

Master thesis

Investigation on the potential application
of MSWI bottom ash as substitute material
in Portland cement concrete



Yubo Sun

Colophon

Report

Title	Investigation on the potential application of MSWI bottom ash as substitute material in Portland cement concrete
Type	Master thesis
Place	Delft, the Netherlands
Date	Oct, 2018

Author

Name	Yubo Sun
Student number	4614887
Department	Structural engineering, Faculty of Civil Engineering and Geosciences, Delft University of Technology
Specialization	Concrete Structures

Assessment Committee

Chair holder:

Dr. G. Ye	Materials- Mechanics- Management & Design, Faculty of Civil Engineering and Geosciences
-----------	---

Committee members:

Ir. B. Chen	Materials- Mechanics- Management & Design, Faculty of Civil Engineering and Geosciences
Dr. Ir. C. B. M. Blom	Concrete Structures, Faculty of Civil Engineering and Geosciences & Gemeente Rotterdam
Dr. Ir. M. Lukovic	Concrete Structures, Faculty of Civil Engineering and Geosciences

Acknowledgements

This thesis is the final report of my master thesis, and the whole study process lasted for about 9 months, which is an extraordinary and unforgettable experience in my life. Looking back, I could really feel my progress from someone who hardly knew anything about material science, and I really appreciate everything happened in this period. The study was conducted in Microlab, CiTG, TU Delft with the greatest help and supporting from many people and companies, and here I would like to give my sincere gratitude and heartfelt tribute to everyone who helped me with every tiny step forward in this process.

First of all, I would like to thank Gemeente Rotterdam and the Heros, who provided the funding and materials for this study. Further, I would also give my deepest gratitude to everyone in my committee:

The chair holder, Assoc prof. Dr. Guang Ye: He provided me this valuable opportunity to perform the study on this interesting topic, even though I'm from structural engineering who almost knew nothing about material science. Moreover, I would also like to thank him for the kind guidance and suggestions in this study.

Ir. Boyu Chen: She is my daily supervisor and contributed greatly to my study. I would like to express my thanks to her for pushing me forward and cheering me up every time I feel disorientated in my study, and also for the generous suggestions and pleasant cooperation.

Dr. ir. C. B. M. Blom: Thank him for building up the bridge between the university and companies, and it's my honor to have him in my committee.

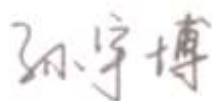
Dr. Ir. M. Lukovic: Big congratulations for her that she had her baby in the middle of this year, and thank her for the suggestions in my research. It was always pleasant working with her.

I also greatly appreciate my colleagues in Microlab for their assistance and suggestions, especially Ir. Shizhe Zhang and Ir. Zhenming Li. A special thank also gives to the technicians in our lab, Mr. Maiko van Leeuwen, Mr. John van den Berg, Mr. Ton Blom and Mr. Arjan Thijssen, thank them for the great help on my experiments.

I would also say thank you to all my dear friends, it was nice meeting you and thank you for sharing the happiness and everything. Thank you for giving me the motivation.

Finally, I would like to give my deepest appreciate to my family, especially my parents and my elder sister for their constant caring and supporting. Thank you for always pushing me forward and accepting my shortcoming. Thank you for always being my strongest shield.

Thank you everyone, for everything you've done.



Yubo Sun
Delft, the Netherlands
October, 2018

Abstract

It has been reported [1] that due to the rapid urbanization and economic growth the municipal solid waste (MSW) would double in volume from 1.3 billion tons per year (in 2012) annually by the end of 2025, challenging environmental and public health management worldwide. Given that, most of the MSW incineration (MSWI) bottom ash (BA) are disposed in landfill currently, and technically and economically viable techniques for the reuse and recycling of MSWI BA is still at a premium. This issue would seriously challenge the environmental and public health management worldwide.

In some European countries and the US, MSWI BA has been utilized as aggregate in pavement construction [20, 28] or as aggregate in concrete [18]. Previous studies also proved the feasibility of using MSWI BA in concrete, either as aggregates [18, 35] or binder [30, 36] substitute materials. However, it is worth noticing that there are several significant drawbacks of using MSWI BA in concrete, including the potential risk of leaching [63, 64] due to the existence of heavy metals and harmful salts, the low reactivity due to high content of quartz and unburned organic matters [71-73], and the metallic aluminum-induced expansion [36].

Therefore, in this study, a characterization of as-received MSWI BA was conducted at the beginning to find out the potential problems when used in concrete, namely the metallic aluminum content, low reactivity and unburned organics. A comprehensive pretreatment was performed subsequently to solve the problems. Specifically, both physical and chemical treatments were carried out to get rid of the metallic aluminum in BA. Afterwards, thermal treatment was conducted to enhance the reactivity of BA and remove the unburned organics. Pre-treated BA samples were characterized again to reveal the effectiveness of pretreatment. The results showed that both chemical and physical treatment were highly effective in removing metallic aluminum. Meanwhile, thermal treatment was proved to be a proper activation method which also removed the remaining organic matters through the high-temperature process.

Subsequently, the investigations of the effects of pre-treated BA addition on compressive strength, reaction products and hydration heat development were conducted on cement paste level by varying the replacement material (BA with different treatment methods) and ratio. A proper method of pretreatment was proposed as well as an optimization of a maximum replacement level of BA in cement paste without detrimentally influence the performance of concrete paste was studied. Compared with nonreactive micronized sand (only works as filler) and pure cement, the addition of physically treated BA has a certain amount of contribution to the hydration process from the viewpoint of heat release. Results show that BA do have pozzolanic activity but is much lower than cement, and physically treated BA is suitable to be used as filler in concrete. Additionally, physically treated BA was further activated through thermal treatment according to the result of compressive strength test, which delivered the highest strength among all the treated BA under the same replacement ratio.

Finally, to extend the application of MSWI BA in concrete, the mix design was made by blending treated BA with the highest compressive strength into concrete and make it suitable for structural application. The effects of treated BA addition on the workability and compressive strength of concrete were investigated. The addition of treated BA

brought slight negative impact both in workability and strength due to the existence of nonreactive phases in BA (quartz and organics).

Accordingly, this study proved the potential of BA with proper treatment to be used as a cement substitute material in concrete as well as promoted the understanding of the influence of BA on the hydration process, which also brings the possibility that BA could be widely reused in concrete system in future industry.

Keywords: MSWI BA, cement substitute material, pretreatment, characterization, cement paste

Content

Colophon	I
Acknowledgements.....	II
Abstract	III
Content	V
Abbreviations.....	IX
List of Nomenclature	IX
Roman letters	IX
Standard	XI
List of Figures.....	XII
List of Tables.....	XV
1. Introduction	1
1.1. Background.....	1
1.1.1. Municipal solid waste (MSW).....	1
1.1.2. Municipal solid waste incineration (MSWI) bottom ash (BA).....	4
1.2. Problem statement.....	5
1.3. Research aim and objective	5
1.4. Methodology	6
1.5. Scope of research	7
1.6. Outline.....	7
2. Literature review.....	10
2.1. Composition of MSWI BA	10
2.2. Current Utilization	10
2.3. Potential problems	13
2.3.1. High-porosity structure	13
2.3.2. Chemical properties	14
2.3.2.1. Low reactivity	14
2.3.2.2. Decrement of strength.....	14
2.3.2.3. Expansion and swelling	14
2.3.2.4. Leaching properties.....	16
2.3.2.5. Organic matters	16
2.4. Pretreatment	17
2.4.1. Washing.....	18
2.4.2. Weathering and accelerated carbonation.....	18
2.4.3. Physical treatment.....	19
2.4.3.1. Grinding and sieving.....	19
2.4.3.2. Thermal treatment.....	19
2.4.4. Chemical treatment	20
3. Materials and methods.....	22
3.1. Materials	22
3.1.1. Cementitious materials.....	22
3.1.1.1. Ordinary Portland cement	22
3.1.1.2. MSWI BA	22
3.1.1.3. Reference substitute materials	23

3.1.2.	Chemical solutions.....	23
3.2.	Experimental methods	24
3.2.1.	Investigation on substitution materials	25
3.2.1.1.	Particle size distribution.....	25
3.2.1.2.	Morphology.....	27
3.2.1.3.	Crystalline phases	27
3.2.1.4.	Chemical composition	28
3.2.1.4.1.	XRF.....	28
3.2.1.4.2.	LOI.....	28
3.2.1.4.3.	Metallic aluminum content	28
3.2.1.5.	Removal of metallic aluminum.....	28
3.2.1.5.1.	Chemical treatment	29
3.2.1.5.2.	Physical treatment	30
3.2.1.5.3.	Mortar strength test.....	31
3.2.1.6.	Activation of treated BA.....	31
3.2.2.	Investigation on cement paste level	31
3.2.2.1.	Compressive strength of paste	31
3.2.2.2.	Hydration heat.....	32
3.2.2.3.	Hydration products.....	34
3.2.2.3.1.	XRD	34
3.2.2.3.2.	TGA	34
3.2.3.	Investigation on concrete level	35
3.2.3.1.	Workability.....	36
3.2.3.2.	Compressive strength.....	36
3.3.	Sample preparations.....	37
3.3.1.	Drying of as-received BA	37
3.3.2.	Fine powders preparation.....	37
3.3.3.	Stopping hydration process.....	38
3.3.4.	ESEM samples preparation.....	38
4.	Characterization of raw BA	39
4.1.	Physical properties	39
4.1.1.	Moisture content	39
4.1.2.	Particle size distribution.....	39
4.1.3.	Morphology.....	40
4.2.	Crystalline phases	41
4.3.	Chemical composition	43
4.3.1.	XRF.....	43
4.3.2.	LOI.....	43
4.3.3.	Metallic aluminum content	44
5.	Pretreatment of BA	47
5.1.	Removal of metallic aluminum.....	47
5.1.1.	Chemical treatment	47
5.1.1.1.	Na ₂ CO ₃ solution.....	47
5.1.1.2.	NaOH solution.....	47

5.1.2.	Physical treatment.....	48
5.1.2.1.	Grinding and sieving.....	48
5.1.2.2.	Preliminary cast	51
5.1.3.	Mortar strength test.....	52
5.2.	Thermal activation	54
6.	Characterization of treated BA	56
6.1.	Physical properties	56
6.1.1.	Particle size distribution.....	56
6.1.2.	Morphology.....	57
6.2.	Crystalline phases	58
6.3.	Chemical composition	60
6.3.1.	XRF.....	60
6.3.2.	Metallic aluminum content	61
7.	Development of materials properties of cement paste and concrete by using BA as replacement.....	62
7.1.	Investigation on cement paste level	62
7.1.1.	Effects of different pretreatment method	62
7.1.1.1.	Compressive strength.....	62
7.1.1.2.	Hydration heat.....	63
7.1.1.3.	Hydration product	66
7.1.1.3.1.	XRD	66
7.1.1.3.2.	TGA	68
7.1.2.	Effects of various replacement ratio	71
7.1.2.1.	Compressive strength.....	71
7.1.2.2.	Hydration heat.....	73
7.1.2.3.	Hydration product	75
7.1.2.3.1.	XRD	76
7.1.2.3.2.	TGA	77
7.2.	Investigation on concrete level	80
7.2.1.	Workability.....	80
7.2.2.	Compressive strength.....	80
8.	Results and discussion	82
8.1.	Investigation on substitution materials	82
8.1.1.	Characterization of raw BA	82
8.1.2.	Pretreatment	82
8.1.3.	Characterization of treated BA	83
8.2.	Investigation on cement paste level	84
8.2.1.	Effect of different treatment method.....	84
8.2.2.	Effect of various replacement ratio.....	85
8.3.	Investigation on concrete level	86
9.	Conclusions and recommendations	87
9.1.	General conclusions	87
9.2.	Recommendations.....	88
References	90

Appendix A	Results of compressive strength tests	97
A1	Compressive strength of mortar	97
A2	Compressive strength for paste	97
A3	Compressive strength of concrete	98
Appendix B	Results of TGA tests	99
Appendix C	Results of DTG tests	101
Appendix D	Results of DSC tests	103

Abbreviations

MSW	Municipal solid waste
MSWI	Municipal solid waste incineration
BA	Bottom ash
FA	Fly ash
GGBFS	Ground-granulated blast furnace slag
CFA	Coal fly ash
MBA	Milled bottom ash
CBA	Chemically treated bottom ash
MTBA	Milled and thermally treated bottom ash
QMBA	Quenched and milled bottom ash
OPC	Ordinary Portland cement
BFS	Blast furnace slag
M300	Micronized sand
PSD	Particle size distribution
ESEM	Environmental scanning electron microscopy
XRD	X-Ray diffraction
XRF	X-Ray fluorescence
LOI	Loss on ignition
TG	Thermalgravimetric
TGA	Thermalgravimetric analysis
DTG	Derivative thermalgravimetric
DSC	Differential scanning calorimetry
CH	Portlandite
C-S-H	Calcium silicate hydrate
C ₂ S	Dicalcium silicate
C ₃ S	Tricalcium silicate
C ₃ A	Tricalcium aluminate
C ₄ AF	Tetracalcium aluminoferrite
AFm	Al ₂ O ₃ – Fe ₂ O ₃ – mono
AFt	Ettringite
RH	Relative humidity
CEN	European Committee for Standardization

List of Nomenclature

Roman letters

$m_{Ref,sand}$	Mass of reference sand
m_{cem}	Mass of cement
m_{water}	Mass of water
m_{BA}	Mass of bottom ash
$C_{p,cem}$	Specific heat of reference sand

$C_{p,water}$	Specific heat of water
$C_{p,BA}$	Specific heat of bottom ash
$C_{p,sand}$	Specific heat of sand
P_0	Normal condition of pressure
T_0	Normal condition of pressure
v_{H2}	Volume of hydrogen gas released
v_0	Molar volume
M_{Al}	Molar mass of aluminum
m_{Al}	Mass of metallic aluminum
T	Room temperature in dissolving test
v_1	Volume of water in cylinder before dissolving test (aluminum content determination)
v_2	Volume of water in cylinder after dissolving test (aluminum content determination)
v_3	Volume increment of water in dissolving test (aluminum content determination)
M_{Fe}	Molar mass of iron
m_{Fe}	Mass of metallic iron
v_4	Volume of hydrogen gas generated by both metallic Fe and Al
v_5	H ₂ generated in acid solution by equivalent amount of metallic aluminum
v_6	Volume of hydrogen gas generated by both metallic Fe
q_1	The minimum heat flow
t_1	The time when minimum heat flow occurs
q_2	The maximum heat flow
t_2	The time when peak value of heat flow occurs
Q_{12}	Cumulative heat at 12 hours
Q_{24}	Cumulative heat at 24 hours
Q_{120}	Cumulative heat at 5 days
w_{ne}	Non-evaporable water content
w_1	Mass loss in TGA from 105°C to 1000°C
w_2	Mass loss in TGA from 400°C to 550°C
w_3	Mass loss in TGA from 700°C to 900°C
L_i	LOI of each kind of substitute material
L_c	LOI of cement
r_i	Mass percentage of each substitute material
r_c	Mass percentage of cement

Standard

<i>NEN-EN 15169</i>	Characterization of waste – Determination of loss on ignition in waste, sludge and sediments
<i>EN 1097-6</i>	Tests for mechanical and physical properties of aggregates – Part 6: Determination of particle density and water absorption
<i>EN 196-2</i>	Methods of testing cement – Part 2: Chemical analysis of cement
<i>EN 196-1</i>	Methods of testing cement – Part 1: Determination of strength
<i>EN 12350-2</i>	Testing fresh concrete – Part 2: Slump test

List of Figures

Fig. 1-1 MSW generated per person in European countries (2004 and 2014)	2
Fig. 1-2 MSW recycling in European countries (2004 and 2014).....	3
Fig. 1-3 MSW Management from 1960 to 2015 according to EPA ¹	4
Fig. 1-4 Waste-to-energy technology ([2]).....	4
Fig. 1-5 Schematization of research methodology	7
Fig. 1-6 Outline of this study	8
Fig. 2-1 Total MSW combusted with energy recovery by EPA (2015)	10
Fig. 2-2 MSWI BA utilization and technology of treatment ([27])	11
Fig. 2-3 High-porosity surface texture of BA particles (<i>Vegas et al. [56], Meima et al. [22], Zevenbergen et al. [57], Izquierdo et al. [58]</i>)	13
Fig. 2-4. (a) Expansion during setting due to the generation of hydrogen gas. (b) Entrapped voids due to hydrogen gas on the fracture surface. [39].....	15
Fig. 2-5 Al(OH) ₃ product of oxidation of aluminum metal ([36])	15
Fig. 2-6 Fe ₂ O ₃ product of oxidation of iron ([36])	16
Fig. 2-7 In-plant ash treatment process (INDAVER).....	18
Fig. 2-8 Design of setup to determine metallic aluminum content in BA	20
Fig. 3-1 Pretreatment route	23
Fig. 3-2 Dry sieving test.....	26
Fig. 3-3 Eye Tech laser diffraction machine	26
Fig. 3-4 Philips XL30 ESEM electron microscope	27
Fig. 3-5 Philips PW 1830 powder X-Ray diffractometer	28
Fig. 3-6 Chemical treatment with Na ₂ CO ₃ solution	29
Fig. 3-7 Retsch PM100 planetary ball miller.....	30
Fig. 3-8 TAM-Air-314 thermometric isothermal conduction calorimeter with 8 channels.....	33
Fig. 3-9 TG-449-F3-Jupiter instrument for TGA.....	35
Fig. 3-10 Steel mold.....	37
Fig. 3-11 MATEST compression machine.....	37
Fig. 3-12 XRD sample	38
Fig. 4-1 Particle size distribution (BA1).....	40
Fig. 4-2 Particle size distribution (BA2).....	40
Fig. 4-3 ESEM 200x of BA particles	41
Fig. 4-4 ESEM 2000x of BA particles	41
Fig. 4-5 XRD diffractograms of BA2 in different fractions	41
Fig. 4-6 XRD diffractograms of BA2 in 0.5-1.6mm, 0.25-0.5mm, 0.125-0.25mm fractions.....	42
Fig. 4-7 Testing system to determine metallic aluminum content	45
Fig. 5-1 Metallic Al content after grinding	49
Fig. 5-2 Mechanisms of grinding and sieving treatment	50
Fig. 5-3 Mass percentage of < 63µm particles after grinding	51
Fig. 5-4 Preliminary cast.....	52
Fig. 5-5 Particle size distribution (CEM I 42.5 R, M300, BFS, MBA).....	52
Fig. 5-6 Compressive strength of mortars with binder substitution (CEM I 42.5N,	

10%MBA, 30%MBA, 10%BFS and 30%BFS).....	53
Fig. 5-7 Compressive strength of mortars with filler substitution (10%MBA, 30%MBA, 10%M300 and 30%M300)	53
Fig. 5-8 DTG curve of MBA	54
Fig. 5-9 TG curve of MBA	55
Fig. 6-1 Particle size distribution (250rpm-30min, 300rpm-20min, 400rpm-10min, 400rpm-40min, CEM I 42.5N and CEM I 52.5R).....	56
Fig. 6-2 Particle size distribution (CEM I 42.5N, MBA, QMBA, MTBA and CEM I 52.5R).....	57
Fig. 6-3 ESEM 200x of BA particles after thermal treatment	58
Fig. 6-4 ESEM 2000x of BA particles after thermal treatment	58
Fig. 6-5 XRD diffractograms of treated BA samples	59
Fig. 6-6 Color change of BA sample (left-MBA, right-MTBA).....	60
Fig. 7-1 Compressive strength of cement paste with CBA, MBA MTBA and M300	63
Fig. 7-2 Rate of hydration as a function of time given by isothermal calorimetry measurements ([106])	63
Fig. 7-3 Definition of characteristic points of heat flow and cumulative heat curves	64
Fig. 7-4 Heat flow normalized to mass of paste at 20°C with w/c=0.5 (CEM I 42.5N, 10% MTBA, 10%MBA, 10%M300)	65
Fig. 7-5 Amount of heat released normalized to mass of paste at 20°C with w/c=0.5 (CEM I 42.5N, 10%MTBA, 10%MBA, 10%M300).....	65
Fig. 7-6 XRD diffractograms of paste with pure cement, MTBA, MBA, CBA and M300	67
Fig. 7-7 TGA curves of cement paste with CBA, MBA MTBA and M300	68
Fig. 7-8 DTG curves of cement paste with CBA, MBA MTBA and M300	69
Fig. 7-9 Mass loss in TGA	70
Fig. 7-10 Hydration products of cement paste with CBA, MBA MTBA and M300 per weight of binder	71
Fig. 7-11 Compressive strength of cement paste with MTBA and M300	72
Fig. 7-12 Compressive strength development of cement paste with MTBA and M300	73
Fig. 7-13 Heat flow normalized to mass of paste at 20°C with w/c=0.5 (CEM I 42.5N, 10%MTBA, 20%MTBA, 30%MTBA).....	73
Fig. 7-14 Calorimetry curve of Portland cement, showing typical shoulder peak where a secondary formation of ettringite occurs and subsequent broad peak corresponding to the formation of AFm phase ([106])	74
Fig. 7-15 Amount of heat released normalized to mass of paste at 20°C with w/c=0.5 (CEM I 42.5N, 10%MTBA, 10%MBA, 10%M300).....	75
Fig. 7-16 XRD diffractograms of paste with different ratio of MTBA and M300	76
Fig. 7-17 TGA curves of cement paste with different replacement ratio of MTBA and M300	77

Fig. 7-18 DTG curves of cement paste with different replacement ratio of MTBA and M300	78
Fig. 7-19 Hydration product of cement paste with different replacement ratio of MTBA and M300 per weight of binder	79
Fig. 7-20 Slump measurement	80
Fig. 7-21 Compressive strength of B40 concrete and 10% MTBA replacement in cement	81
Fig. 8-1 Route of the best pretreatment method within this study.....	85

List of Tables

Table 1-1 Problems of as-received BA derived from characterization and solutions used in this study	9
Table 2-1 Chemical compositions of cement, MSWI BA/FA, GGBFS and CFA12	
Table 2-2 Problems of BA and corresponding solutions according to literature study.....	17
Table 3-1 Characterization of raw and treated BA	24
Table 3-2 Pretreatment	24
Table 3-3 Hydration process	25
Table 3-4 Design of chemical treatment with Na_2CO_3 solution.....	29
Table 3-5 Design of chemical treatment with NaOH solution (by Loic)	30
Table 3-6 Mixture design of mortar cubes (40*40*40 mm)	31
Table 3-7 Mixture design for paste cubes	32
Table 3-8 Mixture design and mass of reference sand.....	33
Table 3-9 Specific heat of each substance	33
Table 3-10 Decomposition reactions of cement paste with the increase of temperature	34
Table 3-11 Proportions of concrete mixtures prepared	36
Table 4-1 Moisture content of BA1 and BA2	39
Table 4-2 Chemical composition of OPC, BA1 and BA2 (by fraction)	44
Table 4-3 Metallic aluminum content in each content.....	46
Table 5-1 Result of treatment with Na_2CO_3 solutions.....	47
Table 5-2 Results of treatment with NaOH solutions.....	48
Table 5-3 Metallic aluminum content and output rate after treatment.....	49
Table 5-4 Preliminary cast design with MBA.....	51
Table 6-1 Volume dimensions of powders with median size (250rpm-30min, 300rpm-20min, 400rpm-10min, 400rpm-40min, CEM I 42.5N and CEM I 52.5R).....	56
Table 6-2 Volume dimensions of powders with median size (CEM I 42.5N, MBA, QMBA, MTBA and CEM I 52.5R)	57
Table 6-3 Chemical composition of raw BA, MBA and MTBA	60
Table 6-4 Metallic aluminum content in raw BA, MBA and MTBA	61
Table 7-1 Compressive strength of cement paste with CBA, MBA and MTBA. 63	
Table 7-2 Characteristic calorimetric parameters of 10% substitution	66
Table 7-3 Characteristic values of TGA, DTG and DSC curves of cement paste with CBA, MBA MTBA and M300.....	69
Table 7-4 CH and non-evaporable water content of cement paste with CBA, MBA MTBA and M300	70
Table 7-5 Compressive strength of cement paste with MTBA and M300.....	72
Table 7-6 Characteristic calorimetric parameters of MTBA and M300	74
Table 7-7 Characteristic values of TGA, DTG and DSC curves of cement paste with different replacement ratio of MTBA and M300.....	78
Table 7-8 CH and non-evaporable water content of cement paste with different replacement ratio of MTBA and M300.....	78

Table A-0-1 Compressive strength of mortar with pure cement, 10% MBA, 30% MBA, 10% BFS, 30% BFS, 10% M300 and 30% M300	97
Table A-0-2 Compressive strength of pastes with pure cement, 10% M300, 10% CBA, 10% MBA and 10% MTBA	97
Table A-0-3 Compressive strength of pastes with pure cement, 10% M300, 10% MTBA, 20% M300, 20% MTBA, 30% M300 and 30% MTBA.....	98
Table A-0-4 Compressive strength of B40 concrete and substituted with 10% MTBA	98

1. Introduction

The introduction first gives the background on the current situation of MSWI production, as well as the treatment and utilization of MSWI BA, especially as a substitute material in concrete. Subsequently, the research problem in this study is proposed, and the research goal, methodology and scope are set as well. Finally, the outline of this report is schematized.

1.1. Background

1.1.1. Municipal solid waste (MSW)

According to the report ‘Solid waste management’ published by *World Bank Group*, the amount of municipal solid waste (MSW), one of the most important by-products of urban lifestyle, is growing even faster than the rate of urbanization. The report showed that in the year of 2012 about 3 billion residents generating 1.2 kg per person per day (1.3 billion tons per year), and an estimation was made that by 2025 this will likely increase to 4.3 billion urban residents generating about 1.42kg per person per day of MSW (2.2 billion tons per year) [1]. The Online service conducted by *Worldwatch Institute* for its *Vital Signs* also estimated that due to the rapid urbanization and economic growth the MSW would double in volume from 1.3 billion tons per year (in 2012) annually by the end of 2025, challenging environmental and public health management worldwide.

According to the investigation carried out by EEA¹, the MSW generated and recycled per person in European countries in 2004 and 2014 are illustrated in Fig. 1-1 and Fig. 1-2 separately. In general, an increment amount of MSW generated per person was observed, while the recycling ratio increased as well. Moreover, MSW generated per person even decreased in some countries such as Cyprus, Luxembourg, Ireland etc. However, the recycling ratio of MSW is still poor while large amount of MSW is still generated, e.g. Serbia, Turkey, Bosnia and Herzegovina. Therefore, both the policy and technique of treating MSW is still inadequate.

¹ European Environmental Agency



Fig. 1-1 MSW generated per person in European countries (2004 and 2014)

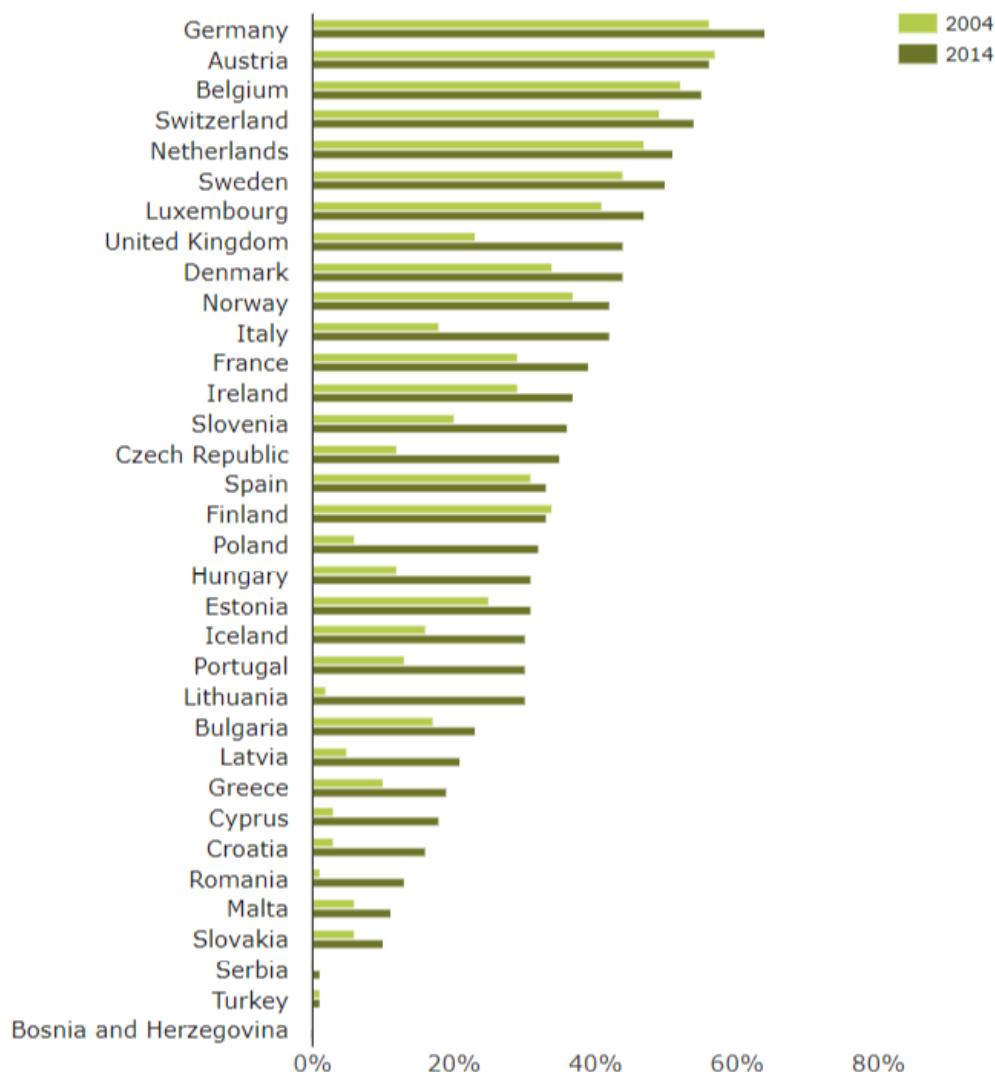


Fig. 1-2 MSW recycling in European countries (2004 and 2014)

Fig. 1-3 depicts the data collected by EPA² on MSW management from 1960 to 2015 in the US, which shows an increasing amount of MSW generation annually. Meanwhile, from the 80's last century, the amount of recycled MSW has been become more and more attractive. However, most of the MSW incineration (MSWI) bottom ash (BA) are disposed in landfill currently, and technically and economically viable techniques for the reuse and recycling of MSWI BA is still at a premium so that most of the MSW is still landfilled, which brings immense pressure and great challenges on the waste management and environment protection.

² United States Environmental Protection Agency



Fig. 1-3 MSW Management from 1960 to 2015 according to EPA¹

1.1.2. Municipal solid waste incineration (MSWI) bottom ash (BA)

Currently, the waste-to-energy technology (as shown in Fig. 1-4) [2] is considered as an efficient method to deal with the increasing amount of MSW. The incineration process reduces the mass and volume of solid waste [3] dramatically (by 70% and 90%, respectively [4, 5]), as well as the demand of landfilling [6]. However, a considerable amount of incineration residues is generated after combustion (typically bottom ash, fly ash, grate sifting, air pollution control (APC), etc. [5, 7, 8]), of which bottom ash (BA) accounts for about 80% by weight [9]. At present, most of MSWI residues are landfilled, which may raise environmental issue and potential loss of resources [5, 10-12]. Previous studies have indicated that MSWI BA is suitable to be reused as construction materials, especially in pavement construction [13-15] and concrete structures [16-19]. In this way the waste materials are recycled, reused and reduced (3Re) in an environmental-friendly way.

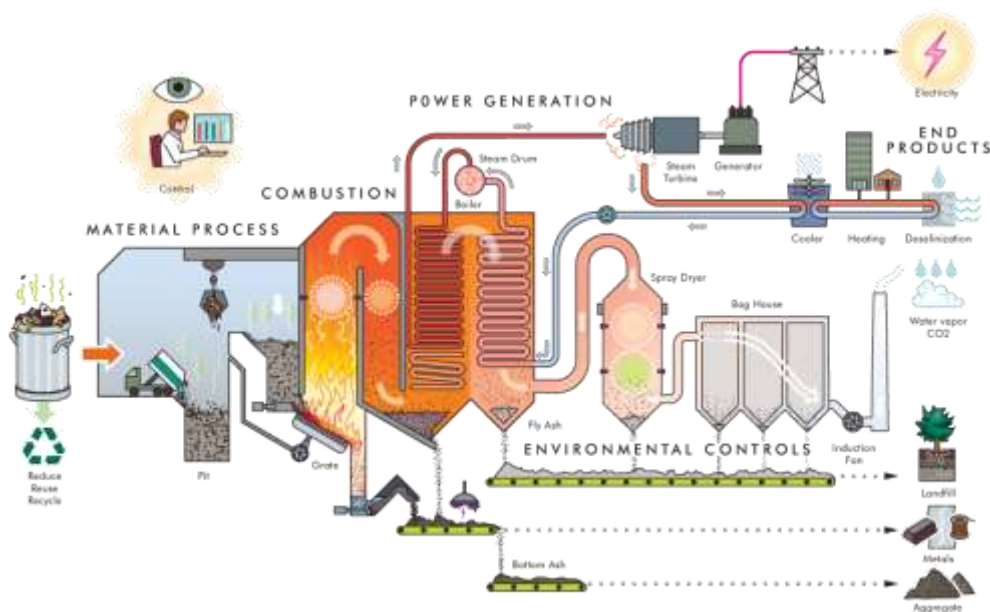


Fig. 1-4 Waste-to-energy technology ([2])

1.2. Problem statement

As a by-product of incineration plant, treated MSWI BA could be used as aggregate in pavement construction or concrete structures. However, the scope of such utilization is relatively limited due to the existing issues such as leaching, expansion. Moreover, the poor pozzolanic reactivity of BA is also reported when used as cement substitute materials. According to the present studies, MSWI BA has a similar chemical composition as cement with an abundant amount of crystalline phases, which is a potential substitute material in concrete as binder or aggregate. Currently, more investigations have been focusing on the pretreatment technologies to remove the less desired substances in the concrete system (such as metallic aluminum, unburned organic matters, heavy metals and harmful salts) which seldom contribute to the hydration process and get BA activated by creating new reactive phases. However, most of them only focused on improving a single or few properties of those mentioned above that a comprehensive study on pretreatment and a standard or proper method of BA treatment is still in scarce.

The performance of treated BA in concrete systems has seldom been studied and the investigation on BA substitution cement is still scarce as well, especially in the following aspects:

- The effect of different treatment methods on MSWI BA.
- The feasibility and effect of using treated BA in concrete system as binder substitute materials in cement paste.
- The reactivity of BA before and after treatment as binder in cement paste.
- The effect of blending treated BA with cement as binder in concrete on the hydration process, including temperature development and hydration products.
- The maximum replacement ratio without detrimentally influencing the compressive strength.

1.3. Research aim and objective

Previous studies have been focusing on the characterization, application of treated BA (details are provided in Chapter 2). However, in the literature, few attention has been paid to the treatment and activation of fine particles (0-2mm provided by *Heros*³) MSWI BA as a substitution material in Portland cement concrete. This project aims to study the pretreatment method to upgrade MSWI BA as substitute material in Portland cement concrete system, and derive a maximum replacement level without detrimentally influence the compressive strength. The initial goal of this project was to cast a bench with BA and concrete, and accordingly a threshold was set that the decrement of 28-day compressive strength of cement paste with BA substitution should be smaller than 30% comparing with pure cement paste so that the compressive strength of concrete could still be obtained by adjusting mix design.

In the research program, as-received MSWI BA with the particle size of 0-2 mm is firstly sieved and divided into several groups according to its particle size to check whether the properties of each fraction are identical to each other. If a severe difference

³ Oostkade 5, 4541 HH Sluiskil, the Netherlands

is detected, the fraction with the most similar property of cement will be selected for further investigation. The crystalline phases, chemical compositions and morphology of BA with different particle size are characterized. According to the nature of BA, pretreatment was performed to get rid of the undesired content when used as substitute material in cement (such as metallic aluminum and unburned organics). Treated BA samples are characterized again and derive the optimum treatment method. Additionally, mechanical properties of mortars with BA are analysed after different curing times, isothermal calorimetry is applied to investigate the hydration process of cement with treated BA and reveal the reactivity of treated BA. Furthermore, hydration products are investigated by TGA and XRD. In this way, an explanation of how treated BA contribute to the hydration process (comparing with pure cement) could be derived, and a reasonable maximum replacement ratio could be proposed as well. Finally, the treated BA with certain replacement ratio will be examined by compressive strength on the concrete level.

Detailed objectives of this research are:

- Find out a proper route of pretreatment and determine the composition and properties of treated BA.
- Check the compressive strength, hydration heat development and hydration product of cement paste with treated BA.
- Evaluate the performance of treated BA as binder substitute material in concrete by compressive strength and workability.
- Derive a maximum replacement level and give recommendations on substitution of treated BA in concrete systems.

1.4. Methodology

The methodology is schematized in Fig. 1-5. In the beginning, research problem is set according to the background, and objective and methodology of this study are proposed separately. A literature study is conducted to show the current situation of MSWI BA, including the production and utilization. Meanwhile, the existing knowledge and solutions of MSWI BA in concrete system are reviewed. In phase 3 the investigation is performed on the material level, focusing on the characterization of as-received BA. Different pretreatments are performed on BA as well to improve the performance, and the treated BA samples are characterized again to show the effect of pretreatment. Subsequently, the contribution of BA samples with different pretreatments to the hydration process are investigated on the paste level, including the compressive strength of paste, the hydration heat development and the hydration products. Finally, the performances of BA samples are evaluated on concrete level according to the results of compressive strength, and conclusions and recommendations are provided as well at the end.

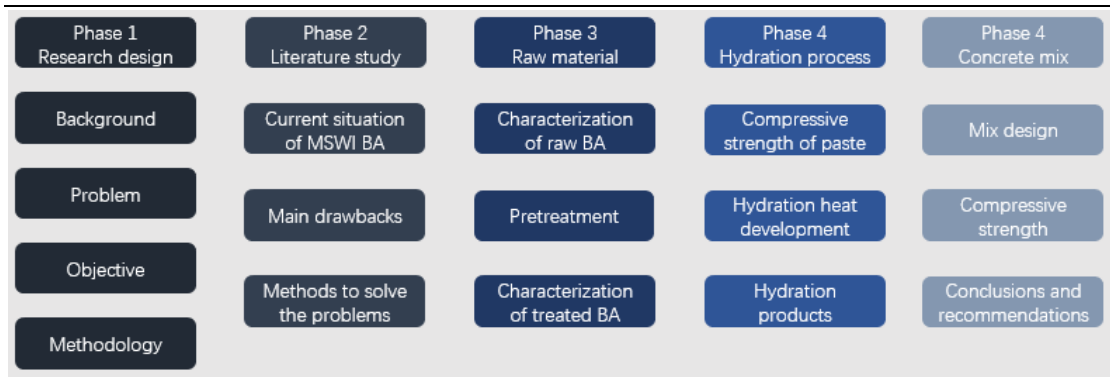


Fig. 1-5 Schematization of research methodology

1.5. Scope of research

In this study, the research was mainly conducted on two aspects, namely the properties of substitute material itself (BA) and the contribution of BA to the hydration process in cement paste comparing with pure cement. On the material level, as-received BA was characterized, and several treatments were performed to get rid of the undesirable contents in cement and get the samples activated. Subsequently, the treated BA samples were characterized again to evaluate the effect of different treatment methods. Then the hydration process was detected by blending treated samples into cement paste. The performances of different samples were evaluated by testing compressive strength, hydration heat and amount of hydration products, in which the compressive strength respond to the quality of BA substituted cement intuitively, and hydration heat and products could help explain how much BA contribute to the hydration process comparing to pure cement and the decrement in compressive strength. Eventually, the best method of treatment with the highest strength of paste was found out and the performance of the best BA sample in concrete was checked by compressive strength test, and the workability of the concrete mix was tested as well.

BA samples after different pretreatment methods were blended with cement paste. Meanwhile, pure cement and pure sand (with no reactivity) were selected as reference materials to evaluate the reactivity of each treated BA. Properties of different pastes were investigated within the following restrictions:

- Each BA and reference material with various property and reactivity was regarded as cement substitute material when blended into the paste and assumed to have a certain amount of contribution to the hydration process when compared with pure cement and BFS.
- BA is regarded as filler substitute material when compared with M300 with no reactivity.
- Water to cement ratio of each mixture was kept at 0.5 according to the sample preparation method in *EN 196-1*.
- All samples were cured under the same condition (demolded after 24 hours and then transferred into a curing room with room temperature 20°C and RH>95%).

1.6. Outline

Outline of this study is illustrated in Fig. 1-6.

Chapter 1-3 mainly gives a general impression on this study. The first chapter provides the background of this study, problem statement, research goal and scope, while the second chapter gives a literature survey related to this study including characterization of materials and technologies of treatment and investigation on the effects of treatment. The third chapter gives an overview of the materials and experimental methods involved in this study, including the details of the experimental setup, mixture design and sample preparation.

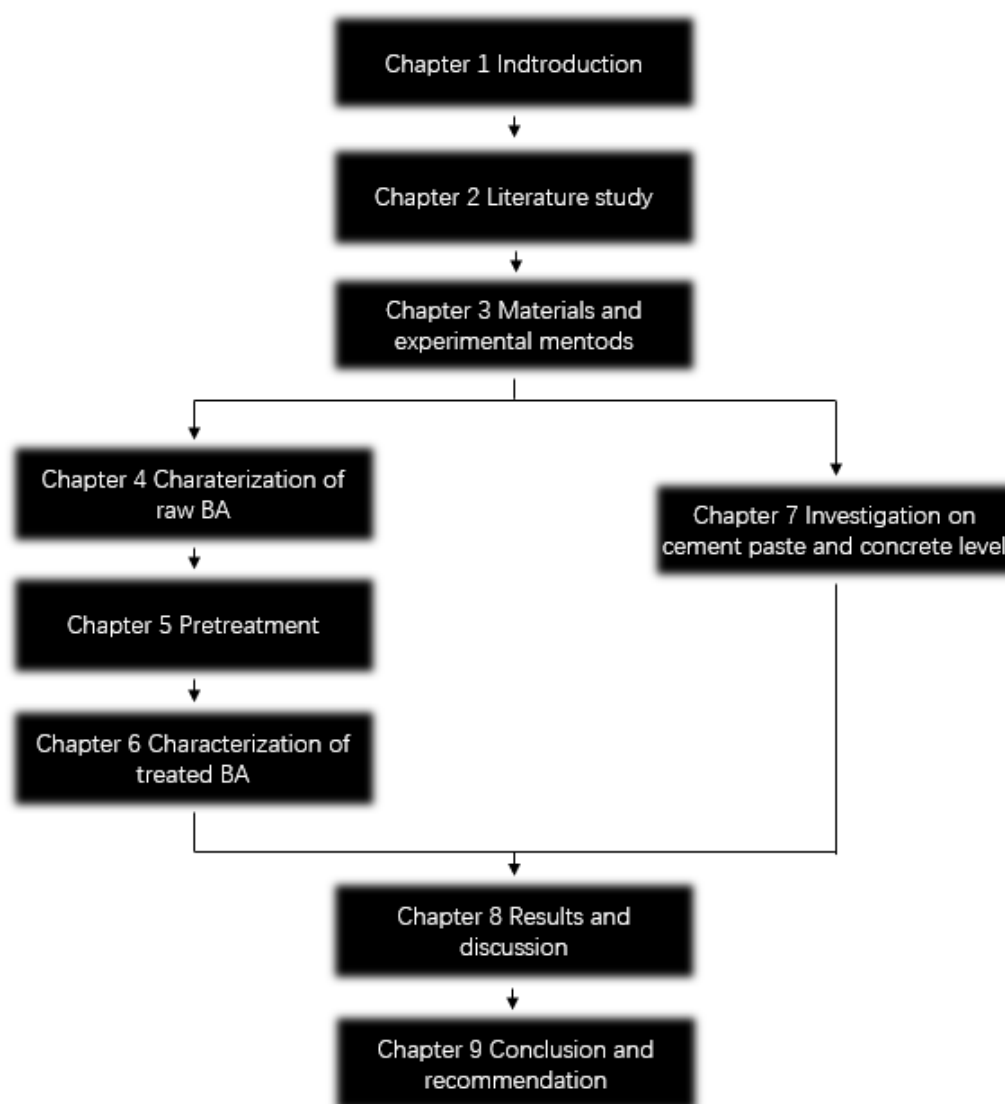


Fig. 1-6 Outline of this study

Consequently, chapter 4-6 are focused on the study of substitution material itself. Chapter 4 shows the result of the characterization of raw BA, including particle size distribution, morphology, crystalline phases and chemical compositions (elemental composition, unburned organic content, metallic aluminum). The properties were compared to those of the target of substitution, the pure cement, and several main problems of as-received BA were found out, namely the metallic aluminum content, relatively low reactivity and unburned organic contents.

Chapter 5 gives the details of pretreatment to solve the problems of as-received BA mentioned in previous chapter (summarized in Table 1-1). In the first stage, both physical and chemical treatments were performed to get rid of the metallic aluminum content in as-received BA. A mortar strength test was performed after the first stage of treatment to show the effect of removing the metallic aluminum content. Both chemical and physical treatment were effective enough to remove the metallic and physically treated BA is already good enough to be used as filler in concrete. Subsequently, thermal treatment was performed as well to get BA activated after removing the aluminums to investigate the feasibility of BA to be used as cement replacement materials. The temperature of thermal treatment was determined as 1000°C according to a TGA test so that a phases transition was detected accompanied by the continuous mass loss corresponding to the decomposition of organics.

Table 1-1 Problems of as-received BA derived from characterization and solutions used in this study

Problems of as-received BA	Solution
Metallic aluminum content	Chemical/physical treatment
Low reactivity	Thermal treatment
Unburned organic content	Thermal treatment

Similarly, the treated BA samples were characterized again in chapter 6, and the effects of pretreatment is revealed by comparing the result of treated BA samples to that of as-received BA and pure cement.

Chapter 7 provides the performance of treated BA on paste and concrete level. Compressive strength, hydration product and hydration heat were measured at different treated BA replacement levels to show the influence of blending cement with treated BA. The best pretreatment method within this study was proposed as well as a maximum replacement level without detrimentally influence the performance of concrete paste was derived. Subsequently, investigations on concrete level were conducted by blending certain amount of treated BA with the best performance according to the results of paste investigation in cement paste and casting into concrete. Compressive strength and workability of concrete cubes with pure cement and BA were measured separately.

Results of experiments are summarized in chapter 8, and the discussion about the results with their interrelations are given as well in perspective of the research aim and problem statement.

Finally, the conclusions are summarized in chapter 9 and recommendations of BA as substitute material in concrete are given as well.

2. Literature review

According to the investigation of other researchers, the results of characterization show several significant drawbacks of BA substitution in concrete. Different methods of improving the properties of BA are proposed to solve the issues occurred. An overview of previous studies shows that the potential utilization of BA in concrete system.

2.1. Composition of MSWI BA

As a by-product from MSWI, the composition of BA could be complex, containing stone, ceramic, glass, brick, metals and unburned organics [9, 20]. Meanwhile, the content of BA could be affected by multiple reasons, such as incineration processes, weathering conditions, separation technologies, geographical and seasonal factors, which may differ from plant to plant, country to country [9, 21-23]. The composition of MSWI BA is highly variable, depending on the nature of the feedstock to the incinerator, and include metal, plastic and putrescible waste [24, 25]. Fig. 2-1 describes on the complexity of combusted MSW, which results in the complex composition of MSWI BA. On the other hand, *Tang et al.* tested the chemical compositions of BA from different plants over time, and the results show that the compositions are stable and mostly independent of the raw solid waste before incineration and different production process [26], which proved the feasibility of the application in industry.

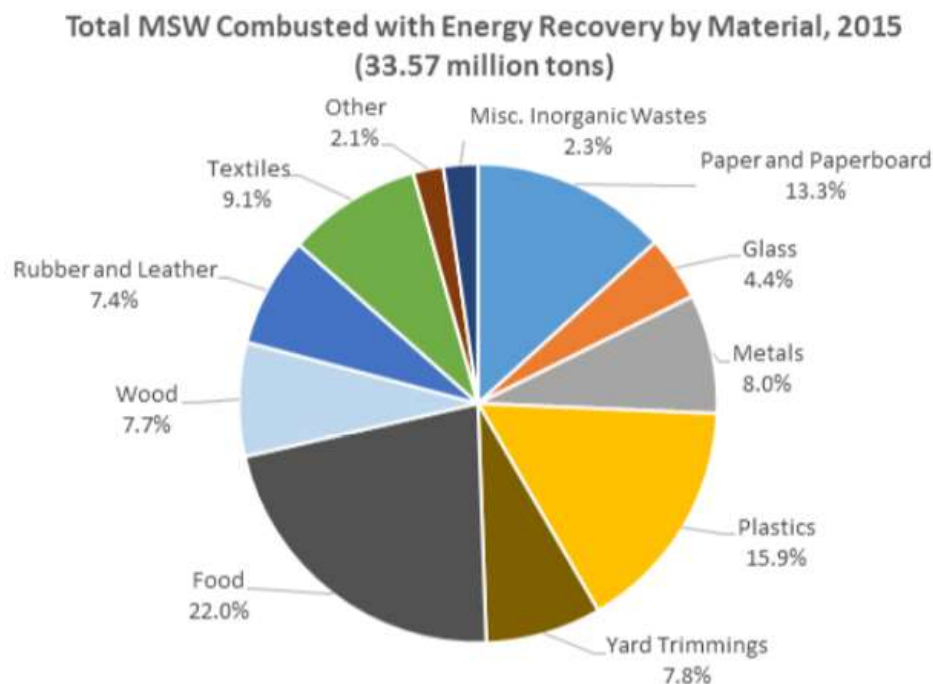


Fig. 2-1 Total MSW combusted with energy recovery by EPA (2015)

2.2. Current Utilization

Due to the increased landfilling cost and awareness of the circular-economy, MSWI BA is now gaining more attention and regarded as an underutilized material [27]. However, BA is now seldom used as a substitute material in the industry directly due to its low

strength and high-content of pollutants. *Bram et al.* [27] summarized the current technology of BA treatment and utilization, as shown in Fig. 2-2, which indicates that the property and utilization of BA is limited by the chemical barriers and treatment technology.

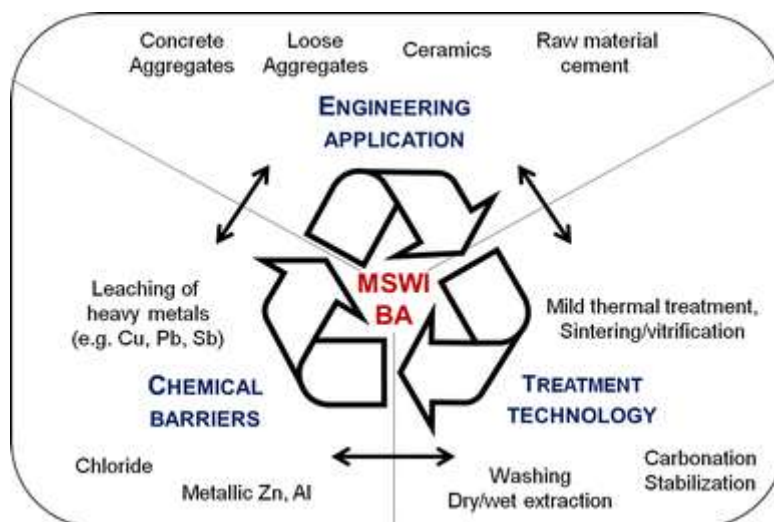


Fig. 2-2 MSWI BA utilization and technology of treatment ([27])

Recently, in the US and some European countries (Germany, France and the Netherlands) the MSWI BA could be used as a substitute material of aggregates in asphalt, road sub-base and embankments [20, 28]. Several methods have been proposed to meet the leaching requirement especially the heavy metals, such as weathering, chemical carbonation and physical stabilization [28]. *Eymael et al.* also concluded that BA could be potentially used as a substitute of natural aggregate in asphalt mixtures up to 25% [29].

In existing studies, MSWI BA has been widely used in concrete investigations, either as substitute material (aggregate [18, 35] and cement [30, 36]). According to the previous studies, MSWI BA is mainly composed of aluminum, iron, silica and calcite oxide [20, 30, 31]. As shown in Table 2-1, significant similarities in chemical compositions have been observed among MSWI BA/FA, Portland cement and other cement additions (such as ground granulated blast furnace slag (GGBFS) and coal fly ash (CFA)) [32-34]. This suggest that MSWI BA could be potentially blended with cementitious materials and contribute to the hydration process in concrete systems [30]. in concrete or raw material for clinker production [37, 38]. However, the investigation of proper treatment and utilization of BA is still limited that BA is seldom used in the industry currently.

Table 2-1 Chemical compositions of cement, MSWI BA/FA, GGBFS and CFA

Chemical composition (% wt.)		CaO	SiO ₂	Fe ₂ O ₃	Al ₂ O ₃	MgO	Na ₂ O	K ₂ O	CuO	ZnO	P ₂ O ₅	TiO ₂	Cl	SO ₃	other
Cement	<i>Bertolini et al. [39]</i>	62.7	23.7	1.93	4.71	1.99	0.2	0.8	-	-	0.15	0.19	-	3.48	0.07
			4					4							
	<i>Tang et al. [31]</i>	64.9	17.1	3.59	3.80	1.56	0.00	0.1	0.0	0.1	0.63	0.27	0.0	3.96	3.74
		9	1					6	2	5			2		
MSWI BA	<i>Gupta et al. [40]</i>	25.9	27.8	4.0	9.9	3.3	3.3	1.8	-	-	6.9	2	0.2	-	14.9
													3		
	<i>Wei et al. [41]</i>	33.4	31.9	5.97	16.6	3.33	2.53	0.8	-	-	0.02		1.0	0.40	3.84
		0	3		5			5					8		
	<i>Pera et al. [17]</i>	11.1	54.6	8.5	8.0	1.5	12.8	1.3	-	-	2.1	-	-	-	0.1
	<i>Muller et al. [35]</i>	11.9	55.7	8.8	14.1	2.7	1.4	1.2	0.5	0.3	-	-	-	0.7	2.7
	<i>Andreola et al. [42]</i>	26.3	46.7	4.7	6.9	2.2	4.6	0.9	0.3	0.7	0.9	0.8	0.2	2.2	2.6
	<i>Gines et al. [18]</i>	14.7	49.4	8.4	6.6	2.3	7.8	1.4	1.3	0.4	-	-	-	0.6	7.1
	<i>Rendek et al. [43]</i>	16.3	49.3	7.6	7.5	2.6	6.0	1.1	1.5	-	1.2	0.6	0.4	0.3	5.6
	<i>Tang et al. [31]</i>	19.3	35.9	11.54	9.00	1.81	1.35	1.1	0.4	0.8	1.02	1.11	0.6	4.95	0.69
		4	8					5	3	0			6		
	<i>Qiao et al. [44]</i>	20.2	36.2	6.21	8.48	1.58	2.93	1.0	0.3	0.3	1.59	0.89	0.8	2.34	12.8
		0	0					4	0	7			9		0
MSWI FA	<i>Aubert et al. [45]</i>	25.2	20.7	2.7	10.0	2.7	1.4	1.4	2.3	4.6	13.6	1.7	-	11.6	2.1
	<i>Wan et al. [46]</i>	22.7	23.6	4.83	8.18	2.64	5.28	5.6	0.1	0.9	2.49	1.36	6.4	13.9	1.74
		8	4					0	4	3			0	9	
CFA	<i>Kim et al. [47]</i>	1.54	51.1	12.2	22.9	0.73	0.38	2.5	-	-	0.14	1.01	-	0.07	7.4
								5							
	<i>Nathan et al. [48]</i>	4.9	58.6	6.7	24.4	1.6	0.05	0.1	-	-	0.8	1.2	-	0.6	0.42
								3							
GGBFS	<i>Zhang et al. [49]</i>	40.9	32.9	0.46	11.8	9.23	-	0.3	-	-	-	-	-	1.60	2.67
		6	1		4			3							
	<i>Richardson et al. [50]</i>	41.7	37.2	0.38	11.0	7.74	0.64	0.5	-	-	-	0.68	-	3.68	0.73
		0	0		0			5							

2.3. Potential problems

The utilization of MSWI BA in concrete structures was obstructed due to the weakness in both physical (high-porosity structure) and chemical properties (low reactivity, high content of metallic aluminum, leaching of harmful elements and unburned organics). Some important aspects are discussed as following and will be dealt with by using certain pretreatment methods.

2.3.1. High-porosity structure

Physically, as a result of the extremely high temperature of the combustion process, a high-porosity and irregular morphology of BA particles are formed, making the particles easily crushed [51, 52]. *Bayuseno* et al. proposed that the angular and porous fragments in BA were formed due to the release of trapped gases in the inorganic components which were partial or wholly melt during the incineration or quenching process [53]. *Brami* et al. also revealed that BA particle could be divided into two fractions, namely cenospheres (empty hollow spheres) and planispheres (hollow spheres packed with large numbers of smaller spheres) [54]. As a result of the high-porosity structure and the vesicular textures, which may be considered as small water reservoirs affecting moisture transport in concrete, extra water absorption may eventually reduce the amount of water available to react with cement and result in higher water demand in mixture design and lower strength in concrete [26, 55]. Therefore, the high-porosity morphology of BA would result in strength decrement when used as substitution material in cement, directly (pores and microcracks induced failure) and indirectly (water absorption and less water reacting with cement).

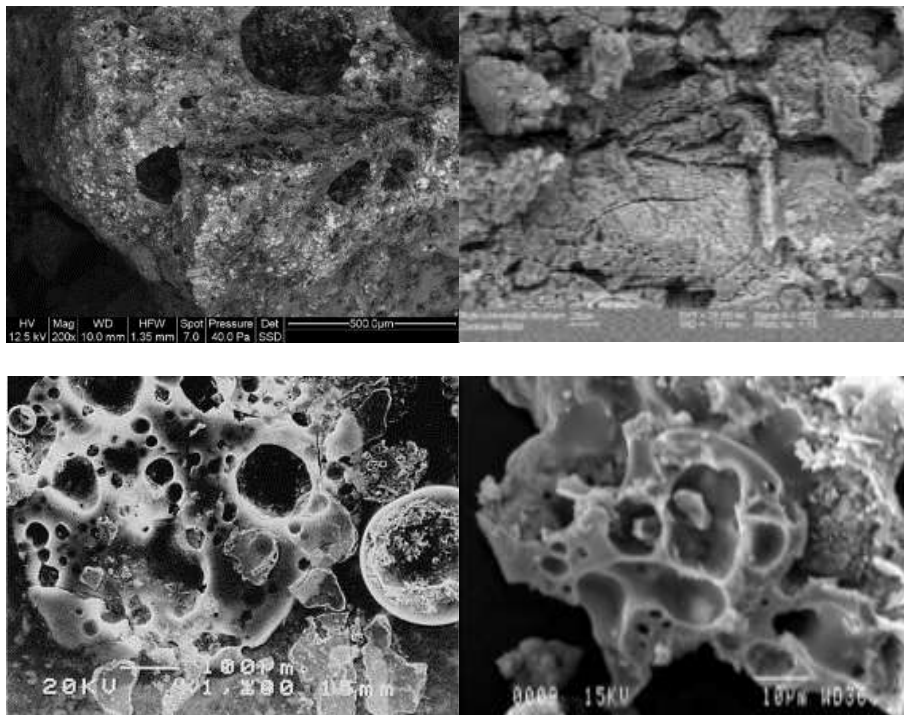


Fig. 2-3 High-porosity surface texture of BA particles (*Vegas* et al. [56], *Meima* et al. [22], *Zevenbergen* et al. [57], *Izquierdo* et al. [58])

2.3.2. Chemical properties

2.3.2.1. Low reactivity

As for chemical properties, in general, the relatively low reactivity of BA (comparing to pure cement) is reported in previous studies. The low reactivity wastes contain little or no detectable levels of lime or Portlandite [59]. *Filipponi et al.* suggested that MSWI BA exhibited weak pozzolanic activity as a consequence of the appearance of amorphous contents and highly reactive silica, according to the result of unconfined compressive strength (UCS) tests [60]. *Tang et al.* mentioned that BA samples have deficient hydraulic activity and their addition to cement would lead to the retardation of cement hydration according to calorimetric results [26]. *Li et al.* indicated that the addition of MSWI BA slowed down the hydration process [30]. *Bertolini et al.* also pointed out that the finely grounded MSWI BA could have pozzolanic or hydraulic behavior and its addition could have a beneficial role in the development of microstructure of the concrete mixture [39]. *Pera et al.* proved that vitrified BA would contribute to the pozzolanic reaction together with Portland cement [61].

2.3.2.2. Decrement of strength

The decrement of strength has been reported in several studies as well [26, 39, 62]. *Gines et al.* reported a linear decay in compressive strength with the increase of the proportions of BA aggregate [18]. *Florea et al.* obtained that the 28-day compressive and flexural strength of mortar with 30% BA replacement is about 16% and 6% lower than the reference mortar, respectively when used as cement replacement [31]. *Li et al.* mentioned that the early strength of cement paste decreases rapidly when the BA content (cement substitution) is over 20%, and the rich silica gel formed when mixing BA with water would result in higher moisture absorption between unhydrated cement particles, and consequently enwraps cement particles and leads to strength reduction and higher water demand [30]. *Pan et al.* found out that the high content of P_2O_5 in BA (>0.5%) would result in the reduction of C_3A production and further reduced the strength of cement [37].

2.3.2.3. Expansion and swelling

It is reported the expansion or swelling of concrete caused by the metallic aluminum contained in BA when it is used as aggregate or filler [36]. Metallic aluminum content will be dissolved in the alkaline environment provided by cement paste and generating large amount of hydrogen (H_2) bubbles and result in severe expansion and swelling with air bubbles and cracks in concrete so that the strength will decrease. The expansive aluminum reaction was identified as the main cause of extensive spalling on the concrete surface [35]. *Bertolini et al.* found that MSWI BA would provide the risk of entrapment of hydrogen bubbles produced by corrosion of aluminum metallic particles [39].

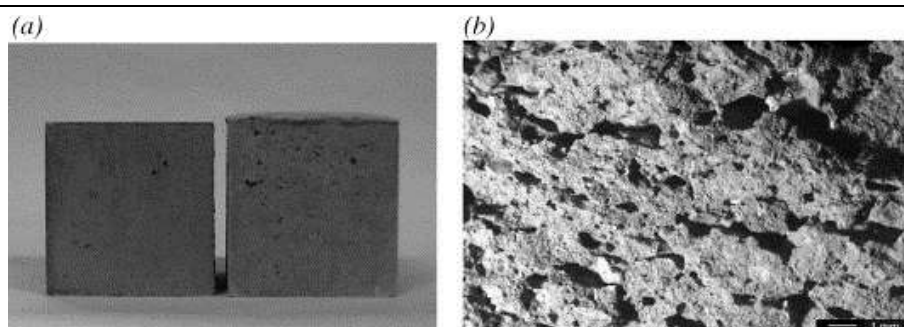


Fig. 2-4. (a) Expansion during setting due to the generation of hydrogen gas. (b) Entrapped voids due to hydrogen gas on the fracture surface. [39]

Meanwhile, due to the high content of bottle glass particles as part of BA, which may contribute to alkali-silica reaction (ASR) and result in cracks and corrosion of reinforcement, the durability of concrete could be negatively affected as well [24, 62]. However, the ASR induced expansion is proved to be less severe than those caused by the aluminum corrosion [35]. The technique for the removal of metallic *Al* and *Si* by slow milling (and the formation of metal plates which can be sieved out) has been proposed and its applicability has been proven by *Tang et al* [31]. *Pecqueur et al.* also proposed that the swell deformation could result from the oxidation of metals such as aluminum or iron [36]. The technique for the removal of metallic *Al* and *Si* by slow milling (and the formation of metal plates which can be sieved out) has been proposed and its applicability has been proven by *Tang et al* [31]. *Pecqueur et al.* also proposed that the swell deformation could result from the oxidation of metals such as aluminum or iron [36] and the oxidation products have been observed along the crack path as shown in Fig. 2-5 and Fig. 2-6.

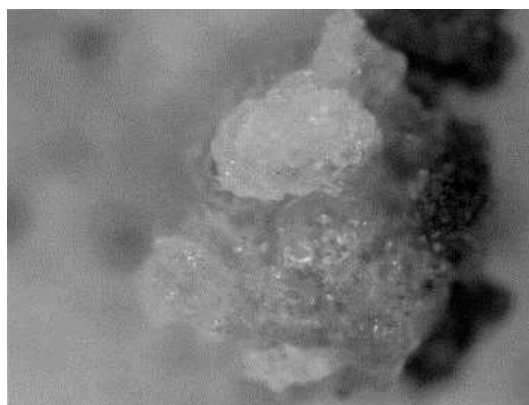


Fig. 2-5 Al(OH)_3 product of oxidation of aluminum metal ([36])

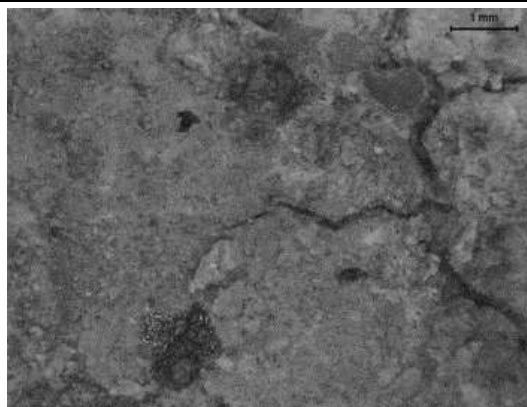


Fig. 2-6 Fe_2O_3 product of oxidation of iron ([36])

2.3.2.4. Leaching properties

MSWI BA contains relatively high concentrations of hazardous elements. Due to the rapid cooling process after incineration process, BA is unstable under atmospheric conditions so that the hazardous elements would be dissolved when water flows through pores and cracks and result in environmental problems, which is called leaching. Previous research also mentioned the potential environmental risk of BA due to the leaching behavior [63, 64]. The number of heavy metals and harmful salts (e.g. Sb, Mo, Cu, chlorides and sulfates) in BA need to be reduced before application in construction field [25, 65]. *Van der Sloot* et al. determined the leaching potential by the risks associated with the presence of potentially hazardous constituents in waste materials together with their leachability and environmental risks [66]. Meanwhile, previous studies already proved that pH is recognized as a dominant factor in element leaching from waste materials and contaminated soils [67, 68]. The evaluation of pH is regarded as an important tool in predicting long-term leaching behavior [66]. *Arickx* et al also addressed that the leaching of Cu could be enhanced by the working together with dissolved organic carbon (DOC) and fulvic acids [69]. *Dijkstra* et al. proved that the leaching of the major components (Al, Ca, SO_4 , Mg, Si, Fe, Na and DOC) and trace elements (Ni, Zn, Cd, Cu, Pb, Mo and Sb) from MSWI BA is a function of time over a wide range of pH [70].

2.3.2.5. Organic matters

The incineration process mainly transforms organic matters in CO_2 and H_2O , but inorganic residues yields [20]. However, due to the inhomogeneous and inadequate incineration process, the remaining unburned organic matters are observed as well in BA samples according to the loss on ignition tests (LOI) [71-73].

As known as a nonreactive phase inhibiting the hydration process in cement paste, organics is undesirable in cementitious materials, which is suspected to be another factor besides the metallic aluminum content resulting in a decrease in concrete strength. *Chimenos* et al. mentioned that the composition of unburned organics could be complex, including carbonaceous semi-burned particles, paper and cardboard, fragments of cotton, synthetic fibers, bone fragments and some fruit skins which are practically unaltered by the gas flow and able to pass the combustion chamber [9].

Saikia et al. suggested that the presence of harmful organic impurities (fulvic and humic acids along with a hydrophilic portion) in BA may affect the compressive strength development of mortar. On the other hand, the presence of organic matters may release organic acids during microbial degradation which contribute to the carbonation reaction and improve leaching properties [74]. However, the organic matter only has a limited short-term effect by contributing to carbonation, and the organic residue after incineration in BA should be removed when used as cement substitute materials.

2.4. Pretreatment

Currently, more studies have been focusing on the pretreatment of BA to improve the potential problems of MSWI BA mentioned above, including treat options in the incineration plant such as size separation, magnetic separation, washing, weathering, carbonation, as well as some further treatment like physical/chemical treatment and thermal treatment. Specific problem and corresponding solutions are summarized in Table 2-2, and details of each treatment method will be explained in this chapter.

Table 2-2 Problems of BA and corresponding solutions according to literature study

BA	Problems in concrete	Solutions
High-porosity	Decrement of strength	Physical treatment (grinding)
Harmful salts	Leaching	Washing (in the incineration plant)
Heavy metals	Leaching	Weathering and accelerated carbonation (in the incineration plant)
Metallic aluminum	Air bubble and expansion	Physical treatment (grinding and sieving) Chemical treatment (dissolving in alkaline solutions)
Organic impurities	Non-reactive phases inhibiting hydration reaction	Thermal treatment
Quartz etc.	Low reactivity phases	Thermal treatment

The current techniques for in-plant ash treatment are illustrated in Fig. 2-7, during which the washing and separation are performed. Both ferrous and non-ferrous metals are recycled, and some big particles and unburned organic matters are sent back to the incinerators again. The treated granulates could be utilized in pavement construction as well.

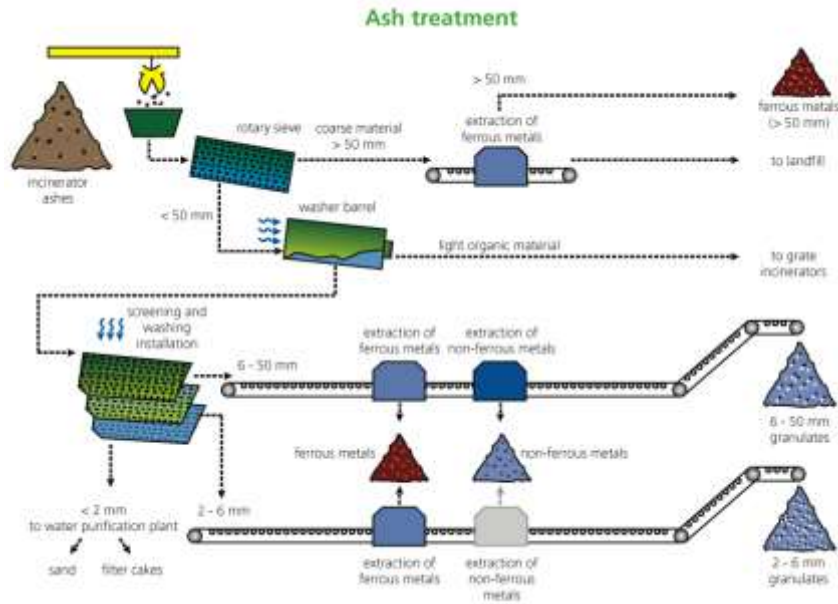


Fig. 2-7 In-plant ash treatment process (INDAVER⁴)

2.4.1. Washing

Washing (with water or acid) [23, 37, 75] is an effective way to remove chloride content and soluble salts in BA. *Chimenos* et al. found out that the water washing process could effectively remove the water-soluble fraction and most of the fine powders stuck on the surface of BA particles (account for a large amount of hazardous heavy metals) [9]. *Pan* et al. removed chloride content in BA by 82% and 90% with water and a combination of water and acetic acid washing separately [37]. *Ito* et al. proposed an effective way to remove insoluble chlorides in BA by washing with sulfuric acid solutions [75].

However, special attention is required to the waste liquid due to the high hazard content, and further treatment is required as well before draining or reusing.

2.4.2. Weathering and accelerated carbonation

Weathering is an in-situ (within the incineration plant) treatment of BA through the contact with earth atmosphere, water and biological organisms, which is considered as an effective way to improve the leaching properties by changing the mineralogical characteristics of BA [22, 23, 76]. Meanwhile, as known as an atmospheric or through aerobic biodegradation process of organic matters during weathering, carbonation is an effective way to develop stable phases.

In Europe countries, the weathering of BA is performed on BA for 1-3 months before final disposal or further utilization due to the low investment and operating costs [77]. The weathering process involves the atmospheric CO₂ dissolution-induced pH drop accompanied with calcite precipitation until the material is in equilibrium with CO₂, during which the unstable heavy metals (Cd, Cr, Pb, Zn) can be trapped in the newly generated minerals [43]. *Saffarzadeh* et al. reported that the carbonation and

⁴ Indaver, Doel Haven 1940, Molenweg 9130, DOEL, BELGIUM

precipitation could effectively mitigate the leaching of heavy metals (Pb, Sb and Zn) at the early days of weathering [11]. *Arichx* et al. found that the natural weather and accelerated carbonation resulted in a significant decrease of Cu leaching and DOC [69]. *Meima* et al. also discovered that carbonation to pH near 8.3 would reduce the leaching of Mo and Cu by 3% and 50% of BA itself separately [76].

Another interesting possibility proposed by other researchers is that the industrial CO₂ emissions could be controlled by the storage capacity of BA (CO₂ are consumed by BA during carbonation), which would be promising in both reducing greenhouse effect and improving BA properties [78].

2.4.3. Physical treatment

2.4.3.1. Grinding and sieving

Grinding and sieving treatment are the most commonly used methods of BA treatment. Grinding process can be used to stabilize the heavy metals in MSWI BA by decreasing particle size and bring about actions of fragmentation or agglomeration [79] as well as increase the reactivity of BA as well by increasing the specific surface area (50 times over that of OPC) [31]. On the other hand, several studies have been focused on the elimination of metallic aluminum content in BA, either by physical or chemical treatment. *Tang* et al. proposed a physical technique for the removal of metallic aluminum by the combination of slow milling and sieving [31]. *Bertolini* et al. discovered that the metallic aluminum induced hydrogen gas emission was exhausted within the slurry before adding to cement during wet grinding [39].

2.4.3.2. Thermal treatment

According to the existing studies, thermal treatment (either by quenching or heating) is widely used in industry to improve the pozzolanic reactivity of clay minerals by generating reactive phases in high temperature [80]. This method has been performed by many researchers to activate the BA. Thermal treatment has been proven to be efficient to reduce the leaching of heavy metals by reducing the content of organics which have been linked to higher leaching elements [81-83]. *Qiao* et al. also reported that thermal treatment at 800 Celsius degrees of milled BA would contribute to the decomposition of calcite as well as the formation of new active phases, and subsequently increasing the reactivity of BA [84]. *Arichx* et al. performed thermal treatment on BA in the range of 100 – 500°C for different duration, and proved that BA treated with 400°C and 30min already met the leaching requirement (according to *EN 12457-2*) [83]. *Hyks* et al. performed thermal treatment at an even higher range of 930–1080°C and observed the changes in surface and mineralogical properties [82]. *Chou* et al. also mentioned that the leaching of Pb, Cu and Cd were decreased after thermal treatment [81]. *Yang* et al. also found out that thermal treatment is more effective in removing soluble chloride than alkali salts [85]. Moreover, thermal treatment on fine particles also further reduces the LOI content by removing the organic matters in BA [31].

2.4.4. Chemical treatment

As mentioned in the previous chapter, metallic aluminum is a big issue in BA resulting in hydrogen-induced expansion and swelling in BA concrete. It is important to determine the metallic aluminum content in as-received BA. A widely used method to determine the metallic aluminum content in previous studies is the dissolving method [45, 86, 87] proposed by Aubert et al. by immersing BA in alkaline solution, and the mass of metallic aluminum could be derived by measuring the amount of hydrogen gas generated during the dissolving reaction. The idea of setup designing is illustrated in Fig. 2-8.

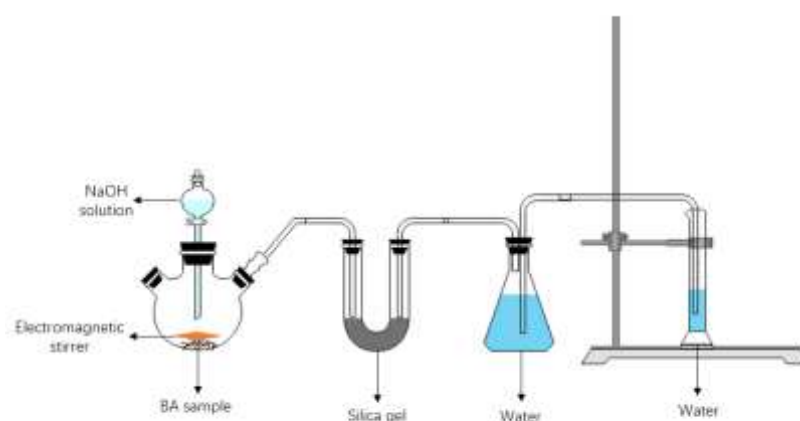


Fig. 2-8 Design of setup to determine metallic aluminum content in BA

Chemical treatment is regarded as another effective way to remove metallic aluminum by washing or immersing BA particles in alkaline solutions. However, other reactive amorphous phases could be attacked or dissolved by alkaline solutions as well during the chemical treatment process. A treatment method of using sodium hydroxide solution to remove the metallic aluminum was proposed by *Pera et al.*, which proved the possibility that up to 50% replacement of gravel in concrete without affecting the durability (the maximum shrinkage under drying-wetting cycles is under control value) [17]. *Penilla et al.* also successfully removed the metallic aluminum content by immersing BA in sodium hydroxide solution for 24 hours [88]. *Aubert et al.* proposed another chemical treatment method with sodium carbonate solution, and the addition of Na_2CO_3 could not only provide a high pH environment to remove the metallic aluminum content but also creating with Na_2SO_4 to form calcite which is regarded as an inert cement-based product [89].

In conclusion, the result of literature study confirms that MSWI BA could be used as substitute materials in the concrete system, but the performance is limited due to its poor chemical and physical properties mentioned in the literature review. Several treatment methods have been investigated and proposed to solve the problems occurred. However, in most studies the investigation was performed only against one specific weakness so that a proper and comprehensive treatment method is still scarce. On the

other hand, previous studies mainly focused on the mechanical properties of concrete with BA substitution that how does it contribute to the hydration process comparing with pure cement is still unclear. In general, according to previous studies, BA could be used as a substitute material in concrete with proper treatment. In this research, the effect of different treatment methods on BA will be studied to find out a proper route of pretreatment, and the contribution of BA as cement substitution to the hydration process will be investigated as well.

3. Materials and methods

3.1. Materials

3.1.1. Cementitious materials

Four kinds of cementitious materials were used throughout this study, namely ordinary Portland cement (OPC), MSWI BA, blast furnace slag (BFS) and micronized sand (M300). OPC is the fundamental cementitious material which was replaced by other substitute materials. Meanwhile, BFS and M300 were selected as references to evaluate the performance of MSWI BA.

3.1.1.1. Ordinary Portland cement

CEM I 42.5N cement was selected in this study as fundamental cementitious material provided by *ENCI B.V.*⁵ the Netherlands.

3.1.1.2. MSWI BA

The MSWI BA (0 – 2 mm) investigated in this study was kindly provided by Heros, a recycling production company located in *Sluiskil*, the Netherlands.

Different types of pretreatments were performed on raw BA to improve the performance of BA as a substitute material in the concrete system. According to the method and order of pretreatments, the following four kinds of BAs were prepared in this study:

- **MBA (milled bottom ash):** Physical treatment was performed on raw BA by grinding with a planetary ball miller at 250rpm for 30min. After the grinding process, the crushed fine powder was separated by a 63 μm sieve and selected as cement substitute material, and bigger particles with high metallic aluminum content were sieved out. Particle size distribution was checked by laser.
- **CBA (chemically treated bottom ash):** Raw BA was chemically treated by immersing a certain amount of BA in 0.1M NaOH solution for 15 days at a solid to liquid ratio of 0.2 to get rid of the metallic aluminum content. The treated BA was then washed with running water and oven-dried until a constant mass. Additional grinding was performed on dried BA (250rpm 20min) to get a similar particle size distribution as MBA (checked by laser).
- **MTBA (milled and thermally treated bottom ash):** After removing the metallic aluminum content, MBA was activated by further thermally treated by heating up to 1000°C in a ventilated furnace for 2h, and then cooling down to room temperature. Severe agglomeration was observed after the heating process, and grinding (200rpm, 10min) was performed again to adjust the particle size distribution (checked by laser).
- **QMBA (quenched and milled bottom ash):** As-received BA was heated up to 1000°C for 2h. The melted BA was immediately poured into an iron bucket and quenched by water. Then the BA was collected by vacuum filtration and oven-dried at 105°C until a constant mass. Grinding was performed as well

⁵ Lage Kanaaldijk 115, 6212 NA Maastricht

(250rpm 30min) to remove metallic aluminum content and get a similar particle size as MBA (checked by laser).

The pretreatment route is illustrated in Fig. 3-1.

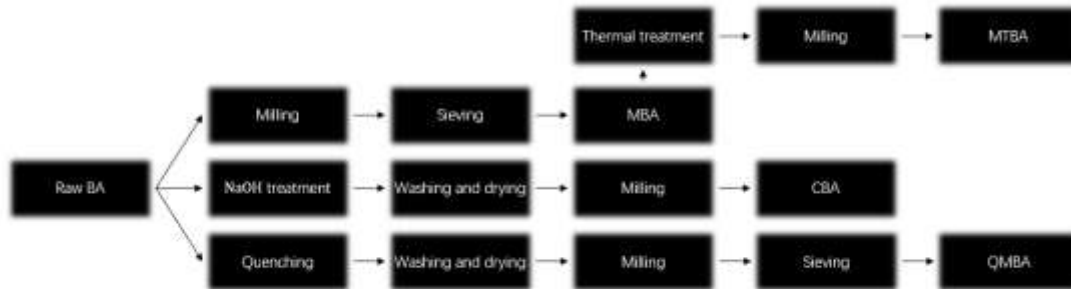


Fig. 3-1 Pretreatment route

3.1.1.3. Reference substitute materials

Two kinds of reference cement substitute materials were selected in this study due to the similar particle size distribution as *CEM I 42.5N* cement as reference, namely blast furnace slag (BFS) and micronized sand (M300).

- BFS is known as a by-product of iron and steel industry, which is obtained by quenching molten iron slag from a blast furnace in water or steam. A glassy and granular product is formed and later dried and ground into fine powder. Currently, BFS has been widely used as a cement substitute material in Europe and the US, especially in making durable concrete structures (blending with OPC). A higher proportion of strength-enhancing hydration product has been observed in concrete containing BFS, namely calcium silicate hydrates (CSH) than OPC concrete, which result in even higher ultimate strength than OPC concrete [50]. On the other hand, BFS concrete also exhibits a slower hydration process than OPC concrete, which may result in lower early-stage strength [90].
- Micronized sand M300 is produced by grinding quartz sand which contains high SiO_2 content. Generally, it is considered as a chemically inert cementitious material which could not react with cement or water and contribute rarely to the hydration process [91].

Known that BFS is a substitute material with high reactivity while M300 almost has no reactivity, the reactivity of treated BA could be evaluated through the compressive strength of samples by blending the same amount of BFS, M300 and treated BA into the mixture.

3.1.2. Chemical solutions

In this study the following chemical solutions were prepared, in which Na_2CO_3 and NaOH solutions were used to perform chemical treatment, 2-propanol solution was used to stop the hydration process, ethanol solution was used to determine the particle size distribution and superplasticizer was used to reduce the water demand in the concrete mix.

- Na_2CO_3 solutions: 0.1, 0.5, 1 and 5M Na_2CO_3 solutions were prepared by dissolving certain amount of sodium carbonate powder in distilled water. Na_2CO_3 solutions were later used in removing metallic aluminum content.
- NaOH solutions: 0.1, 1 and 3M NaOH solutions were prepared by dissolving certain amount of sodium hydroxide powder in distilled water. NaOH solutions were later used in removing metallic aluminum content. 1M NaOH solution was used in the determination of metallic aluminum content in the dissolving test.
- 2-propanol solution: 99.8% 2-propanol solution provided by *Honeywell*⁶ was used to stop the hydration reaction so that the hydration products at the end of 28 day could be checked.
- Ethanol solution: 96% ethanol solution provided by *Brenntag Nederland B.V.*⁷ was used for particle size distribution measurement and cleaning.
- Superplasticizer: *SikaPlast Techno 80* provided by *SIKA FRANCE SAS*⁸.
- Distilled water: distilled water was used for making binder, preparing chemical solution and cleaning.

3.2. Experimental methods

In this study, physical and chemical properties of BA were characterized both before and after pretreatment. Consequently, the performance of treated BA was investigated on paste level by blending it with OPC and casting into cement paste. The hydration process was studied by measuring the heat evolution and checking hydration products. Different kinds of tests performed on different stages of this study are summarized in Table 3-1, Table 3-2 and Table 3-3.

Table 3-1 Characterization of raw and treated BA

Properties	Methods	
Particle size distribution	Raw BA	Dry sieving test
	Fine powder	Laser diffraction
Morphology	Environmental scanning electron microscopy (ESEM)	
Crystalline phases	X-Ray diffraction (XRD)	
Chemical composition	X-Ray fluorescence (XRF)	
	Loss on ignition (LOI)	
	Dissolution with sodium hydroxide solution	

Table 3-2 Pretreatment

Remove metallic aluminum	Chemical	Na_2CO_3 solution
		NaOH solution
	Physical	Grinding and sieving

⁶ Wunstorfer Strasse 40, D-30926 Seelze, Germany

⁷ Lindtsedijk 2, 3336 LE Zwijndrecht, the Netherlands

⁸ 84 Rue Edouard Vaillant, 93350 Le Bourget, Frankrijk

Activation	Thermal treatment
Table 3-3 Hydration process	
Compressive strength	According to <i>EN 196-1</i>
Heat evolution	Isothermal calorimetry
Hydration product	X-Ray diffraction
	Thermalgravimetric analysis (TGA)

3.2.1. Investigation on substitution materials

In this part, experiments were performed to find out the physical and chemical properties of BA (both before and after pretreatment). In addition, physical and chemical pretreatment were performed to remove the metallic aluminum content, and thermal treatment was performed to get BA activated as well as remove the unburned organic matters.

3.2.1.1. Particle size distribution

In this study, both particles size distribution (PSD) of coarse as-received BA particles and treated BA fine powders were checked by different methods. In the beginning, coarse BA particles were divided into different groups according to particle size and properties of each group was checked separately. If a severe difference is detected, the fraction with higher mass percentage and similar property to cement will be selected for further investigation. In addition, it is also important to check and control the PSD of each kind of treated BA powder in the same level so that the effect of packing in cement paste could be controlled.

The as-received BA used in this study after weighing was first dried in a ventilated oven at 105°C until a constant mass to determine the moisture content according to *NEN-EN 15169*, and then divided into 5 fractions according to the particle size distribution by a dry sieving test (as shown in Fig. 3-2) according to *EN 1097-6*, namely 1.6-2mm, 0.5-1.6mm, 0.25-0.5mm, 0.125-0.25mm and < 0.125mm to check the properties of each fraction.

BA in each fraction was homogenized by grinding in a planetary ball miller to get fine powders smaller than 0.125mm, and properties of each fraction were later checked separately.



Fig. 3-2 Dry sieving test

The PSD of the treated fine BA powders was checked by Eye tech laser diffraction machine (as shown in Fig. 3-3). A cleaning process was conducted with deionized water and ethanol rinsing each time before the particle size measurement until meeting the cleanness requirement. PSD was measured by dissolving 0.5 gram of sample powder into 800 ml ethanol (rather than water since hydration takes place when mixing cementitious material with water) and pre-mixed by a stirrer for 5 minutes. Meanwhile, an ultrasonic vibration was turned on as well to prevent the agglomeration of fine particles. Eventually, PSD of fine BA powders were measured by laser and a PSD report was made by software.



Fig. 3-3 Eye Tech laser diffraction machine

3.2.1.2. Morphology

As mentioned in the literature review the high-porosity morphology of BA particles will result in strength decrement when used as substitute materials in concrete. Therefore, it is important to check the morphology of BA before and after pretreatment to see whether the high-porosity morphology is improved.

Morphology and microstructure of BA particles were investigated by environmental scanning electron microscopy (ESEM). The X-Ray fluorescence of the surface elements of a sample could be detected when excited by a highly focused energetic beam of electron. ESEM is a system in which electron micrographs of a sample could be collected with an electron beam in a high chamber pressure atmosphere of water vapor. In this study, ESEM was conducted using a Philips XL30 ESEM electron microscope as shown in Fig. 3-4.



Fig. 3-4 Philips XL30 ESEM electron microscope

3.2.1.3. Crystalline phases

In the characterization of substitution materials, crystalline phases of as-received BA, treated BA and OPC were compared to each other to check the effect of pretreatment and detect the difference between BA and OPC.

As known as a nondestructive method for crystalline phases determination in solid powder, X-Ray diffraction (XRD) analysis was performed here on BA to determine the crystalline phases. Due to the atomic and molecular structure of a crystal, a beam of incident X-Ray will diffract in to specific directions. The electron density could be derived by measuring the angles and intensities of these diffracted beams, which provide information of atom position in the crystal, as well as the chemical bond and crystallographic disorder etc. XRD was carried out with Philips PW 1830 powder X-Ray diffractometer as shown in Fig. 3-5(Co $K\alpha$ 1.789Å radiation, Divergence slit V12, scatter screen height 5 mm, 40 kV 40 mA, Coupled θ - 2θ scan 5° - 70° , step size 0.010° 2θ , counting time per step 2s).



Fig. 3-5 Philips PW 1830 powder X-Ray diffractometer

3.2.1.4. Chemical composition

In the characterization of raw materials, chemical composition of as-received BA, treated BA and OPC were checked, and the differences in chemical composition could help detect the difference between as-received BA and OPC and show the effect of pretreatment. X-Ray fluorescence (XRF) analysis was performed to determine the elemental composition, while the organic content and metallic aluminum content were detected by LOI and dissolving tests separately.

3.2.1.4.1. XRF

XRF is a nondestructive analytical technique to determine the elemental composition of materials. By measuring the fluorescent (or secondary) X-Ray emitted from the material when excited by a X-Ray source (each element produces a characteristic fluorescent X-Ray as a “fingerprint”), the elemental compositions could be determined.

3.2.1.4.2. LOI

LOI of each fraction was performed according to *EN 196-2*. Raw BA was pre-dried in a ventilated oven at 105°C until a constant mass. BA was transferred into a pre-ignited crucible and then ignited in a temperature-controlled furnace for 1 hour. Ignition temperature was determined to be 550°C and 950°C separately allowing different kinds of volatile substances to escape until a constant mass. Eventually, LOI was presented by a loss of total sample mass.

3.2.1.4.3. Metallic aluminum content

An optimized setup was built up according to Aubert’s research [45] to determine the metallic aluminum content by dissolving test in as-received BA, detailed explanation of calculation will be given in chapter 4.

3.2.1.5. Removal of metallic aluminum

Both chemical and physical method were performed to remove the metallic aluminum content in BA. The remaining metallic aluminum contents were checked again after

treatments.

3.2.1.5.1. Chemical treatment

In the chemical treatment, as shown in Fig. 3-6, BA was immersed in alkaline solutions (Na_2CO_3 and NaOH) with different solid to liquid ratio in sealed buckets for a fixed time. Details of treatment design with Na_2CO_3 and NaOH solutions are given in Table 3-4 and Table 3-5 separately. Treated BA was subsequently washed with running water and oven dried at 105°C until a constant mass. Eventually, the metallic content was determined again.

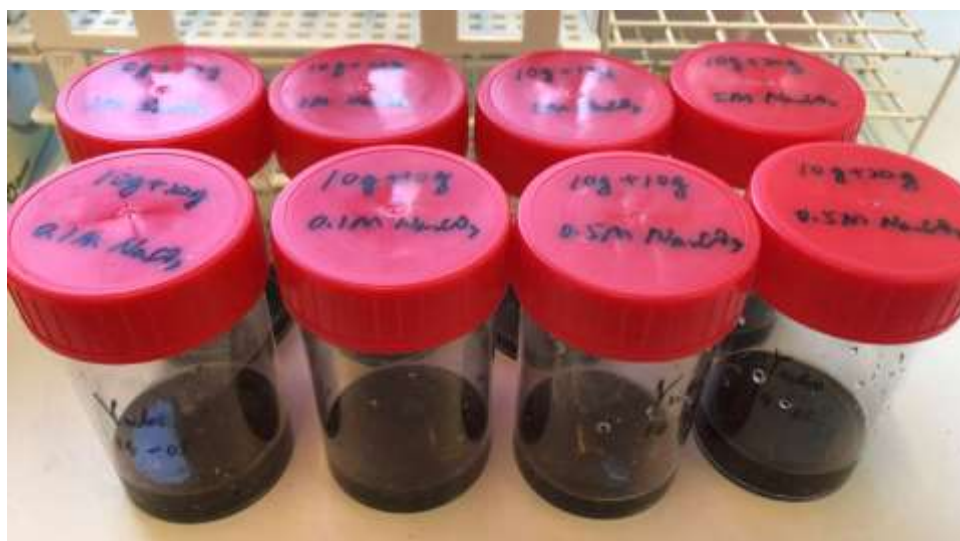


Fig. 3-6 Chemical treatment with Na_2CO_3 solution

Table 3-4 Design of chemical treatment with Na_2CO_3 solution

Treatment	Solid/liquid	Initial pH value
10g BA+10g 0.1M Na_2CO_3	1.0	11.5
10g BA+20g 0.1M Na_2CO_3	0.5	11.5
10g BA+10g 0.5M Na_2CO_3	1.0	12.0
10g BA+20g 0.5M Na_2CO_3	0.5	12.0
10g BA+10g 1.0M Na_2CO_3	1.0	12.5
10g BA+20g 1.0M Na_2CO_3	0.5	12.5
10g BA+10g 5.0M Na_2CO_3	1.0	13.5
10g BA+20g 5.0M Na_2CO_3	0.5	13.5

Table 3-5 Design of chemical treatment with NaOH solution (by Loic⁹)

Treatment	Duration (days)	Solid/liquid	Initial pH value
0.1M NaOH	5	0.2	13.5
0.1M NaOH	5	0.1	13.5
0.1M NaOH	15	0.2	13.5
0.1M NaOH	15	0.1	13.5
1.0M NaOH	5	0.2	14.0
1.0M NaOH	5	0.1	14.0
1.0M NaOH	15	0.2	14.0
1.0M NaOH	15	0.1	14.0
3.0M NaOH	5	0.2	14.0
3.0M NaOH	5	0.1	14.0
3.0M NaOH	15	0.2	14.0
3.0M NaOH	15	0.1	14.0

3.2.1.5.2. Physical treatment

The physical treatment is a combination of grinding and sieving to get rid of metallic aluminum. To be specific, the metallic aluminum content in BA particles would be ground into metal plates in low speed and short-term grinding so that could be sieved out while the fine powder of remaining BA could be collected.

BA was ground in Retsch PM100 planetary ball miller at different speed for different time-period, and then the metallic aluminum particles which were ground into metal plates were sieved out by using a 63 μm sieve.



Fig. 3-7 Retsch PM100 planetary ball miller

⁹ Bachelor student, Microlab, Civil engineering and geosciences, TUDelft

3.2.1.5.3. Mortar strength test

The mortar compressive strength test was performed to study the effect of removing metallic aluminum content. Treated BA was blended with *CEM I 42.5N* cement with different replacement level (10% and 30%). Mortar was prepared according to *EN 196-1*, and samples were demolded after 24h and cured in a curing room (room temperature and 95% RH). The compressive strength of 1d, 7d and 28d were derived as well. Moreover, two groups of parallel tests were performed as well by blending the same amount of blast furnace slag (BFS) and micronized sand (M300) in cement. BFS and M300 were selected as the reference here due to the similar particle size distribution as *CEM I 42.5N*[98]. Details of the mixture design are given in Table 3-6.

Table 3-6 Mixture design of mortar cubes (40*40*40 mm)

(grams)	Cement				Sand (mm)					water
	CEM I 42.5N	MBA	BFS	M300	0.08-0.16	0.16-0.5	0.5-1	1-1.6	1.6-2	
CEM	337.5	0	0	0	101.25	202.5	354.375	253.125	101.25	168.75
10% MBA	303.75	33.75	0	0	101.25	202.5	354.375	253.125	101.25	168.75
30% MBA	236.25	101.25	0	0	101.25	202.5	354.375	253.125	101.25	168.75
10% BFS	303.75	0	33.75	0	101.25	202.5	354.375	253.125	101.25	168.75
30% BFS	236.25	0	101.25	0	101.25	202.5	354.375	253.125	101.25	168.75
10% M300	303.75	0	0	33.75	101.25	202.5	354.375	253.125	101.25	168.75
30% M300	236.25	0	0	101.25	101.25	202.5	354.375	253.125	101.25	168.75

3.2.1.6. Activation of treated BA

According to the literature review, thermal treatment could not only get BA activated by generating more reactive amorphous phases but also effectively remove the unburned organics in BA. Two kinds of thermal treatments were carried out either before or after removing the metallic aluminum content to investigate the effect of treatment order, and the treated BA samples were labelled as MTBA and QMBA separately as mentioned in the previous chapter. The one day paste compressive strength test was performed to make a choice between two thermal treatment methods.

3.2.2. Investigation on cement paste level

In this part, experiments were carried out to investigate the hydration process of pastes with different substitution materials. The compressive strength of hardened paste samples at different curing ages was examined to show the degree of hydration in different mixtures directly. Furthermore, hydration heat and amount of hydration products were measured to reveal the details of the hydration process.

3.2.2.1. Compressive strength of paste

The compressive strength of hardened paste samples at different curing ages was examined to show the degree of hydration in different mixtures directly. Strength test

was performed according to *EN 196-1* to reveal the influence of blending BA with different pretreatment methods into cement powders. Details of mixture design is given in

Table 3-7. Blended pastes were poured into 20*20*20 mm cubic molds. Samples were demolded after 24 hours and transferred into the curing room (room temperature and 95% RH). 1-day, 7-day, 14-day and 28-day compressive strength was tested to investigate the strength development of different mixtures.

Table 3-7 Mixture design for paste cubes

(grams)	Cementitious materials				Water
	CEM I 42.5N	MBA	MTBA	M300	
Ref. Cement	200				100
10% MBA	180	20			100
10% MTBA	180		20		100
20% MTBA	160		40		100
30% MTBA	140		60		100
10% M300	180			20	100
20% M300	160			40	100
30% M300	140			60	100

3.2.2.2. Hydration heat

As known as the dominant reaction that bring about the hardening of cement paste, the hydration process is accompanied by the liberation of heat, and this heat of hydration is an important factor in concrete. The heat of hydration is the product of the exothermic chemical reaction between cement and water and regarded as an important indicator of the hydration process.

The hydration heat development was detected by using an isothermal calorimeter (TAM-Air-314 thermometric isothermal conduction calorimeter as shown in Fig. 3-8). A calibration was done at 20°C before each measurement. Each group of tests consists of two same mixtures accompanied with two references. 5 grams of fresh mixture was poured into a glass container and transferred into the calorimeter in A-channels, while the reference sand was placed in the same kind of container and transferred into the calorimeter in B-channels. History of temperature development was detected and recorded in computer.



Fig. 3-8 TAM-Air-314 thermometric isothermal conduction calorimeter with 8 channels

Details of mixture design and mass of reference sand is given in Table 3-8, and the mass of reference sand was determined according to the following equation:

$$m_{Ref,sand} = \frac{m_{cem}C_{p,cem} + m_{water}C_{p,water} + m_{BA}C_{p,BA}}{C_{p,sand}} \quad (1)$$

where $m_{Ref,sand}$, m_{cem} , m_{water} and m_{BA} are the mass of each substance in gram, while $C_{p,cem}$, $C_{p,water}$, $C_{p,BA}$ and $C_{p,sand}$ are the specific heat of cement, water, BA and sand respectively (specific heat values are given in). An estimation was made here that the specific heat of BA is unknown and estimated to be equal to that of sand.

Table 3-8 Mixture design and mass of reference sand

(grams)	Cementitious materials				Water	sand
	CEM I 42.5N	MBA	MTBA	M300		
CEM I 42.5N	20				10	12.77
10% MBA	18	2			10	12.75
10% MTBA	18		2		10	12.75
20% MTBA	16		4		10	12.72
30% MTBA	14		6		10	12.70
10% M300	18			2	10	12.75
20% M300	16			4	10	12.72
30% M300	14			6	10	12.70

Table 3-9 Specific heat of each substance

Specific heat (J/(g k))	
Cement	0.8
Water	4.18
Sand	0.75
BA	0.75

3.2.2.3. Hydration products

The hydration products of different paste mixtures were studied at the age of 28 days. At the end of 28 days the hydration process in each paste mixture was stopped and hydration products were studied by XRD and TGA analysis.

3.2.2.3.1. XRD

Crystalline phases of hardened paste samples were checked at the end of 28 day to reveal the hydration products with different substitutions in cement paste.

3.2.2.3.2. TGA

Thermalgravimetric analysis was conducted to detect the mass loss of sample during the heating process, which would help to evaluate the amount of different kinds of hydration products as well as provide information about physical and chemical phenomena as well as solid-gas reactions. According to the existing studies, the main product of hydration process are portlandite (CH) and calcium silicate hydrate (C – S – H), and the hydrated cement paste is mainly consisting of four kinds of compounds, namely dicalcium silicate (C_2S), tricalcium silicate (C_3S), tricalcium aluminate (C_3A) and tetracalcium aluminoferrite (C_4AF) [92]. The decomposition reaction of cement paste with the increase of temperature could be described by the following 5 phases summarized in Table 3-10.

Table 3-10 Decomposition reactions of cement paste with the increase of temperature

Temperature interval	Decomposition reactions
30 – 120°C	Evaporation of free water and part of the bound water[93]
120 – 180°C	Decomposition of gypsum, ettringite and part of carboaluminate hydrates[93-95]
180 – 300°C	Loss of water from the decomposition of C – S – H and carboaluminate hydrates[93, 96]
400 – 550°C	Dihydroxylation of portlandite[96, 97]
700 – 900°C	Decomposition of calcium carbonate[96, 97]

The powder of pastes (about 30 mg) at a curing age of 28-day were put in an aluminum oxide crucible and heated from 40°C to 1300°C in the TG-449-F3-Jupiter instrument (as shown in Fig. 3-9) for TGA. The heating process was set with a rate of 10°C/min under the protection of argon atmosphere (flow rate 50μL/min).



Fig. 3-9 TG-449-F3-Jupiter instrument for TGA

3.2.3. Investigation on concrete level

According to the result of the investigation on paste level, treated BA with the best performance and a reasonable replacement ratio was studied on the concrete level. Two series of concrete mixtures were prepared with the water to cement ratio of 0.5. 10% of MTBA was blended in to the mixture substituting *CEM I 42.5N* as binder. Since the addition of dry aggregates would absorb part of the water in the binder, which results in the decrement in water to cement ratio, certain amount of extra water was added into the mixture to saturate the dry aggregates. The water absorption factor for each proportion selected here is according to Zhenming's¹⁰ research. Superplasticizer was added to ensure the workability. Details of the concrete mix design are summarized in Table 3-11.

¹⁰ PhD student, Microlab, Civil engineering and geosciences, TUDelft

Table 3-11 Proportions of concrete mixtures prepared

		Density (g/cm^3)	Concrete mix proportions (kg/m^3)	
			CEM I 42.5N	10% MTBA
Water		-	155	155
Cement	CEM I 42.5N	3.11	320	288
	MTBA	2.55	0	32
Water/cement			0.48	0.48
Fine aggregate	0-0.25 mm	2.64	242.7	242.7
	0.25-0.5 mm		202.25	202.25
	0.5-1 mm		202.25	202.25
	1-2 mm		80.9	80.9
	2-4 mm		80.9	80.9
	Sum		809	809
Coarse aggregate	4-8 mm	2.65	539	539
	8-16 mm		500	500
	Sum		1039	1039
Admixture	Superplasticizer		1.73	1.73
Extra water		-	10.67	10.67

3.2.3.1. Workability

A slump test was conducted to determine the workability of the fresh concrete mixture according to *NEN-EN 12350-2*. A truncated conical mold was prepared and filled with approximately six liters of fresh concrete mixtures. The introduction of fresh concrete was divided into three layers with respect to the height of the mold, and each layer was compacted with a steel rod for 25 strokes to ensure uniform filling of the mold. Excess concrete was removed by the rod. After about 30 seconds, the mold was lifted smoothly in vertical direction in 5 seconds so that the height of the slump was measured.

3.2.3.2. Compressive strength

Fresh concrete mixtures were collected after the slump test and casted into cubic samples. Cubes (100*100*100 mm in dimension) were casted in steel molds (as shown in Fig. 3-10) and compacted on a vibrating table.

The top surface was then sealed with a plastic foil. Subsequently, cubes were demolded after 24 hours and transferred into a curing room (room temperature and 95% RH). 1, 7, 14 and 28-day compressive strength were measured. Compressive tests were performed with MATEST compression machines (as shown in Fig. 3-11).



Fig. 3-10 Steel mold



Fig. 3-11 MATEST compression machine

3.3. Sample preparations

According to the experimental methods used in this study, different samples were prepared as the following.

3.3.1. Drying of as-received BA

A high moisture content was detected in as-received BA samples, which is highly variable with the increase of storage time. Drying process was performed to get rid of the effect of the humidity in samples, that as-received BA was pre-dried in a ventilated furnace at 105°C until a constant mass before further tests.

3.3.2. Fine powders preparation

The properties of BA sample is highly depended on the composition of each BA particle since the particle size of as-received BA is relatively large (0-2 mm). Therefore, BA

samples were ground into fine powder smaller than 125 μm by a planetary ball miller to achieve a homogeneous property, and then further tests (XRD, XRF and TGA) were performed. To conduct a XRD analysis, powder of sample should be compressed into an aluminum holder (as shown in Fig. 3-12) and surface finished by pressing with a glass sheet.



Fig. 3-12 XRD sample

3.3.3. Stopping hydration process

In this study the hydration products of different pastes were checked at the age of 28 days so that they could be compared to each other. After the 28-day compressive strength tests, samples were crushed into smaller pieces. The hydration reaction was then stopped by immersing the crushed pieces in 2-propanol solution for 24 hours. Consequently, the samples were dried by a vacuum chamber for another hour before other tests.

3.3.4. ESEM samples preparation

ESEM tests were performed to check the morphology of BA particles. The powder samples were prepared by spraying a homogenous layer of sample on the surface of a carbon sticker. The unattached particles were removed by blowing compressed air. The sticker was then fixed on a holder and transferred into the ESEM machine.

The crushed 28-day samples were immersed in 2-propanol solution for 24 hours, and then made into ESEM samples by epoxy impregnation, cutting, grinding and polishing [99]. The crushed paste pieces were collected in a cylindrical mold and evacuated at 30 mbar for 1 hour. Epoxy (made by blending base liquid with hardener) was poured into the mold from a cup outside the vacuum chamber through a tube until all samples were immersed. The impregnation process lasted for about ten minutes so that the air pores could be adequately filled with epoxy. Subsequently, the impregnated ESEM samples were cured at 40°C for 24 hours before further treatment. After demolding, the samples were split into proper pieces and the surface of samples was prepared by grinding (on a middle-speed lap wheel with p320, p500 and p1200 sand papers) and polishing (on a lap wheel with a mixture of ethanol together with 6, 3, 1 and 0.25 μm diamond paste).

4. Characterization of raw BA

Two batches of MSWI BA have been received from *Heros* in this study (BA1 and BA2), and the main difference is that a cleaning process has been performed on BA2 comparing with BA1. Several tests have been performed to determine the physical properties and chemical composition of MSWI BA. BA2 was selected as the raw material for further investigations.

4.1. Physical properties

4.1.1. Moisture content

As-received BA was firstly weighed and then dried in a ventilated oven at $105 \pm 5^\circ\text{C}$ until a constant mass. Moisture content is expressed as a loss in weight percentage after the drying process. Results are given in Table 4-1, and there's no big difference in moisture content between two batches of BA.

Table 4-1 Moisture content of BA1 and BA2

	Before drying (g)	After drying (g)	Moisture content (%)
BA1	75.3	58.8	21.91
	98.2	74.7	23.93
	111.4	85.6	23.16
	94.97	73.03	23.10
BA2	217.9	170.0	21.98
	223.4	176.2	21.13
	250.0	201.8	19.28
	230.43	182.67	20.73

4.1.2. Particle size distribution

A dry sieving test has been carried out to determine the particle size distribution of BA and washed BA. Results are given in and, separately.

In BA1, the mass of fraction 0.5-1.6 mm is the highest which contribute approximately 46% to the total mass, while the mass of fraction of 2-4 mm is the second highest and contribute about 21% to total mass. However, things are different BA2 that there are only 4% mass content left of fraction 2-4 mm, while the content in fractions 0.25-0.5 mm and 0.125-0.25 mm increase significantly which contribute 27% and 21% separately to the total mass. Meanwhile, the mass content of fraction 0.5-1.6 mm still remains the highest (37%).

It is evident that the particle size distribution has changed obviously after the washing process. The amount of big particles (>4mm, 2-4mm and 1.6-2mm) drops significantly while the amount of small particles (0.25-0.5mm, 0.125-0.25mm and <0.125mm) increased, which means big particles were divided into smaller particles during the washing process. The content of fraction 0.5-1.6mm remains the highest after washing. Special attention is paid to fraction 0.5-1.6mm, 0.25-0.5mm and 0.125-0.25mm since the contents are relatively high in washed BA.

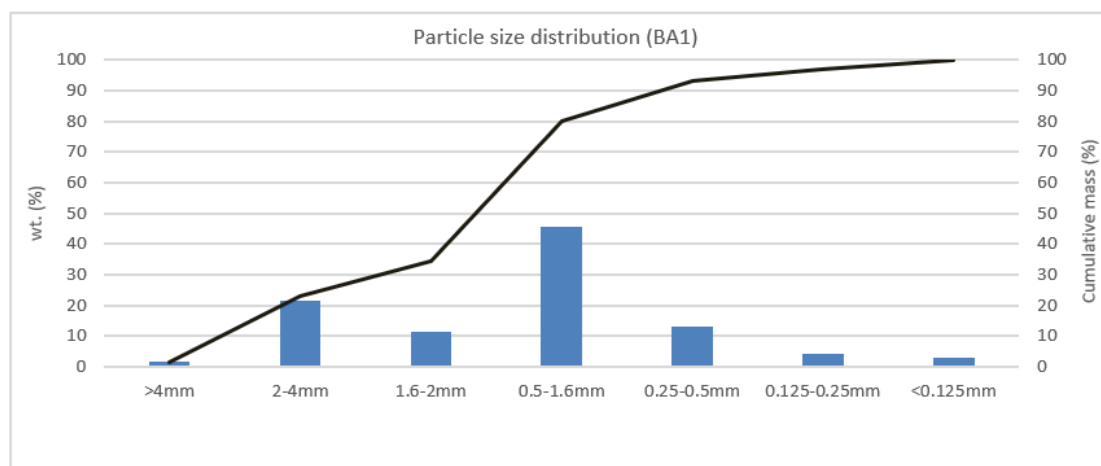


Fig. 4-1 Particle size distribution (BA1)

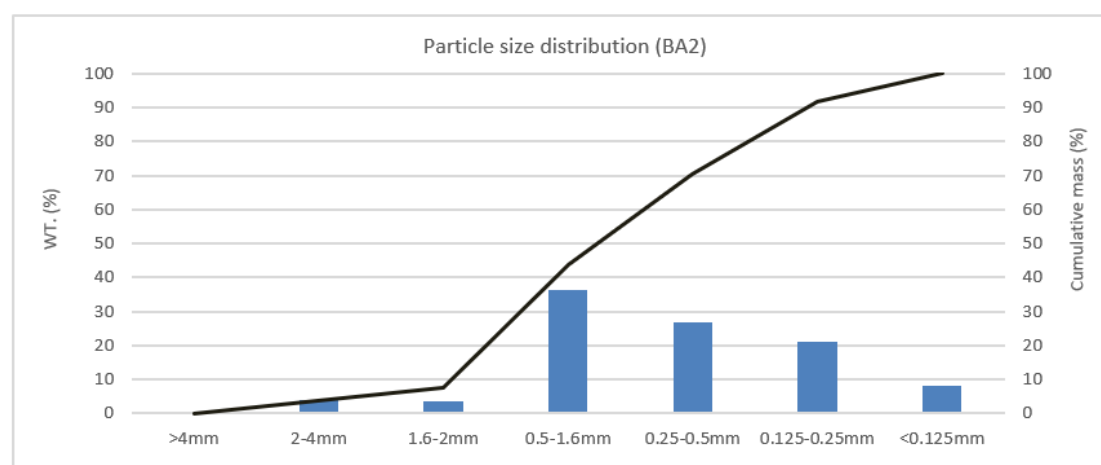


Fig. 4-2 Particle size distribution (BA2)

4.1.3. Morphology

The microstructure and surface appearance of BA were investigated by the environmental scanning electron microscopy (ESEM) method. A slightly rough texture with high porosity structure and microcracks have been observed on the surface of BA particles as shown in Fig. 4-3 and Fig. 4-4, and some of the pores even penetrate through the whole BA particle (dark-colored holes) or connected to each other (overlap of holes in different diameters), which will result in the decrease in strength of BA particles. Moreover, some dust-like finer powders are observed on the surface of the coarse BA particles, which are suspected to be heavy metal or hazardous salts according to the literature survey.

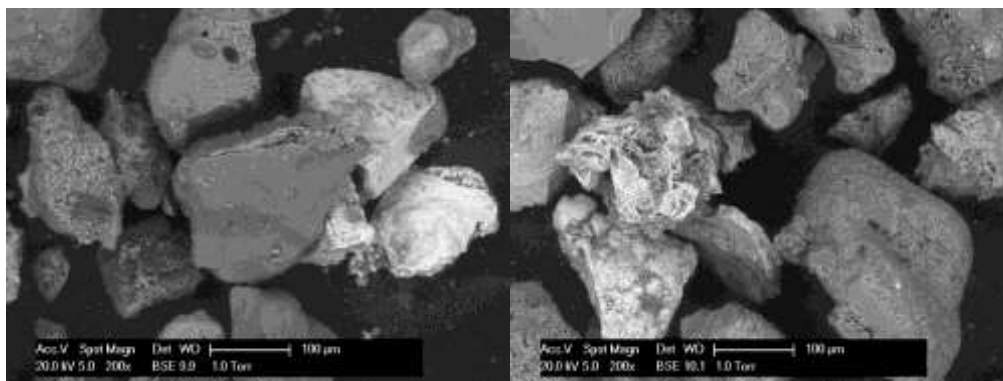


Fig. 4-3 ESEM 200x of BA particles

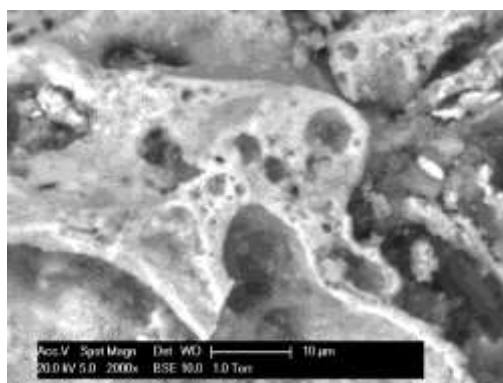


Fig. 4-4 ESEM 2000x of BA particles

4.2. Crystalline phases

The X-Ray diffraction analysis was performed on two batches of BA at a detection angle between 5° and 75° , and results are given in Fig. 4-5.

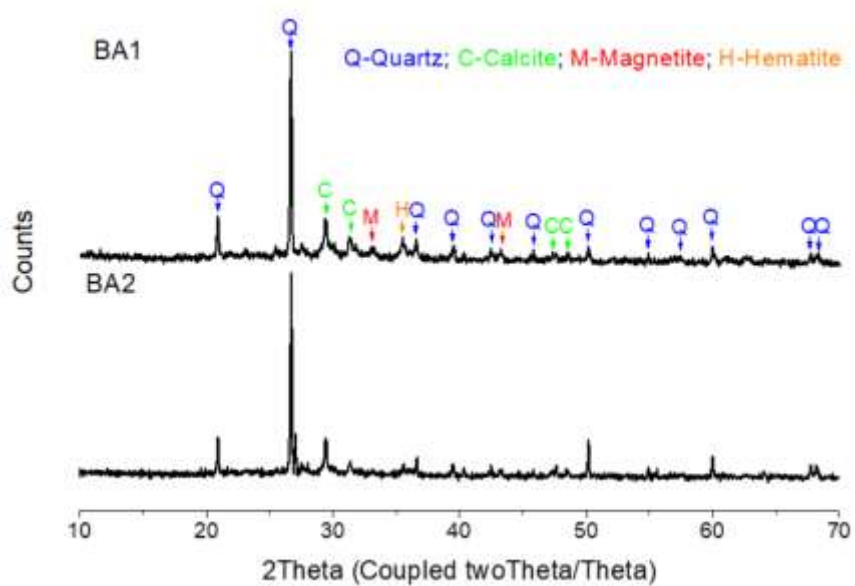


Fig. 4-5 XRD diffractograms of BA2 in different fractions

No obvious difference was observed between BA1 and BA2, and the main mineral components identified are quartz (SiO_2), calcite (CaCO_3), hematite (Fe_2O_3) and magnetite (Fe_3O_4). A main peak of quartz is detected at around 26.6° in all samples, which is in agreement with other studies [31, 84]. Meanwhile, it is observed that all peaks in BA2 exhibited lower intensity and became more narrow comparing with BA1, which indicates that part of the existing crystalline phases were attacked during the washing process while no new phases were generated.

Furthermore, XRD of 0.5-1.6 mm, 0.25-0.5 mm and 0.125-0.25 mm in BA2 were checked due to the higher mass content according to particle size distribution (as shown in Fig. 4-6). Comparing the result of each group, more peaks were detected as the particle size became smaller. Meanwhile, both the intensity and width of subpeaks increased with the decrease of particle size. Moreover, some amorphous phases were detected between 20° and 40° next to the main quartz peak. This is attributed to that smaller particle size fractions contains higher content of dust like impurities (hazardous heavy metals, soluble salts and organic matters) which were originally absorbed on the surface of BA particles [9]. Therefore, a comprehensive treatment is required on BA before it could be used as a substitute material in cement.

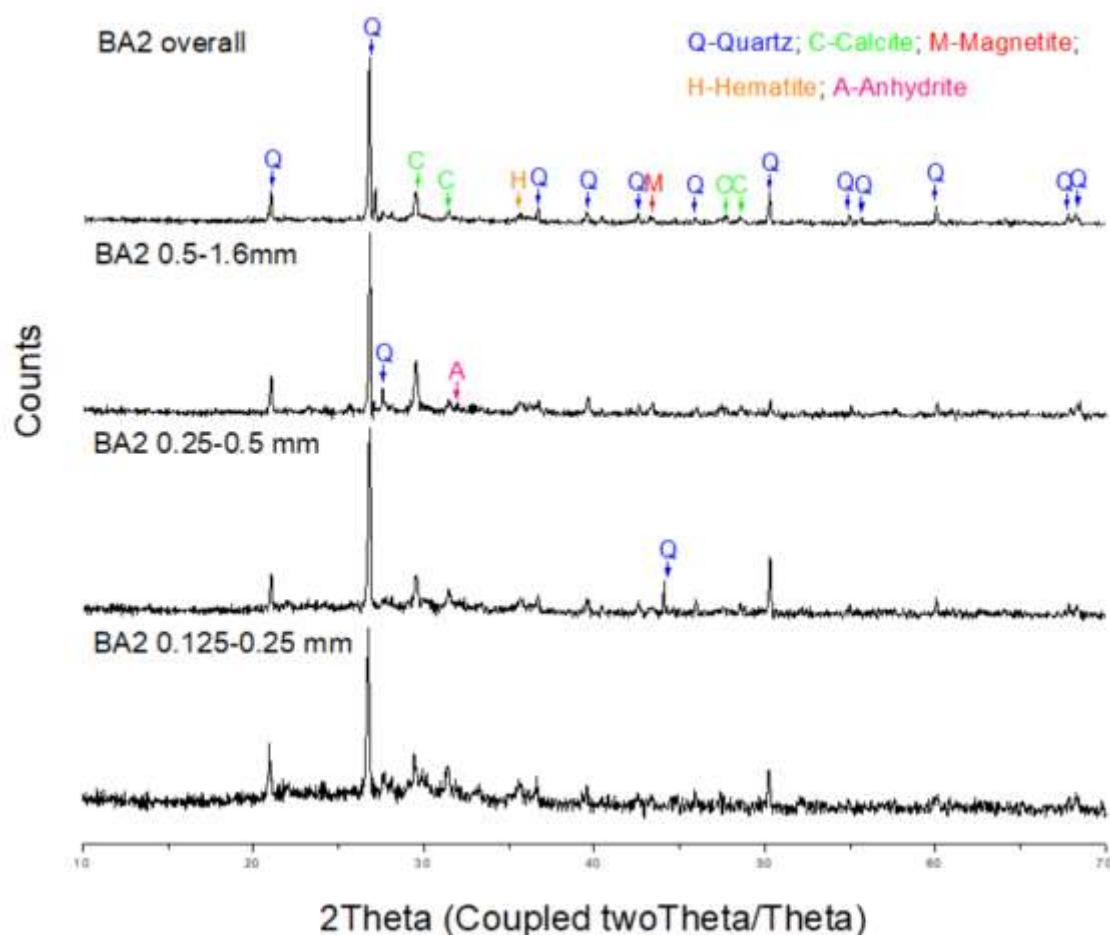


Fig. 4-6 XRD diffractograms of BA2 in 0.5-1.6mm, 0.25-0.5mm, 0.125-0.25mm fractions

4.3. Chemical composition

Chemical compositions of BA1 and BA2 in each fraction were detected by XRF and LOI tests, and the results were compared to that of pure cement to reveal the difference in chemical composition between raw material and cement.

4.3.1. XRF

The chemical compositions of BA1 and BA2 were analyzed separately by X-Ray fluorescence, and results are presented in Table 4-2. Ordinary Portland cement *CEM I 42.5N* is selected as a reference material to show the difference in chemical composition between OPC and BA.

Comparing with OPC, identical chemical elements were detected in BA samples. However, the content of each element varies that all BA samples contain more SiO_2 , Fe_2O_3 and Al_2O_3 , and less CaO than the reference cement. Meanwhile, the heavy metal (CuO, ZnO) and harmful salt (Cl^- , SO_4^{2-}) contents are much higher than that in OPC, which means further treatments are required before it could be used as cement materials concerning the leaching behavior. Moreover, comparing the samples BA1 and BA2 it can be observed that the content of harmful salts such as Cl^- and SO_4^{2-} decreased significantly after the washing process.

4.3.2. LOI

In addition, loss on ignition (LOI) tests were performed on OPC, BA1 and BA2 as well to determine the unburnt organic content in each fraction according to *EN 196-2*. Here, LOI of each fraction is determined by igniting 5 grams of sample at $550 \pm 25^\circ\text{C}$ and $950 \pm 25^\circ\text{C}$ for 1 hour in a ventilated furnace, allowing the volatile substances to escape (hydrates and labile hydroxy-compound and carbon dioxide from carbonates), and expressed by loss in mass after the heating process. In general, the LOI content of BA2 is a little bit lower than that in BA1, which indicates that part of the unburnt organics has been removed during the process. However, LOI of both BA1 and BA2 are much higher than that in *CEM I 42.5N*, which means the nonreactive organics should be removed before BA could be used in cement, otherwise the strength of concrete would decrease. The average LOI content at 950°C is 7.3% in BA2. It is interesting to notice that, as the particle size become smaller, LOI content keeps increasing. It is suspected that the unburned organic particles which are lighter than other contents in BA were crushed and fell into finer fractions during the washing process.

Table 4-2 Chemical composition of OPC, BA1 and BA2 (by fraction)

Chemical composition (% wt.)	CEM I		BA1 (mm)					BA2 (mm)					
	42.5N	Over	1.6-2	0.5-1.	0.25-	0.125	<0.12	Over	1.6-2	0.5-1.	0.25-	0.125	<0.12
		all	6	6	0.5	-0.25	5	all	6	6	0.5	-0.25	5
CaO	64.99	23.86	24.39	23.91	36.80	35.54	38.41	22.39	20.88	20.12	20.43	23.78	26.45
SiO ₂	17.11	37.28	36.59	35.14	20.14	23.31	15.46	43.67	49.17	46.35	47.38	43.45	30.23
Fe ₂ O ₃	3.59	15.27	15.00	16.06	14.48	13.09	11.69	12.29	9.23	11.84	11.79	12.17	19.60
Al ₂ O ₃	3.80	10.48	10.64	11.29	10.22	11.05	15.68	11.66	10.03	11.48	11.32	11.08	11.81
MgO	1.56	2.68	2.91	2.95	2.10	2.17	2.79	2.47	3.58	3.02	2.18	2.07	2.25
Na ₂ O	0	0.83	0.72	0.73	0.57	0.42	0.36	0.34	0.91	0.77	0.27	0.22	0.11
K ₂ O	0.16	1.02	1.01	1.05	1.26	1.17	1.19	0.94	1.07	1.03	0.94	0.89	0.74
CuO	0.02	0.58	0.49	0.59	1.07	1.58	1.20	0.62	0.42	0.48	0.53	0.56	0.91
ZnO	0.15	0.90	0.88	0.97	2.21	1.75	1.54	0.90	0.57	0.71	0.81	0.95	1.47
P ₂ O ₅	0.63	0.89	1.05	0.94	0.58	0.69	0.63	0.84	0.89	0.79	0.83	0.92	1.06
TiO ₂	0.27	1.49	1.55	1.54	1.98	1.94	2.07	1.30	1.36	1.16	1.16	1.38	1.74
Cl	0.02	1.33	1.13	1.33	2.98	2.36	2.98	0.16	0.16	0.17	0.15	0.15	0.19
SO ₃	3.96	2.32	2.28	2.39	4.15	3.68	4.67	1.40	0.99	1.21	1.33	1.42	1.84
other	2.01	1.08	1.37	1.11	1.47	1.26	1.33	1.02	0.74	0.89	0.89	0.96	1.62
LOI(550°C)	1.64	-	-	-	-	-	-	2.84	4.59	4.62	4.65	6.77	7.27
LOI(950°C)	3.10	8.84	7.25	7.51	8.77	9.79	12.79	7.26	5.96	6.24	7.32	9.08	10.30

4.3.3. Metallic aluminum content

According to the previous literature survey hydrogen bubbles produced by corrosion of metallic aluminum particles in BA samples will cause a decrease in strength and serious expansion or swelling problems. Therefore, it is important to determine the metallic aluminum content in each fraction. *Aubert et al.* (2004) developed a method to determine the metallic aluminum content by immersing samples in alkaline solution and measuring the amount of hydrogen gas [45]. A similar dissolving test method was used in this study to determine the metallic aluminum content in BA samples.

In high pH, metallic aluminum will be dissolved, accompanied with the emission of dihydrogen according to the following reaction



In this test OH^- ions were provided by 1M sodium hydroxide solution and the volume of dihydrogen generated was measured. As shown in Fig. 4-7, a testing system was set up in *Mircolab TUDelft*¹¹ to determine the volume of dihydrogen by measuring water volume pumped out by gas generated in dissolving process at normal conditions of pressure and temperature ($P_0 = 101.3\text{kPa}$, $T_0 = 273\text{K}$). Silica gel pellets were filled in the U-shaped tube to get rid of water vapor, and the water pumped out by hydrogen gas was collected and measured by the cylinder.

The relationship between the volume of hydrogen gas released and the amount of metallic aluminum in the sample is given by

¹¹ Stevinweg 1, 2628 CN Delft, the Netherlands

$$v_{H_2} = \frac{3m_{Al}}{2M_{Al}} v_0 \quad (3)$$

where v_0 is the molar volume, equal to 22.4L/mol and M_{Al} is the molar mass of aluminum, equal to 27g/mol. In case the room temperature of measurement is higher than 273K, according to *General gas law* ($\frac{p_1 v_1}{T_1} = \frac{p_2 v_2}{T_2}$, and $p_1 = p_2 = P_0 = 101.3\text{kPa}$), the equivalent volume of H_2 at 273K could be expressed as:

$$v_{H_2} = \frac{273}{273+T} v_m \quad (4)$$

where T is room temperature in Celsius degree, and $v_3 = v_2 - v_1$ is the volume increment of H_2 . Therefore, the mass of metallic aluminum in BA sample could be represented by the following equation:

$$m_{Al} = \frac{2v_3}{3v_0} M_{Al} = \frac{2(v_2 - v_1) \frac{273}{273+T}}{3v_0} M_{Al} \quad (5)$$

Accordingly, the mass percentage of metallic aluminum in BA could be determined as well by dividing m_{Al} by total mass of BA sample.



Fig. 4-7 Testing system to determine metallic aluminum content

The BA of each fraction was milled into fine powder by a ball mill to reduce the particle size and make it more homogenous before the test. Results of metallic aluminum content of BA2 in each fraction are given in Table 4-3. In general, metallic aluminum content in BA is 0.8% by weight in BA samples, which is much higher than the acceptable level and will generate a large amount of air bubbles in concrete structure and lead to drop in strength. A relatively high amount of metallic aluminum is present in fraction 1.6-2mm and 0.5-1.6mm. Further treatments are required to remove the aluminum before the BA could be applied in OPC concrete system.

Table 4-3 Metallic aluminum content in each content

Fraction	Content (wt. %)
Overall	0.80 ± 0.02
1.6-2mm	1.81 ± 0.04
0.5-1.6mm	1.36 ± 0.05
0.25-0.5mm	0.43 ± 0.02
0.125-0.25mm	0.28 ± 0.03
<0.125mm	0.16 ± 0.01

5. Pretreatment of BA

According to the result of the characterization of as-received BA, the main problem are the high metallic aluminum content and low reactivity. Several methods of pretreatment were performed on BA to improve the properties of BA (chemical composition, packing density and reactivity). Both chemical and physical methods were carried out in this study to get rid of metallic aluminum, and the effect was checked by a group of preliminary cast by blending treated BA into cement paste. The remaining aluminum content is acceptable if no obvious air bubbles were observed on the surface of the samples. Meanwhile, BA after physical treatment will be activated by thermal treatment so that it could work better when used as cement substitute materials.

5.1. Removal of metallic aluminum

5.1.1. Chemical treatment

The main aim of chemical treatment is to remove the metallic aluminum content in BA. It has been reported that Na_2CO_3 and NaOH solutions are suitable to remove the metallic aluminum content in BA [17, 88, 89]. Therefore, in this study, BA samples are immersed in Na_2CO_3 and NaOH solutions with different concentration and liquid to solid ratio. Metallic aluminum content and pH values are measured both before and after the treatment.

5.1.1.1. Na_2CO_3 solution

Firstly, treatment with Na_2CO_3 solutions was performed. Samples were immersed in different Na_2CO_3 solutions for a week, and results are shown in Table 5-1. Metallic aluminum content was determined again only for the groups with the highest Na_2CO_3 concentration, and no severe decrease in aluminum content was detected. The result shows that Na_2CO_3 solution is not strong enough to remove the metallic aluminum in BA. Otherwise, Na_2CO_3 treatment might be time-consuming.

Table 5-1 Result of treatment with Na_2CO_3 solutions

Solution	Solid/Liquid	pH before treatment	pH after treatment	Al before treatment (wt. %)	Al after treatment (wt. %)
0.1M Na_2CO_3	1.0	11.5	8.2	0.80 ± 0.03	-
0.1M Na_2CO_3	0.5	11.5	9.5	0.80 ± 0.03	-
0.5M Na_2CO_3	1.0	12.0	10.5	0.80 ± 0.03	-
0.5M Na_2CO_3	0.5	12.0	11.0	0.80 ± 0.03	-
1.0M Na_2CO_3	1.0	12.5	11.5	0.80 ± 0.03	-
1.0M Na_2CO_3	0.5	12.5	12.0	0.80 ± 0.03	-
5.0M Na_2CO_3	1.0	13.5	12.5	0.80 ± 0.03	0.71 ± 0.03
5.0M Na_2CO_3	0.5	13.5	13.0	0.80 ± 0.03	0.62 ± 0.03

5.1.1.2. NaOH solution

Meanwhile, BA samples were treated with NaOH solutions as well. This part of study was done by *Loic*, a bachelor student in *TU Delft*. Results are given in Table 5-2. Result

indicates that NaOH solution has a much better performance than Na_2CO_3 solution in metallic aluminum elimination.

After the chemical treatment process, BA was washed by running water and dried until a constant mass in a ventilated oven. Subsequently, BA was sieved into different fractions according to *EN 196-1* and blended with CEN standard sand, which will be used as fine aggregate in the mortar.

Table 5-2 Results of treatment with NaOH solutions

	Duration (days)	Solid/Liq uid	pH before treatment	pH after treatment	Al before treatment (wt. %)	Al after treatment (wt. %)
0.1M NaOH	5	0.2	13.5	13.0	0.80 ± 0.03	0.16 ± 0.03
0.1M NaOH	5	0.1	13.5	13.0	0.80 ± 0.03	0.06 ± 0.03
0.1M NaOH	15	0.2	13.5	11.5	0.80 ± 0.03	0.02 ± 0.03
0.1M NaOH	15	0.1	13.5	11.5	0.80 ± 0.03	0
1.0M NaOH	5	0.2	14.0	14.0	0.80 ± 0.03	0.09 ± 0.03
1.0M NaOH	5	0.1	14.0	14.0	0.80 ± 0.03	0.04 ± 0.03
1.0M NaOH	15	0.2	14.0	14.0	0.80 ± 0.03	0.12 ± 0.03
1.0M NaOH	15	0.1	14.0	14.0	0.80 ± 0.03	0.03 ± 0.03
3.0M NaOH	5	0.2	14.0	14.0	0.80 ± 0.03	0.07 ± 0.03
3.0M NaOH	5	0.1	14.0	14.0	0.80 ± 0.03	0
3.0M NaOH	15	0.2	14.0	14.0	0.80 ± 0.03	0.04 ± 0.03
3.0M NaOH	15	0.1	14.0	14.0	0.80 ± 0.03	0.05 ± 0.03

5.1.2. Physical treatment

Physical treatments were performed on BA samples as well. A combination of grinding and sieving have been carried out to get rid of metallic aluminum, adjust the particle size distribution and increase the packing density.

5.1.2.1. Grinding and sieving

A technique for the removal of metallic Al by slow milling and sieving has been proposed by *Tang et al* [31]. Coarse BA particles could be crushed into fine powders and metallic aluminum inside could be exposed and ground into metal plates, which could be easily sieved out during the subsequent sieving process. Meanwhile, the oxidation of the remaining metallic aluminum could be promoted as well in the high temperature environment provided by the grinding process.

In addition, it is also reported that grinding is an effective way to improve the reactivity of BA by increasing particle fineness and surface area [80, 84, 100].

20 groups of grinding tests have been performed in this study to derive an optimum method to remove the metallic aluminum in BA, concerning both aluminum content after treatment and output rate of treated powder. In each group, 100 grams of dried sample was ground in a planetary ball miller at different speed for different duration, and then the obtained fine powders were sieved to pass a 63 μm sieve. Metallic aluminum contents of fractions smaller than 63 μm were determined again by

dissolving test to show the efficiency of treatment. Meanwhile, the mass percentage of fractions smaller than $63\ \mu\text{m}$ to the total mass before grinding and sieving was determined as well. Results are given in Table 5-3.

Table 5-3 Metallic aluminum content and output rate after treatment

Particle size (<63 μm)	200 rpm		250 rpm		300 rpm		350 rpm		400 rpm	
	Al (wt. %)	Mass (%)	Al (wt. %)	Mass (%)	Al (wt. %)	Mass (%)	Al (wt. %)	Mass (%)	Al (wt. %)	Mass (%)
10 min	0.25	34	0.21	35	0.18	43	0.13	48	0.12	53
20 min	0.22	48	0.18	46	0.15	69	0.43	91	0.67	87
30 min	0.18	78	0.13	80	0.27	91	0.74	92	0.50	91
40 min	0.26	66	0.43	89	0.59	82	0.19	89	0.15	86

Considering about the efficiency of grinding and sieving treatment, the remaining metallic aluminum contents in fraction smaller than $63\ \mu\text{m}$ are plotted against grinding time for each grinding speed (as shown in Fig. 5-1). Severe drops in metallic aluminum content after treatment have been observed in several groups (250rpm-30min, 300rpm-20min, 400rpm-10min and 400rpm-40min). However, it is also observed that in each curve the metallic aluminum content increased again as the grinding time became longer (the metallic aluminum content in 350rpm-30min and 400rpm-20min are extremely high that almost all aluminum in BA drops into fraction $<63\ \mu\text{m}$). It is also interesting to notice that the metallic aluminum content dropped again as the grinding time kept increasing (350rpm-40min and 400rpm-40min).

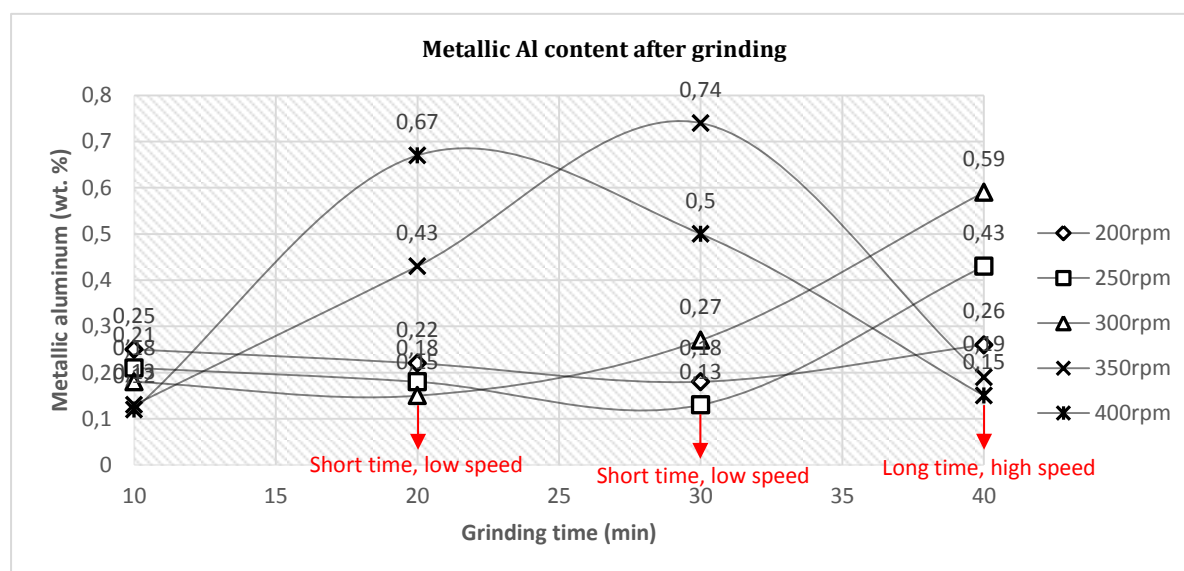


Fig. 5-1 Metallic Al content after grinding

It is clear that grinding time and speed is not the more the better, and multiple mechanisms are affecting the efficiency of grinding and sieving. As shown in Fig. 5-2, at the beginning, for short time and low speed grinding the metallic aluminum were ground into metal plates and could be easily sieved out. On the other hand, two peaks

are observed at 350rpm-30min and 400rpm-20min, which indicates that the metallic aluminum plates were further crushed into fine powders ($< 63 \mu\text{m}$) when grinding period became longer and dropped into smaller particle fraction. Meanwhile, the metallic aluminum content dropped again in high speed grinding groups as the time increased, and it is also detected that the grinding jar became extremely hot in long-term and high-speed groups. Accordingly, it is suspected the high-temperature environment generated by the long-term and high-speed grinding accelerated the oxidation of metallic aluminum which fell into finer fractions during the grinding and sieving process, so that the metallic aluminum content dropped again. However, this method could be energy and time consuming, which is not suitable to be used in industry. Therefore, it is very important to determine the best grinding time and speed to achieve high efficiency in metallic aluminum elimination.

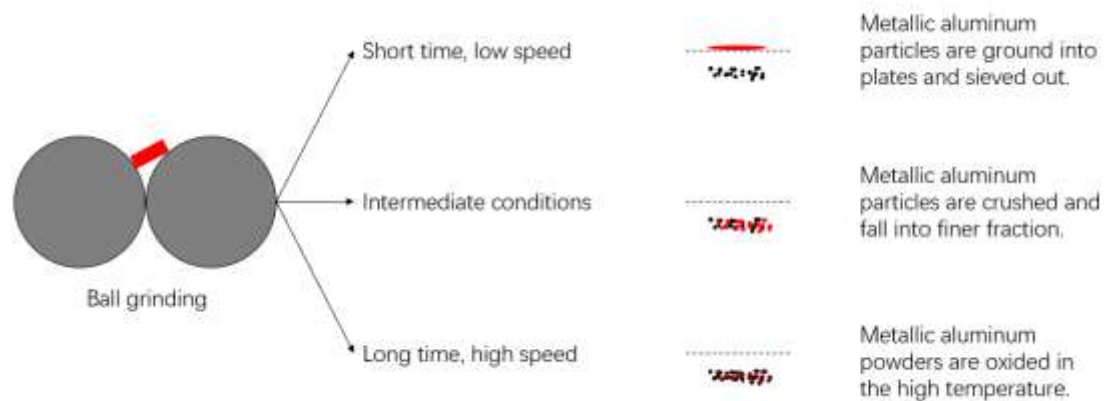


Fig. 5-2 Mechanisms of grinding and sieving treatment

Apart from the efficiency, another important factor is the output rate of fine powders ($< 63 \mu\text{m}$) in grinding and sieving treatment. Mass percentages of $< 63 \mu\text{m}$ particles after grinding against grinding time for different speed are plotted in Fig. 5-3. It is obvious that the output rates for all speeds become relatively high when the grinding time comes to about 30 minutes. A threshold for an acceptable output rate is set here as 80%. Similarly, the grinding time and speed are not the more the better even the output rate is high due to mechanisms mentioned above.

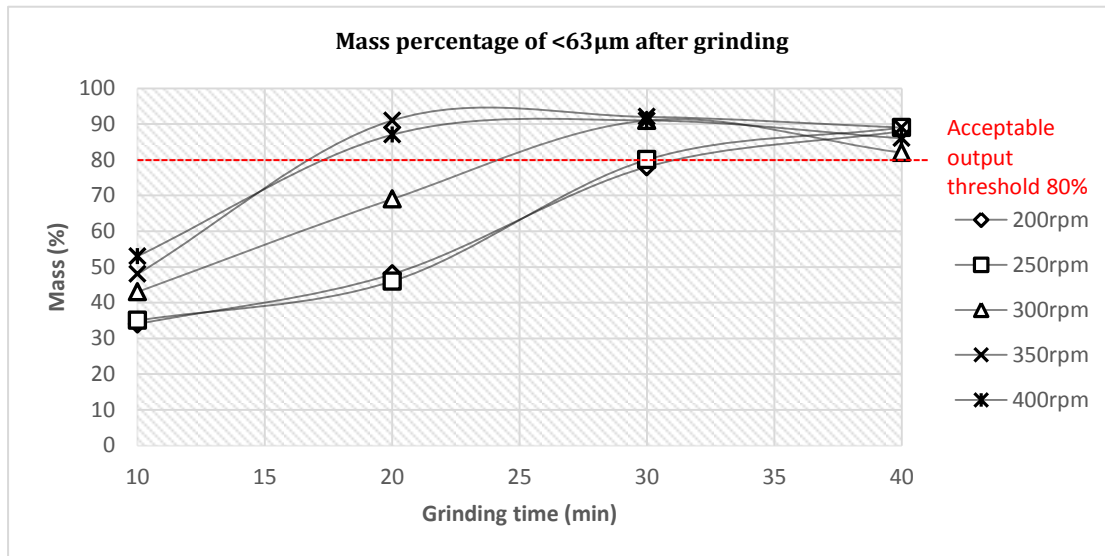


Fig. 5-3 Mass percentage of < 63µm particles after grinding

Therefore, considering both grinding efficiency and output ratio, 250rpm-30min is selected as the standard method of pretreatment to get rid of metallic aluminum content in this research for further investigations and BA treated with this method is labelled as MBA.

5.1.2.2. Preliminary cast

As mentioned in the literature survey, very little amount of metallic aluminum content will already result in high-porosity concrete structures. Besides the metallic aluminum content test, the effect of pretreatment was checked again by some preliminary cast with MBA and OPC. The paste was made with 10 grams of cementitious material (0-60% OPC replaced with MBA) at water/cement ratio of 0.5, and then casted in a cylindrical mold. Specimens were demolded after 24 hours and both the surface and internal structure (degree of expansion and the amount of entrapped voids due to hydrogen bubbles) were checked to get a feeling of the remaining aluminum content in MBA. The mixture design is given in Table 5-4.

Table 5-4 Preliminary cast design with MBA

Replacement level (%)	0	10	20	30	40	50	60
CEM I 42.5 N (g)	20	18	16	14	12	10	8
MBA (g)	0	2	4	6	8	10	12
Water (g)	10	10	10	10	10	10	10

The results of the preliminary cast are illustrated in Fig. 5-4. No obvious air bubbles were observed on the surface of all samples, which proved that the pretreatment for metallic aluminum elimination was effective.



Fig. 5-4 Preliminary cast

5.1.3. Mortar strength test

Subsequently, the performance of MBA in cement was checked on mortar level. As shown in Fig. 5-5, M300 and BFS were selected as reference materials due to the similar particle size distribution as *CEM I 42.5N* and MBA. Sample cubes were casted in 40*40*40mm cubes and demolded after 24 hours, and then transferred to the curing room (room temperature, 95% RH).

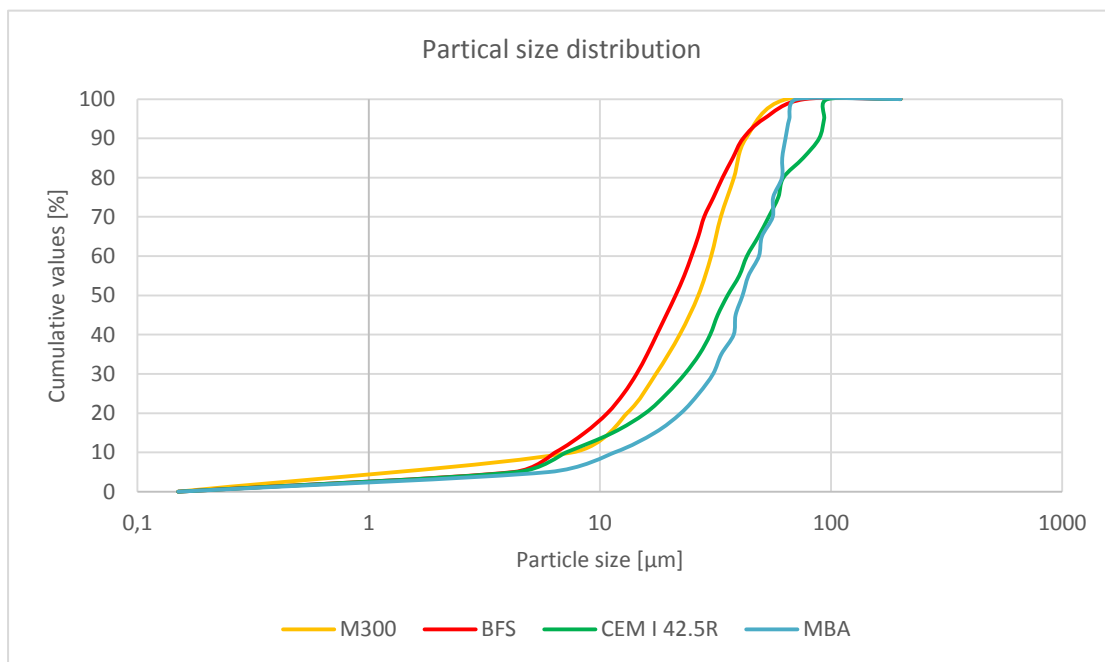


Fig. 5-5 Particle size distribution (CEM I 42.5 R, M300, BFS, MBA)

Results of 1, 7 and 28-days compressive strength test are schematized in Fig. 5-6 and Fig. 5-7 (details of data are given in Appendix A). In Fig. 5-6, all substitute materials are considered as binder in mortar to investigate the performance of MBA as cement substitution. Comparing with *CEM I 42.5N* mortar, different levels of decrements were observed in 10% replacement with MBA and BFS. However, the mortar with 10% BFS exhibited the highest strength among all substitute materials, The result of strength test indicates that the contribution to hydration process or in other words, the reactivity of

MBA is much lower than that in *CEM I 42.5N* or BFS.

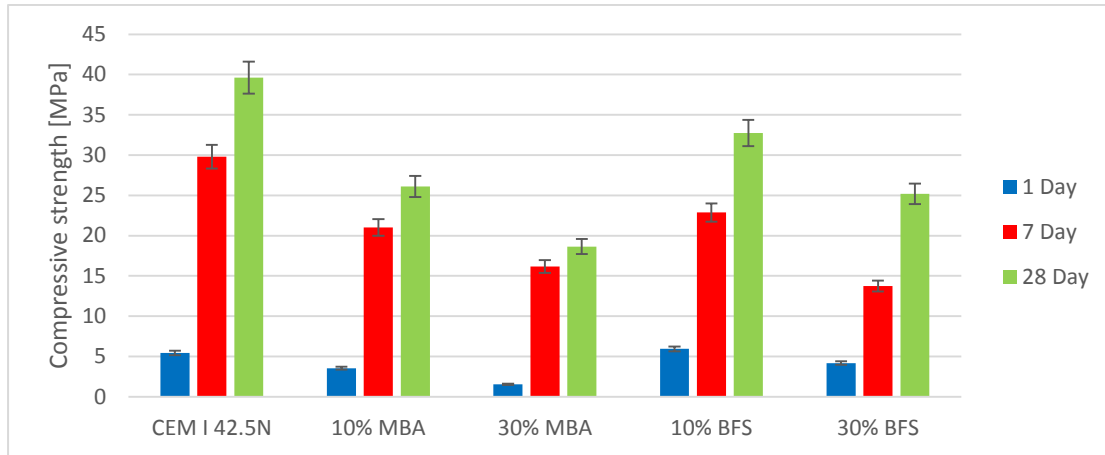


Fig. 5-6 Compressive strength of mortars with binder substitution (CEM I 42.5N, 10%MBA, 30%MBA, 10%BFS and 30%BFS)

Subsequently, the strength of mortars with MBA was plotted together with M300 to investigate the feasibility of MBA used as filler substitution. Mortar with 10% and 30% MBA showed higher 7-day and 28-day compressive strength, while the 1-day strength of mortar with MBA is even worse than that with the same amount of M300, which indicates the addition of MBA retarded the early-stage strength development.

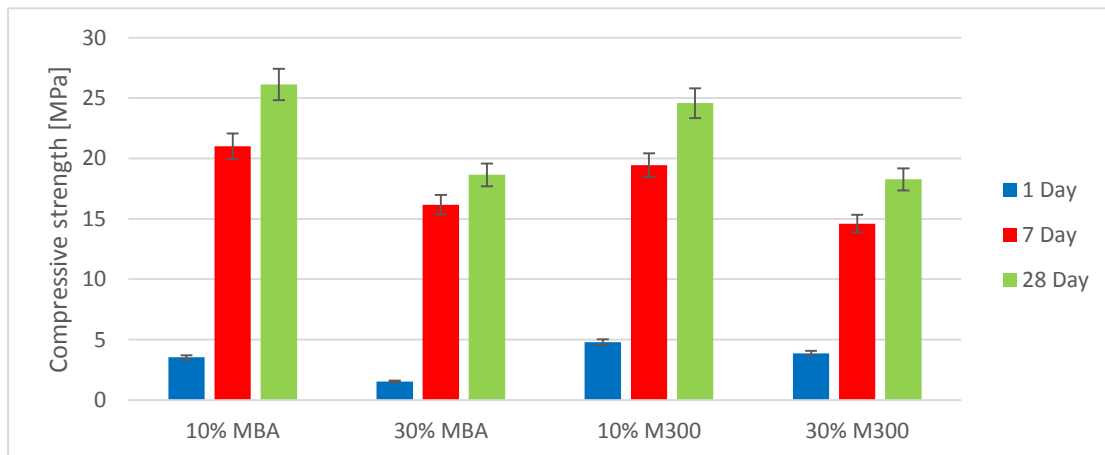


Fig. 5-7 Compressive strength of mortars with filler substitution (10%MBA, 30%MBA, 10%M300 and 30%M300)

Therefore, MBA is already good enough to be used as filler substitute material that the compressive strength is higher than that with sand. However, when MBA is considered as binder substitute materials, the compressive is much lower pure cement and that with the same amount of BFS, which indicates the reactivity of MBA is still poor that works worse than pure cement and BFS. Subsequently, it was decided to perform thermal treatment to get BA activated by generating new phases as well as removing the unburned organics and investigate the possibility of BA to be used as binder substitute material.

5.2. Thermal activation

According to previous studies, thermal treatment is an effective way of both increasing the strength of BA cement and improving the leaching behavior [31, 84]. Thermal treatment will help to remove the unburnt nonreactive organic matters in BA [101, 102] and increase the reactivity of BA by generating new reactive phases and accelerating the decomposition of calcite [31, 60]. Meanwhile, it is also reported that thermal treatment would reduce the leaching of heavy metals (such as Cu, Pb and Mo) [82, 83].

Thermogravimetric analysis (TGA) test was carried out to evaluate the thermal stability of BA and provide information about physical and chemical phenomena as well as solid-gas reactions. The derivative TG (DTG) curve from 40 to 1100°C is shown in Fig. 5-8, and a phase transition is observed at around 771°C accompanied with the emission of CO and CO₂ gas which is suspected to be the decomposition of calcite according to the literature survey mentioned in previous chapters. The mass loss related to calcite decomposition in MBA is about 1.61% according to TG curve as shown in Fig. 5-9.

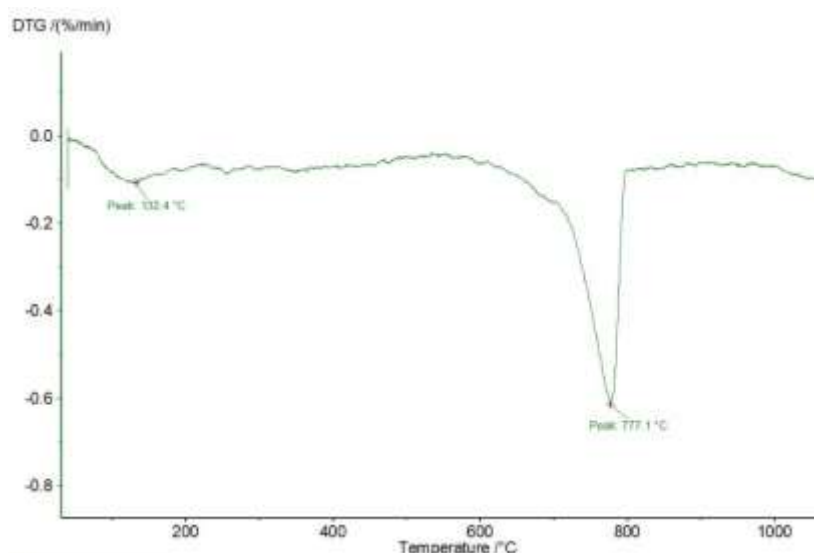


Fig. 5-8 DTG curve of MBA

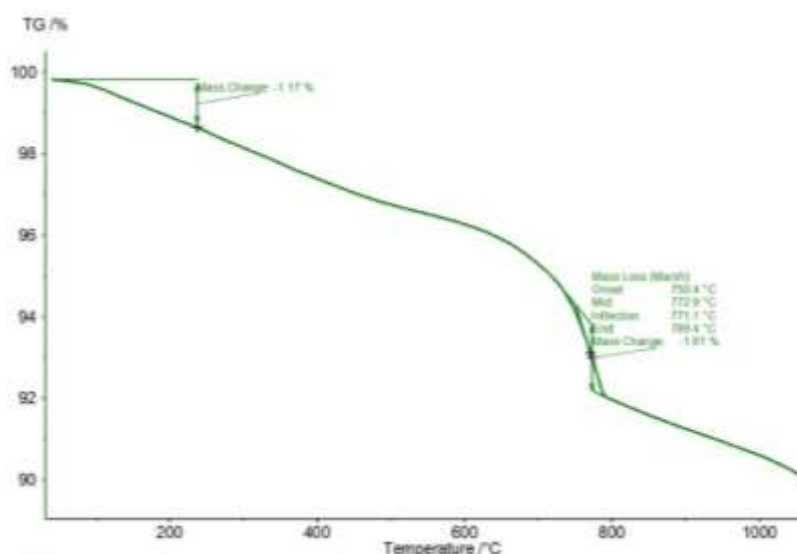


Fig. 5-9 TG curve of MBA

According to the result of TGA test, it was decided to perform thermal treatment at 1000°C on BA samples to get rid of the unburned organic matters and generate new reactive phases.

Two methods of thermal treatment were proposed to investigate the order of treatment. In the first method, MBA derived from physical treatment was heated up to 1000°C in a ventilated furnace for 2 hours and then cool down to room temperature. However, severe agglomeration was observed after the high-temperature process. Therefore, an extra grinding was conducted to adjust the particle size distribution, and the sample derived is labelled as MTBA.

Optionally, the thermal treatment was performed before the thermal treatment. Raw BA was heated up to 1000°C in a ventilated furnace for 2 hours, and then a quenching process was conducted by pouring the BA immediately into a bucket filled with water in room temperature. Then the BA particles were collected by a vacuum pumping, and oven dried at 105°C until a constant mass. Subsequently, an identical grinding and sieving process as that in MBA was performed on quenched BA to get rid of the metallic aluminum content, and the sample derived by this method is labelled as QMBA. However, a large amount of black-colored iron oxide particles were detected in QMBA due to the spalling of crucible wall during the quenching process, which introduced a large number of impurity substance in QMBA.

A one day paste compressive strength test was performed to make a choice between two thermal treatment methods. Cement blended with 10% MTBA replacement showed a higher strength than QMBA, which indicates that MTBA has a better performance than QMBA. Accordingly, MTBA is selected as the thermally treated material and used for latter investigations.

6. Characterization of treated BA

In this chapter, BA with different methods of treatment was characterized again comparing with pure cement to reveal the effect of treatment. Meanwhile, different BA samples were compared with each other as well to derive the best treatment method in this study.

6.1. Physical properties

6.1.1. Particle size distribution

Particle size distribution (PSD) of obtained from each grinding method was checked by laser as well, and results are shown in Fig. 6-1 and Table 6-1. *CEM I 42.5N* and *CEM I 52.5R* were selected as reference. It is clear that all powders obtained from grinding and sieving treatment are finer than *CEM I 42.5N* cement, and have a similar particle size distribution as *CEM I 52.5R*. Meanwhile, BA powder obtained from long-term and high-speed grinding (400rpm-40min) has an even finer PSD than that of *CEM I 52.5R*.

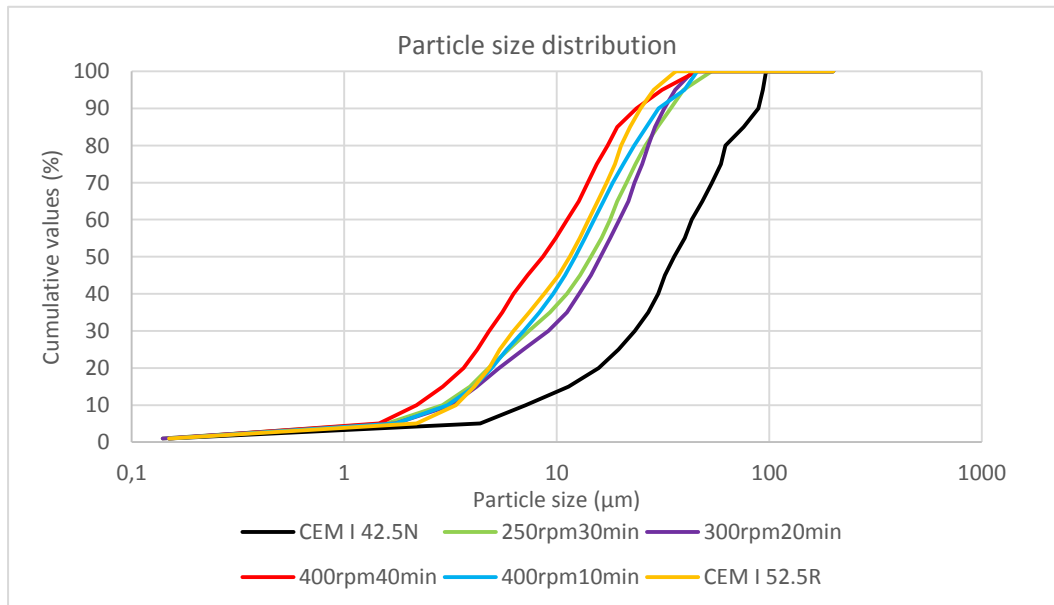


Fig. 6-1 Particle size distribution (250rpm-30min, 300rpm-20min, 400rpm-10min, 400rpm-40min, CEM I 42.5N and CEM I 52.5R)

Table 6-1 Volume dimensions of powders with median size (250rpm-30min, 300rpm-20min, 400rpm-10min, 400rpm-40min, CEM I 42.5N and CEM I 52.5R)

	D ₁₀ (μm)	D ₅₀ (μm)	D ₉₀ (μm)
CEM I 42.5N	7.14	35.70	88.87
250rpm-30min	2.9	14.5	34.35
300rpm-20min	3.19	16.09	32.03
400rpm-10min	3.06	12.24	30.16
400rpm-40min	2.19	8.60	23.75
CEM I 52.5R	3.35	11.51	24.77

Besides, particle size distribution of BA was checked again after thermal treatment. Severe agglomeration was observed due to the high temperature process which result in the coarser particles as shown in Fig. 6-2. Therefore, an additional grinding process was performed to adjust the particle size distribution (similar as MBA) and the BA derived this way was labelled as MTBA. Meanwhile, QMBA behaves more brittle due to the quenching process so that a finer PSD is observed under the same grinding condition as MBA.

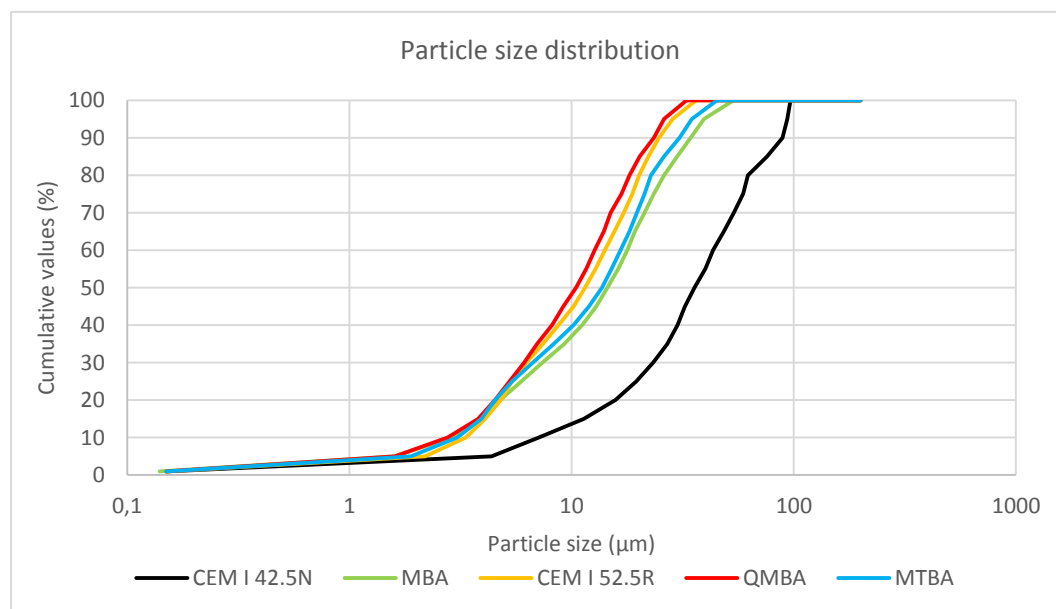


Fig. 6-2 Particle size distribution (CEM I 42.5N, MBA, QMBA, MTBA and CEM I 52.5R)

Table 6-2 Volume dimensions of powders with median size (CEM I 42.5N, MBA, QMBA, MTBA and CEM I 52.5R)

	D ₁₀ (µm)	D ₅₀ (µm)	D ₉₀ (µm)
CEM I 42.5N	7.14	35.70	88.87
MBA	2.9	14.5	34.35
QMBA	2.77	10.49	23.46
MTBA	3.06	13.70	30.60
CEM I 52.5R	3.35	11.51	24.77

6.1.2. Morphology

ESEM was carried out again to compare the morphology of BA particles before and after thermal treatment (as shown in Fig. 6-3 and Fig. 6-4). Comparing with as-received BA before thermal treatment (Fig. 4-3 and Fig. 4-4), the amount of pores decreased significantly and a much denser BA matrix was observed. Therefore, thermal treatment could increase the strength of BA cement by decreasing the porosity of BA particles.

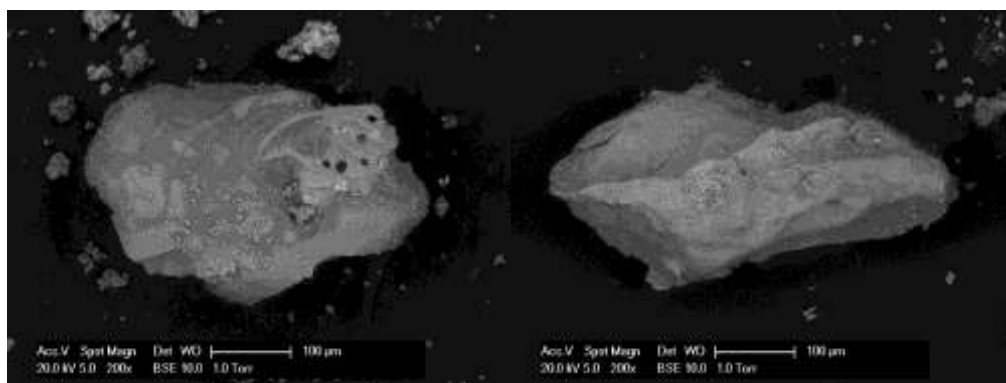


Fig. 6-3 ESEM 200x of BA particles after thermal treatment

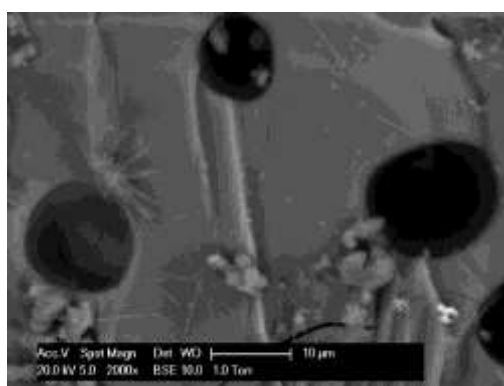


Fig. 6-4 ESEM 2000x of BA particles after thermal treatment

6.2. Crystalline phases

The XRD analysis was performed on raw BA, MBA, CBA, QMBA and MTBA to investigate the crystalline phase changes before and after each kind of treatment, and results are illustrated in Fig. 6-5. The identified dominant crystalline phase in all samples is quartz (SiO_2), and the main quartz peak is observed at around 26.6° in all samples, which is in agreement with other studies [31, 84].

In general, high content of quartz (SiO_2), calcite (CaCO_3), akermanite ($\text{Ca}_2\text{MgSi}_2\text{O}_7$) and magnetite ($\text{Fe} + 2\text{Fe}_2 + 3\text{O}_4$) have been observed in BA MBA and CBA, and no significant difference was observed, which indicates that the grinding or chemical washing process didn't result in obvious phase changes. However, it is observed that both the intensity and width of peaks are decreased in CBA comparing that in BA and MBA, which indicates that those crystalline phases were dissolved as well in NaOH solution during the chemical treatment.

As for QMBA and MTBA, thermally treated BA samples exhibit more complex crystalline phases, that much more peaks were detected between 20° and 70° . In general, peaks representing calcite (CaCO_3) vanished after thermal treatment in both MTBA and QMBA, which is due to the decomposition of calcite in high temperature. Furthermore, newly generated wollastonite (CaSiO_3) phases were observed in both

QMBA and MTBA, which is considered to work as a reinforcing micro-fiber phase in cement contributing to the strength development [103]. In addition, aluminum oxide-containing phases were detected after the thermal treatment, such as gehlenite ($\text{Ca}_2\text{Al}_2\text{SiO}_7$) and albite ($\text{NaAlSi}_3\text{O}_8$), which proved that the oxidation of metallic aluminum content in BA was effectively accelerated during thermal treatment.

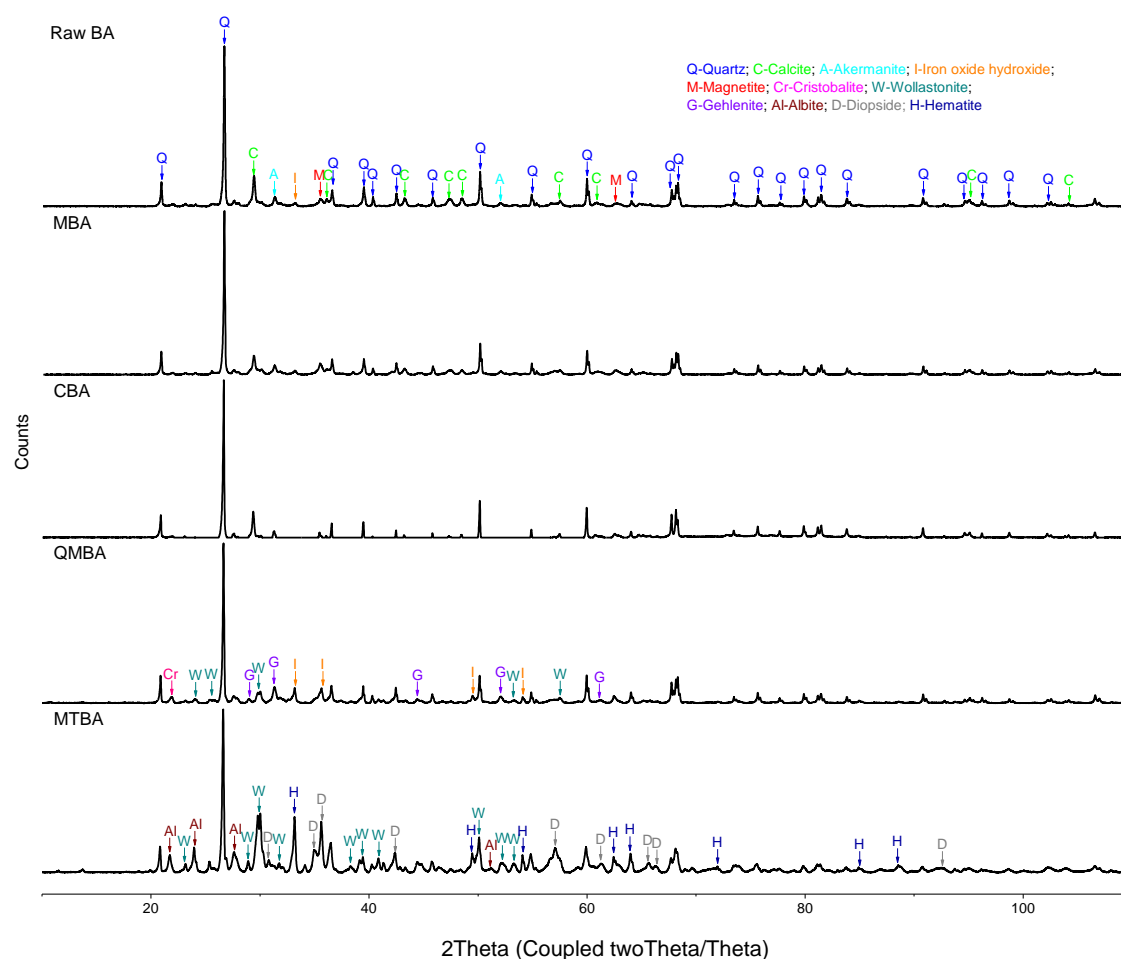


Fig. 6-5 XRD diffractograms of treated BA samples

In MTBA, more newly generated phases were detected and some of which were even distributed between 80° and 100° . Comparing with raw BA and MBA, a decrement was observed in the intensity of the main quartz peak of MTBA, which is in parallel with the XRF result. Moreover, significant increment has been detected in both number and intensity of peaks representing iron oxide, especially hematite (Fe_2O_3), which is also observed by the color change of sample after thermal treatment (as shown in Fig. 6-6). This can be attributed to the accelerated oxidation of iron due to the high temperature during thermal treatment. Meanwhile, however, the composition of iron-containing compounds is even more complicated in QMBA due to the quenching process, so that iron oxide hydroxide was detected. Gehlenite was observed as well in QMBA, which is reported to be an intermediate compound of Portland cement clinker production at the temperature below 1200°C and is characteristic for natural hydraulic lime [104].

In conclusion, BA mainly consists of quartz, calcite, akermanite and magnetite, and grinding or chemical treatment would not result in significant phase changes. However, more crystalline phases were dissolved during the chemical treatment that both intensity and width of existing phases peaks were decreased. Thermal treatment mainly accelerates the decomposition of calcite as well as the oxidation of metallic iron and aluminum content, while some reactive phases such as wollastonite are generated at the same time. Comparing with QMBA, MTBA is more desirable since more peaks of reactive phases and oxidation phases were detected which would contribute more to strength development and mitigate the expansion and swelling due to metallic metals.



Fig. 6-6 Color change of BA sample (left-MBA, right-MTBA)

6.3. Chemical composition

6.3.1. XRF

Chemical compositions of raw BA, MBA and MTBA are listed in Table 6-3, and a similar composition has been observed among three kinds of BA. However, the silica oxide content became higher after treatment while the calcium oxide content dropped. Meanwhile, the treatment also further removed the hazard contents such as heavy metals (Al, Mg, Cu and Zn) and salts (chloride and SO_3).

Table 6-3 Chemical composition of raw BA, MBA and MTBA

Chemical composition (wt. %)	CEM I 42.5N	Raw BA	MBA	MTBA
CaO	64.99	22.39	18.34	18.70
SiO ₂	17.11	48.44	50.40	43.67
Fe ₂ O ₃	3.59	12.29	12.94	13.62
Al ₂ O ₃	3.80	11.66	9.84	10.08
MgO	1.56	2.47	2.21	2.40
Na ₂ O	0	0.34	0.56	0.92
K ₂ O	0.16	0.94	0.82	0.82
CuO	0.02	0.62	0.48	0.48
ZnO	0.15	0.90	0.75	0.77
P ₂ O ₅	0.63	0.84	0.67	0.74
TiO ₂	0.27	1.30	1.12	1.20
Cl	0.02	0.16	0.12	0.03
SO ₃	3.96	1.40	0.86	0.84
other	2.01	1.02	0.89	0.96

6.3.2. Metallic aluminum content

The metallic aluminum content in MTBA was determined by dissolving test again to check the remaining aluminum after treatment, the results are given in Table 6-4. It is proved that the residual metallic aluminum content in MBA is further removed by accelerated oxidation due to the high-temperature process in thermal treatment. Therefore, MTBA is expected to have a better performance than MBA.

Table 6-4 Metallic aluminum content in raw BA, MBA and MTBA

	Raw BA	MBA	MTBA
Metallic aluminum (wt. %)	0.80 ± 0.03	0.13 ± 0.03	0.06 ± 0.04

In conclusion, both chemical treatment with sodium solution (CBA) and physical treatment with grinding and sieving (MBA) are effective enough to remove the metallic aluminum content in as-received BA. However, CBA is more suitable to be used as filler or fine aggregate in concrete since more reactive crystalline phases were dissolved by alkaline solutions as well even though the remaining metallic aluminum content of CBA is even lower than that in MBA. Moreover, two activation methods were proposed by thermal treatment. New reactive crystalline phases generated by thermal treatment in both methods were detected by XRD, and MTBA is more desired comparing with QMBA according to the 1-day strength and XRD results.

7. Development of materials properties of cement paste and concrete by using BA as replacement

In this chapter, the study was divided into two parts, focusing on the development of material properties during the hydration process of cement paste and the properties of concrete when using BA as substitution material.

7.1. Investigation on cement paste level

In cement paste, the studies were carried out on the effect of different pretreatment methods and different MTBA replacement ratio. In the first group, CBA, MBA, MTBA and M300 were blended into *CEM I 42.5N* cement with a 10% replacement ratio separately comparing with pure cement, and MTBA was considered as the best substitute material with the best performance according to the compressive strength, hydration products and heat development. In the second group of study, MTBA and M300 were blended with *CEM I 42.5N* cement with 10%, 20% and 30% replacement ratio and the effect of various replacement ratio was investigated comparing with pure cement.

7.1.1. Effects of different pretreatment method

7.1.1.1. Compressive strength

7-day and 28-day compressive strength tests of cement paste with 10% CBA, MBA, MTBA and M300 were conducted to show the effects of different kinds of pretreatment methods (details of data are given in Appendix A). Three cubes were tested in each group, and the average results are given in Table 7-1 and Fig. 7-1. Unsatisfactorily, comparing with *CEM I 42.5N* cement paste, a drop of compressive strength is observed in each kind of treated BA. On the other hand, comparing the performance among different types of BA samples, 10% MTBA exhibited the highest 7-day and 28-day compressive strength while the strength of 10% CBA was the lowest, which is even lower than that of 10% M300. The result indicates that both MBA and MTBA would contribute more to the hydration process and strength development than pure sand, while the performance of CBA is even worse than pure sand.

However, the differences of compressive strength among CBA, MBA and MTBA is still attractive, which might be attributable to the differences in BA, namely the aluminum content, reactive phases and impurity substances. According to the result reported in the previous chapter, the metallic aluminum content in CBA and MBA were 0.02% and 0.13% separately. Even so, the compressive strength of paste with 10% MBA is still higher than that with 10% M300 and 10% CBA, which proves that MBA contains more reactive phases than CBA despite the higher amount of metallic aluminum residual content which would result in more porous structure and lower strength. On the other hand, grinding and sieving process does no contribution to the generation of new reactive phase at all, which proves that the existing reactive phases in BA were attacked by chemical treatment. Therefore, the chemically treated BA is more suitable to be used as filler in concrete due to the relatively low reactivity. Moreover, the performance of CBA is worse than that of M300, which may be attributed to the impurity substances in CBA such as unburned organic matters.

Table 7-1 Compressive strength of cement paste with CBA, MBA and MTBA

Mixture	Compressive strength (MPa)	
	7-day	28-day
Ref. cement	18.736	41.834
10% CBA	12.287	15.945
10% MBA	14.669	25.314
10% MTBA	17.929	29.877
10% M300	12.494	20.250

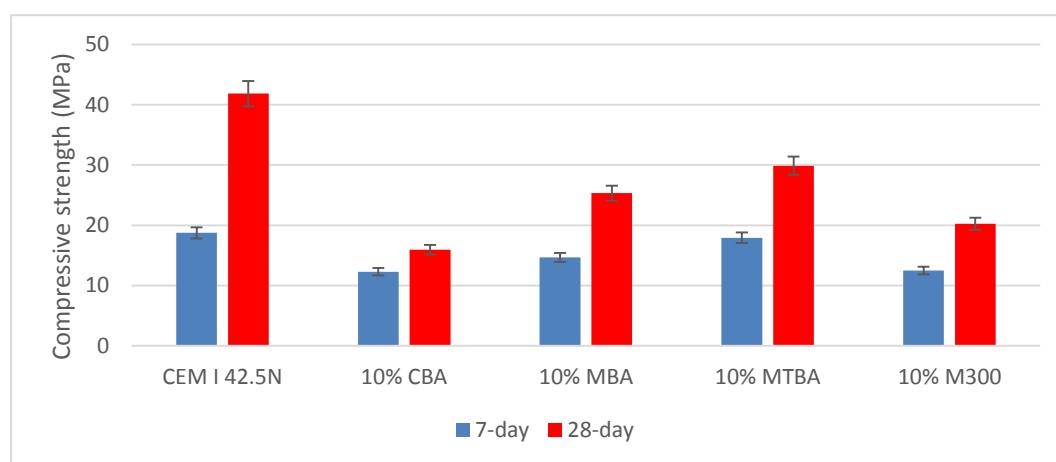


Fig. 7-1 Compressive strength of cement paste with CBA, MBA MTBA and M300

7.1.1.2. Hydration heat

According to the existing studies [105, 106], the overall hydration progress could be divided into four stages indicated in the isothermal calorimetry plot of heat flow against time, namely initial dissolution, induction, acceleration and deceleration periods (as shown in Fig. 7-2). The initial peak with relatively high heat flow is attributed to the initial wetting and dissolution of materials, while the second peak refers to the formation of hydration products [107].

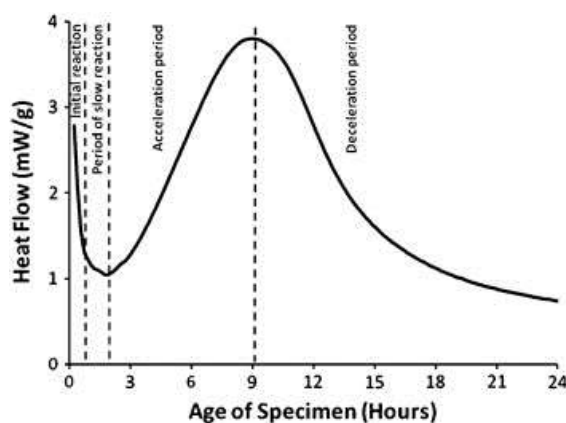


Fig. 7-2 Rate of hydration as a function of time given by isothermal calorimetry measurements ([106])

Isothermal calorimetry measurement was also performed in this study on different kinds of mixtures to reveal the effect of blending various ratios of treated BA into cement on the development of hydration heat. Results are presented in heat flow and total cumulative heat against time, and the cumulative curve is the integration of heat flow. Meanwhile, as shown in Fig. 7-3, some characteristic values are defined as follows:

- q_1 : The minimum heat flow.
- t_1 : The time when minimum heat flow occurs.
- q_2 : The maximum heat flow.
- t_2 : The time when peak value of heat flow occurs.
- Q_{12} : Cumulative heat at 12 hours.
- Q_{24} : Cumulative heat at 24 hours.
- Q_{120} : Cumulative heat at 5 days.

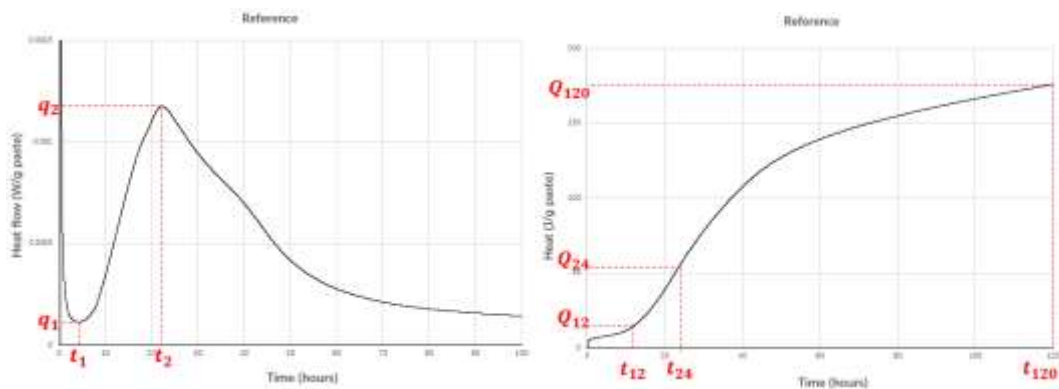


Fig. 7-3 Definition of characteristic points of heat flow and cumulative heat curves

The development of heat flow with different kinds of mixtures (including pure cement, cement blended 10% MTBA, 10% M300 and 10% MBA) during the hydration process are plotted in Fig. 7-4. Different features were observed in each profile. In general, a peak value of heat flow occurred in each curve at around 20 hours during the hydration process. There is no significant difference between the maximum heat flow of pure cement and 10% MTBA, however the maximum heat flow of MBA and M300 decreased 12.18% and 9.29% separately. Meanwhile, a remarkable delay of the peak value is observed in 10% MBA group and the maximum heat release rate is even smaller than 10% M300, which proved that the addition of MBA negatively affected the hydration process and the early-stage performance is even worse than pure sand. Moreover, a heat flow stronger than that in pure cement is detected in 10% MTBA and 10% MBA in deceleration stage.

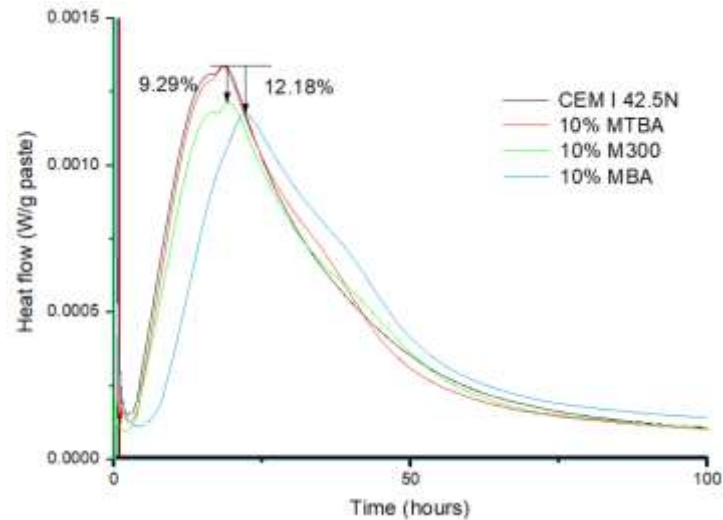


Fig. 7-4 Heat flow normalized to mass of paste at 20°C with w/c=0.5 (CEM I 42.5N, 10% MTBA, 10%MBA, 10%M300)

The total amount of heat released during the hydration process per unit mass of paste is derived by integrating the normalized heat flow over time, and the result is depicted in Fig. 7-5. Cement blended with 10% MBA exhibited rather slow early-stage heat development, so that the cumulative heat before 40 hours is even lower than that of 10% M300. However, a reversal occurred at around 40 hours and after that the total amount of heat release of 10% MBA is higher than that of 10% M300. Eventually, at the end of 5 days, the cumulative heat of 10% MBA and 10% MTBA nearly reached the same level, which is 2.23% lower than that of pure cement. Meanwhile, the cumulative heat of 10% M300 is 15.47% lower than that of pure cement, which proved that BA has a certain pozzolanic reactivity and the contribution of pretreatment to the hydration process. To be specific, the thermal treatment mainly activated the BA and accelerate the early-stage heat development.

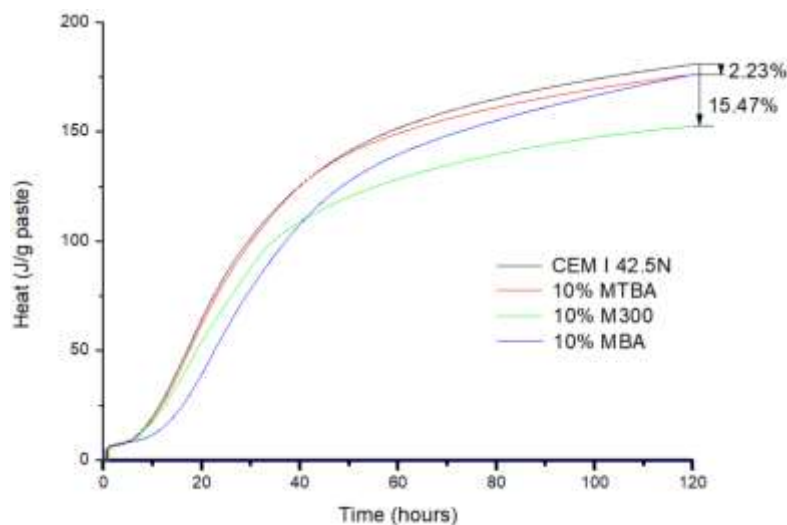


Fig. 7-5 Amount of heat released normalized to mass of paste at 20°C with w/c=0.5 (CEM I 42.5N, 10%MTBA, 10%MBA, 10%M300)

Effect of thermal treatment on the performance of BA could be distinguished by comparing the differences of characteristic parameters in heat flow among different curves (given in Table 7-2). Comparing with pure cement, the addition of MBA retarded and extended the hydration process obviously, so that the maximum heat release rate (q_2) is delayed approximately 240 minutes while the acceleration stage ($t_2 - t_1$) is extended for about 20%. As for the cumulative heat, cement blended with 10% MBA released minimal amount in the early stage (Q_{12} 48% lower than pure cement, and Q_{24} 32% lower than pure cement). However, more heat was released later so that Q_{120} of 10% MBA is almost the same as pure cement, which indicates that the addition of MBA would result in retardation of cement hydration especially in the early-stage. On the other hand, the addition of MTBA didn't result in severe retardation, the identical trend of heat development has been observed between cement blended with 10% MTBA and pure cement.

Table 7-2 Characteristic calorimetric parameters of 10% substitution

	Time (hours)			Heat flow (mW/g)		Cumulative heat (J/g)		
	t_1	t_2	$t_2 - t_1$	q_1	q_2	Q_{12}	Q_{24}	Q_{120}
CEM I 42.5N	2.507	18.23281	15.72581	0.15329	1.338385	27.57863	81.63767	180.91886
10% MTBA	2.576915	18.52477	15.947855	0.128284	1.33528	25.88033	79.18368	176.25869
10% MBA	4.225463	22.2746	18.049137	0.113532	1.175687	14.35983	55.34735	175.848
10% M300	1.941254	19.355265	17.414011	0.095734	1.214052	22.35207	71.48658	171.73444

Therefore, in general, MTBA showed a more beneficial effect on the hydration process when blended with cement. According to the existing studies, the retardation effect of BA on cement hydration could be attributed to the following mechanisms. *Arickx* et al. found out that the remaining organic (mainly fulvic and humic acids) matter may lead to the retardation of cement hydration [83]. *Weeks* et al. mentioned that the heavy metals may disturb the hydration process by attaching on the surface of cement particles [108]. Thermal treatment mainly enhanced the heat development and reduced the retardation in the early-stage throughout the hydration process by removing the unburned organic matters and creating reactive phases.

7.1.1.3. Hydration product

The hydration process was stopped at the end of 28 days, and samples of different pastes were crushed into powders. Crystalline phases generated in hydration reaction and amount of hydration products were checked by XRD and TGA separately.

7.1.1.3.1. XRD

Crystalline phases of hydration products in different mixtures were checked by XRD, and the results are presented in Fig. 7-6. The main products of the hydration process detected are ettringite, portlandite, which is in parallel with the literature study, and a certain amount of calcite was found in pure cement as well. Calcite was detected between 25° and 70° with the main peak at around 29.3° , while the Portlandite was distributed in the full range of XRD detection with main peaks at around 18° , 34° and

70°. Meanwhile, ettringite was detected between 15° and 60°.

It is promising to find out that the XRD curve of 10% MTBA is almost identical to that of pure cement, which means the kind and amount of hydration products detected by XRD of two mixtures are at the same level. The result also proved the contribution of MTBA to the hydration reaction in cement. However, several peaks of quartz were detected in 10% MTBA as well which is attributed to the existence of high SiO₂ content in BA (characterized by XRF).

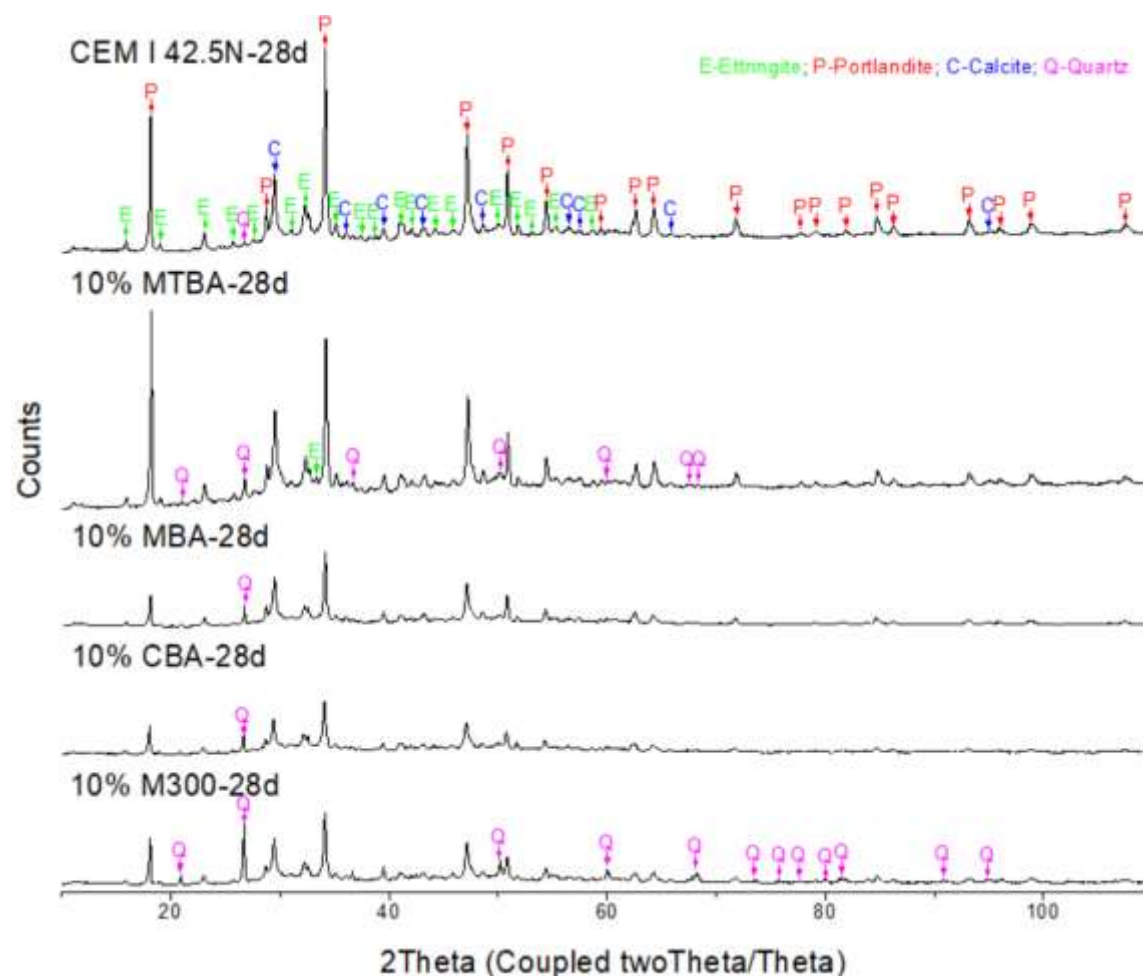


Fig. 7-6 XRD diffractograms of paste with pure cement, MTBA, MBA, CBA and M300

The situation turns much worse in pastes with 10% MBA, 10% CBA and 10% M300 that a dramatic drop was observed in the intensity of peaks corresponding to calcite, portlandite and ettringite, and some of the peaks even vanished. The results proved the poor hydration degree of those mixtures, which is also in agreement with the result of compressive strength tests. On the other hand, more peaks of quartz were detected which is due to the existence of high level SiO₂ content in those substitute materials. Comparing with 10% MBA and 10% M300 paste, the broadness of paste with 10% CBA is even worse that the peaks became more narrow accompanied with the decrement of intensity, and all peaks vanished from 70° to 110°, which proves again that more reactive phases were dissolved during chemical treatment and contribute less

to the hydration products.

In the paste with 10% M300, an obvious main peak of quartz was detected at around 26° with a large number of subpeaks of quartz distributed between 20° and 100° , which is due to the addition of pure sand. However, the peaks representing main hydration products in 10% M300 paste are still stronger than that in 10% CBA.

7.1.1.3.2. TGA

Hydrated cement paste mainly consists of four kinds of compounds, namely tricalcium silicate (C_3S), dicalcium silicate (C_2S), tricalcium aluminate (C_3A) and tetracalcium aluminoferrite (C_4AF) [97]. The most important hydration products are the calcium silicate hydrate ($C - S - H$) and portlandite (CH) [92].

Thermogravimetric (TG) analysis was conducted here to determinate the amount of hydration product in 28-day paste samples. TG curves of pure cement, 10% M300, 10% CBA, 10% MBA and 10% MTBA are plotted against temperature in Fig. 7-7. It is evident that the trends of mass loss throughout the temperature history are, and three rapid weight loss processes are detected.

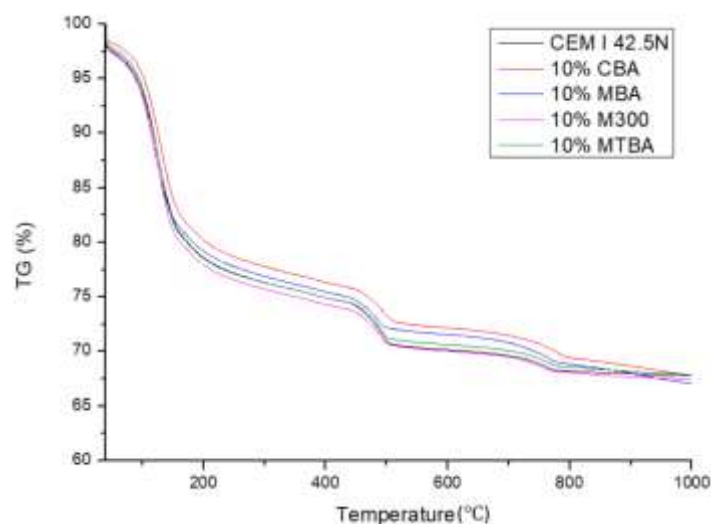


Fig. 7-7 TGA curves of cement paste with CBA, MBA MTBA and M300

The DTG curves of cement paste with CBA, MBA MTBA and M300 are summarized in Fig. 7-8, which better reveals each process by showing the details of inflexion points and plateaus features that are not present in TGA curves. A change in TGA slope is reflected as a marked peak in the DTG [97].

The first peak of mass loss in the DTG curve between 100°C and 300°C corresponds to the dehydration of several kinds of hydration products, such as $C - S - H$, ettringite and carbonaluminum hydrates etc. The second peak of weight loss is mainly related to the water loss from dihydroxylation of another hydration product namely portlandite ($\text{Ca}(\text{OH})_2$ or CH), which is located between 450°C and 500°C . The third peak of weight loss occurs at around 750°C refers to the decarbonation of calcium carbonate (from clinker and filler materials) accompanied with the emission of carbon dioxide

[97].

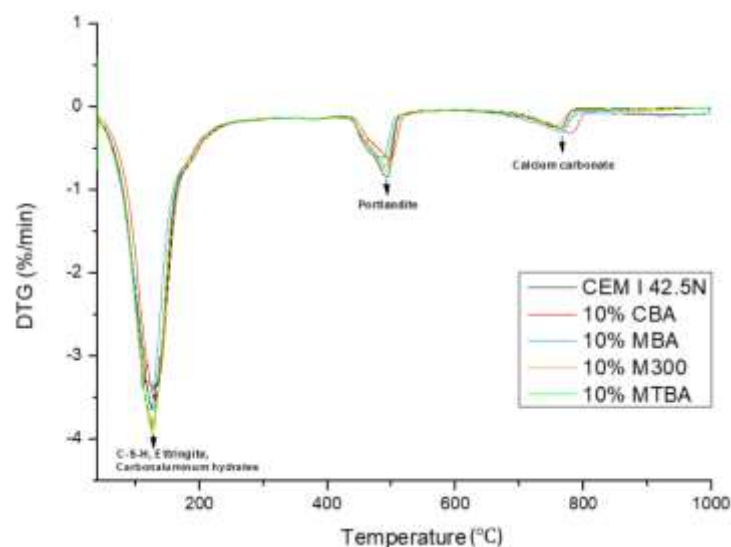


Fig. 7-8 DTG curves of cement paste with CBA, MBA MTBA and M300

Characteristic values of TGA, DTG and DSC curves of the three phases are summarized in

Table 7-3 (details of data are given in Appendix B, C and D), which will be later used for estimation of hydration products in different pastes.

Table 7-3 Characteristic values of TGA, DTG and DSC curves of cement paste with CBA, MBA MTBA and M300

		CEM I 42.5N	10% M300	10% CBA	10% MBA	10% MTBA
105 – 300°C	Mass loss in TG (%)	8.53	8.07	5.68	8.21	8.90
	Peak in DTG (°C)	126.5	124.0	131.3	121.6	127.0
	Area in DSC (mW/mg)	488.6	518.6	484.7	476.3	466.6
400 – 550°C	Mass loss in TG (%)	2.69	2.30	1.98	1.82	2.39
	Peak in DTG (°C)	493.5	489.1	497.3	485.2	492.0
	Area in DSC (mW/mg)	117.01	93.65	86.72	77.86	101.33
700 – 900°C	Mass loss in TG (%)	0.43	0.02	0.54	0.41	0.31
	Peak in DTG (°C)	760.9	752.2	777.3	763.2	765.0
	Area in DSC (mW/mg)	11.96	7.81	19.58	17.08	7.60

In pure cement pastes, the amount of non-evaporable water and calcium hydroxide (CH) contents are usually investigated to indicate the degree of hydration progress [109, 110]. CH contents could be roughly estimated by measuring the mass loss in TGA from 400°C to 550°C. However, the determination of non-evaporable water could be even complex since the loss of mass happens continuously from 105°C to 1000°C, and the detection of which could be disturbed by the incineration of unburned organic matters, the dihydroxylation of CH (400 – 550°C) or the decomposition of calcium

carbonate (700 – 900°C). In this study, the non-evaporable water is determined by the following equation:

$$w_{ne} = w_1 - w_2 - w_3 - (L_i r_i + L_c r_c) \quad (6)$$

where w_{ne} is the non-evaporable water content, w_1 , w_2 and w_3 are the mass loss in TGA as shown in Fig. 7-9 representing the mass loss from 105°C to 1000°C, the dihydroxylation of CH and the decomposition of calcium carbonate, respectively. L_i and L_c are the LOI of each kind of substitute material and cement, while r_i and r_c are representing the mass percentage of each substitute material and cement in paste respectively. Here the LOI of CBA and MBA are estimated to be the same as raw BA since the chemical treatment and grinding process will not result in a decrement in organic content.

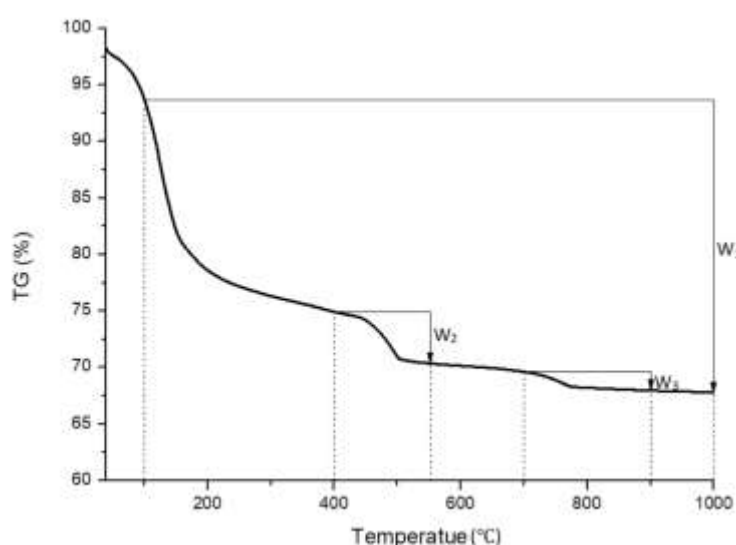


Fig. 7-9 Mass loss in TGA

The result of non-evaporable water and CH content are calculated and summarized in Table 7-4 and Fig. 7-10. The highest content of CH and non-evaporable water are detected in 28-day pure cement, while the content of those is a little bit lower in 10% MTBA and 10% MBA. However, both CH and non-evaporable water contents of 10% CBA is even lower than 10% M300. The result is in agreement with the compressive strength test.

Table 7-4 CH and non-evaporable water content of cement paste with CBA, MBA MTBA and M300

Content (%)	M300				
	CEM I 42.5N	10% M300	10% CBA	10% MBA	10% MTBA
CH	2.69	2.30	1.98	1.82	2.39
Non-evaporable water	11.35	9.43	8.90	9.95	11.06

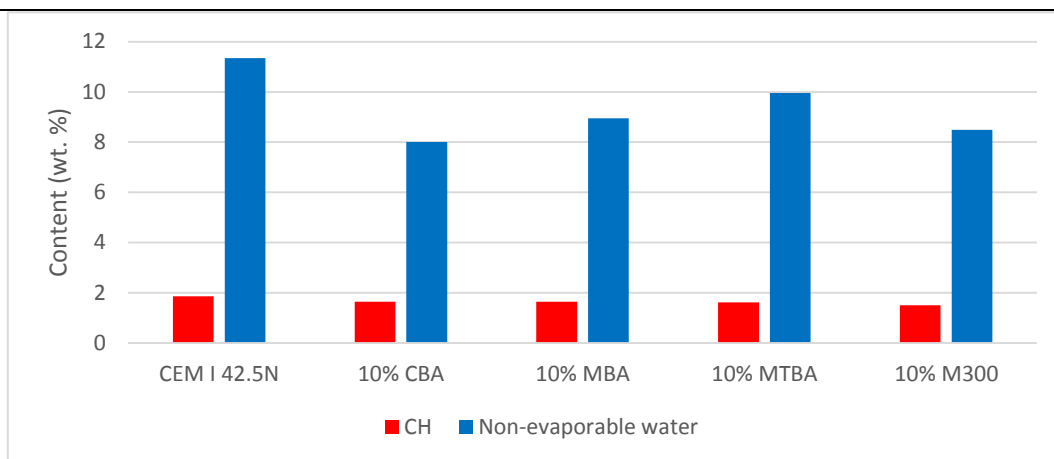


Fig. 7-10 Hydration products of cement paste with CBA, MBA MTBA and M300 per weight of binder

In conclusion, MTBA is the best substitute material with the best performance in compressive strength, hydration heat and hydration products. Comparing with M300, which is pure sand with no pozzolanic reactivity, both MTBA and MBA exhibit better compressive strength with more hydration products. The result indicates the contribution of BA to the hydration reaction. However, MTBA works better than MBA in cement paste, which indicates that thermal treatment removes the unburned organic matters in BA as well as generates new reactive phases. Furthermore, BA is activated and the early-stage heat development is enhanced by the thermal treatment according to the isothermal calorimetry measurement. Nevertheless, the performance of CBA is even worse than that of M300, even though the chemical treatment is regarded as the most effective method in removing metallic content with the lowest residual aluminum content. This could be attributed to that many reactive phases are attacked by alkaline solution during chemical treatment, which is detected by XRD. Therefore, CBA is regarded as a potential filler substitute material, and MTBA is selected as the cement substitute material for further investigation.

7.1.2. Effects of various replacement ratio

7.1.2.1. Compressive strength

Another group of compressive strength test was conducted to investigate the effect of different replacement ratio with MTBA on the compressive strength of cement paste. Meanwhile, micronized sand with no reactivity was selected as the reference. The same ratio of MTBA and M300 were blended with cement and casted into cubes. 1-day, 7-day, 14-day and 28-day compressive strength of different kinds of mixtures were tested according to *EN 196-1*. Three cubes were tested per group, and the average results are given in Table 7-5 and Fig. 7-11 (details of data are given in Appendix A). In general, the compressive strength of pure cement is the highest while 10% MTBA still exhibits better strength than 10% M300. The performance of paste with 10% MTBA was promising that the 7-day and 28-day compressive strength only dropped 4.3% and 28.5 % comparing with *CEM I 42.5N* cement. Unfortunately, a significant drop in compressive strength was observed with the increasing amount of blended MTBA. On

the other hand, however, the performance of MTBA is still much better than that of M300, which proved that the thermal treatment provided certain amount of pozzolanic activity for BA and contributed to the hydration process.

Table 7-5 Compressive strength of cement paste with MTBA and M300

Mixture	Compressive strength (MPa)			
	1-day	7-day	14-day	28-day
Ref. cement	2.946	18.736	34.682	41.834
10% MTBA	2.904	17.929	24.714	29.877
20% MTBA	1.855	10.814	20.441	20.627
30% MTBA	1.36	8.564	16.641	18.106
10% M300	2.217	12.494	17.963	20.250
20% M300	1.245	10.586	16.653	19.133
30% M300	0.998	6.2	10.787	12.024

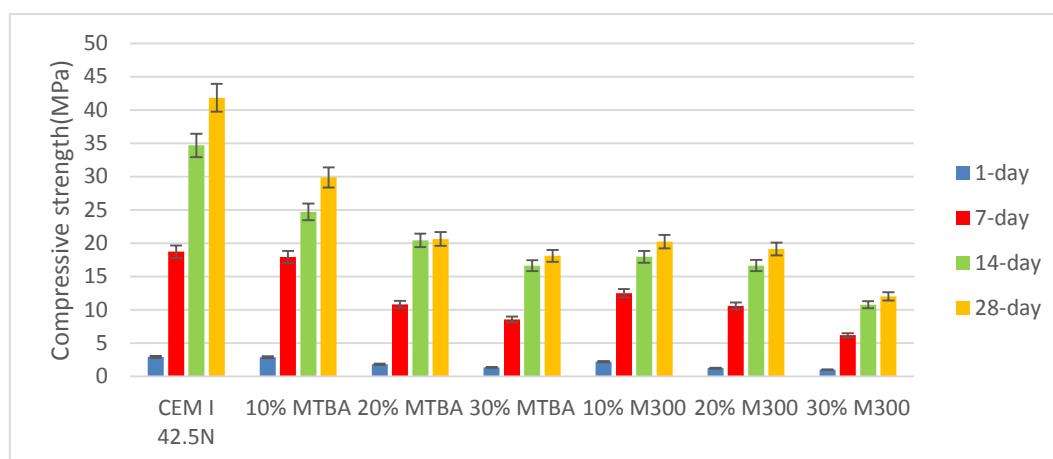


Fig. 7-11 Compressive strength of cement paste with MTBA and M300

The compressive strength development against time of pastes is summarized in Fig. 7-12. It is observed that 10% MTBA almost showed identical strength development as pure cement at the very beginning 7 days. However, the development becomes much slower from 7 to 28 day. The same situations are observed in other pastes as well, that a significant drop in slope of strength development occurs in all groups. Meanwhile, the curves of 20% MTBA, 30% MTBA and all M300 groups from 14 to 28 days are almost parallel to each other, and there is hardly any strength developed in this period. Accordingly, the performance of 10% MTBA is the best among all groups. Moreover, the compressive strength of MTBA is much higher than that of M300 in the same replacement ratio, which proves the contribution of MTBA to the hydration process.

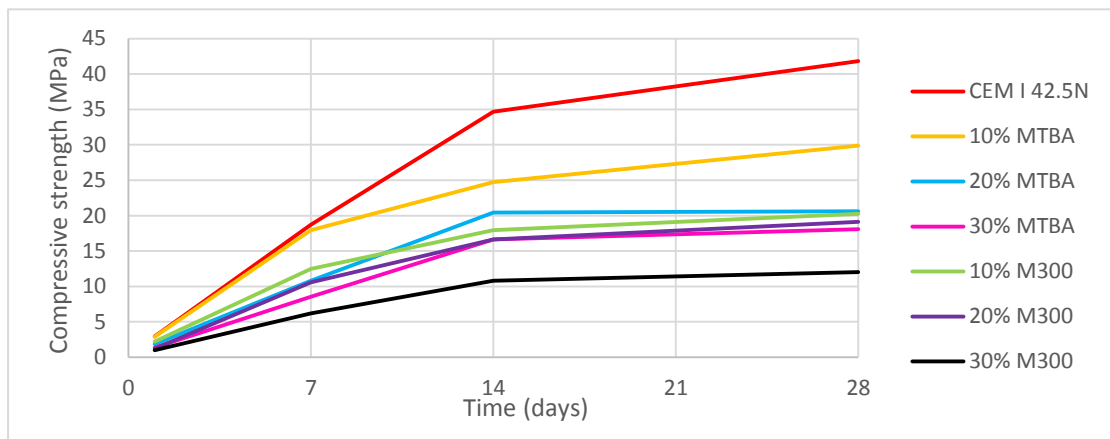


Fig. 7-12 Compressive strength development of cement paste with MTBA and M300

7.1.2.2. Hydration heat

The effect of blending MTBA with cement on hydration process was investigated by blending 10%, 20% and 30% MTBA into cement paste, and the heat flow of each group was measured and plotted against time as shown in Fig. 7-13. Pure cement and same amount of M300 were selected as reference pastes. Characteristic parameters are summarized in Table 7-6.

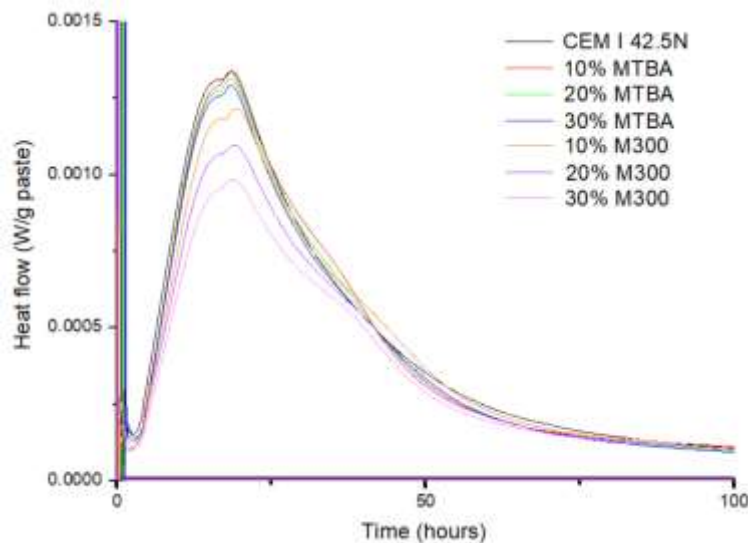


Fig. 7-13 Heat flow normalized to mass of paste at 20°C with $w/c=0.5$ (CEM I 42.5N, 10% MTBA, 20% MTBA, 30% MTBA)

The magnitude of the main peak decreased with the increasing of MTBA substitution rate, while all groups with MTBA reached peak heat flow at around 18.5 hours. All groups with MTBA showed identical heat development trend as pure cement, and the retardation effect of BA has been effectively mitigated by thermal treatment. However, the groups with M300 reached peak heat flow at around 30 minutes later. A more significant drop in peak heat flow intensity is observed in profiles of M300, that the

addition of 30% M300 resulted in q_2 decreased 27% compared with pure cement while the addition of 30% MTBA only decreased 3.5%. The length of acceleration stage is represented by $t_2 - t_1$, so that the addition of M300 leads to this period extended for about 1-2 hours depending on the substitution level, while the addition of MTBA result in neither delay nor extension at all.

Table 7-6 Characteristic calorimetric parameters of MTBA and M300

	Time (hours)			Heat flow (mW/g)		Cumulative heat (J/g)		
	t_1	t_2	$t_2 - t_1$	q_1	q_2	Q_{12}	Q_{24}	Q_{120}
CEM I 42.5N	2.507	18.23281	15.72581	0.15329	1.338385	27.57863	81.63767	180.91886
10% MTBA	2.576915	18.52477	15.947855	0.128284	1.33528	25.88033	79.18368	176.25869
20% MTBA	2.819686	18.34985	15.530164	0.136468	1.313226	26.35936	78.85878	173.97159
30% MTBA	3.017856	18.43976	15.421904	0.142489	1.291508	26.83838	78.53388	171.68449
10% M300	1.941254	19.355265	17.414011	0.095734	1.214052	22.35207	71.48658	171.73444
20% M300	2.336189	19.091212	16.755023	0.102328	1.095603	21.72761	66.05225	158.57204
30% M300	2.544688	18.687621	16.142933	0.106678	0.980414	21.10316	60.61792	145.40965

Besides, a “shoulder” has been detected in each profile with the addition of MTBA in the deceleration stage at around 30-40 hours, which is designated as the “sulphate depletion” peak [111] in pure cement systems and representing the formation of AFm ($\text{Al}_2\text{O}_3 - \text{Fe}_2\text{O}_3 - \text{mono}$) and AFt (ettringite) phases. AFt was formed through the reaction between calcium aluminate and calcium sulphate during the hydration process. The unstable ettringite converted to monosulphate (previously absorbed in C – S – H phase) after the calcium sulphate was completely consumed, which provided free sulphate ions so that the reaction continued [112]. Subsequently, a low broad peak occurred which appears to correlate with the formation of AFm phases [106]. Therefore, the appearance of this “shoulder” in paste containing MTBA (new sulphate source) could be attributed to the formation of AFt and AFm, which is mainly related to sulphate consumption reactions in hydration process [31].

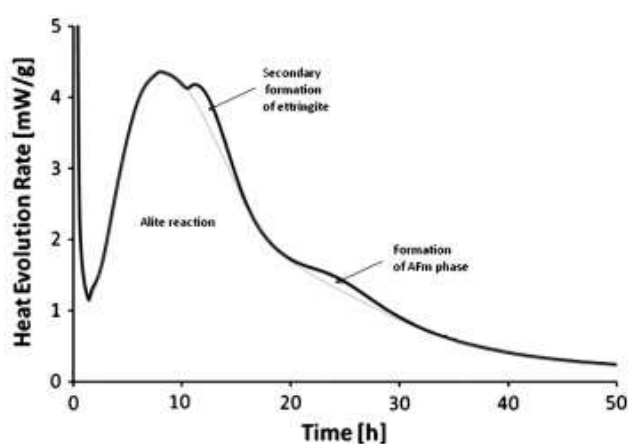


Fig. 7-14 Calorimetry curve of Portland cement, showing typical shoulder peak where a secondary formation of ettringite occurs and subsequent broad peak corresponding to the formation of AFm phase ([106])

Cumulative heat release of each paste is plotted against time as shown in Fig. 7-15. Comparing with pure cement, Q_{24} and Q_{120} of paste with 30% MTBA dropped 4% and 5% separately while Q_{24} and Q_{120} of paste with 30% M300 decreased 26% and 20% separately. Meanwhile, the cumulative heat value of 30% MTBA is always higher than that of 30% M300, which indicates the contribution of MTBA to the hydration process. On the other hand, it is also interesting to find out that Q_{12} increased with the increasing of MTBA substitution rate, which proves that the thermal treatment has effectively eliminated the retardation effect of BA in hydration process and MTBA would contribute more to the early-stage hydration reaction.

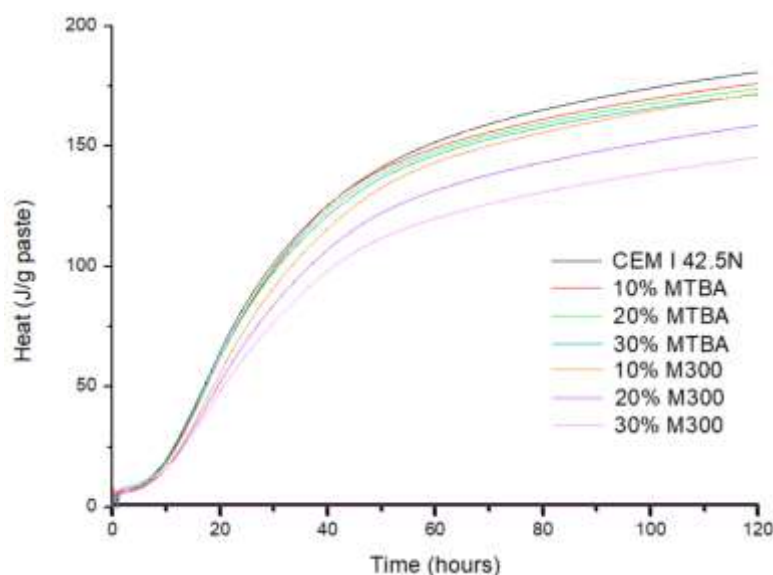


Fig. 7-15 Amount of heat released normalized to mass of paste at 20°C with w/c=0.5 (CEM I 42.5N, 10%MTBA, 10%MBA, 10%M300)

Accordingly, both MBA and MTBA would contribute to the reduction in the total amount of heat release throughout the hydration process. Comparing with pure sand M300, the amount of heat release of MBA at 12 hours is even lower, which indicates the addition of BA in cement paste would result in retardation in the hydration process. However, MTBA exhibited a better performance in early-stage of hydration, which proves that the thermal treatment would effectively fade out the retarding effect of BA by removing the remaining organic matters and creating new reactive phases. Moreover, both MBA and MTBA released much more heat than M300, which indicates the contribution of BA in hydration. Eventually, all groups of MTBA followed the same trend of the heat development of pure cement, and the total amount of heat released by 30% MTBA is still higher than 10% M300. Therefore, MTBA could be a potential substitute material in cement.

7.1.2.3. Hydration product

Crystalline phases generated in hydration reaction and amount of hydration products were checked by XRD and TGA separately at the paste age of 28 days.

7.1.2.3.1. XRD

Crystalline phases of hydration products in different mixtures were checked by XRD, and the results are presented in Fig. 7-16. The main crystalline phases detected by XRD in pure cement were ettringite, portlandite and calcite. The paste with 10% MTBA showed almost identical XRD diffractograms as pure cement with a little bit of quartz detected from 20° to 70° , which could be attributed to the high level of SiO_2 content in BA samples.

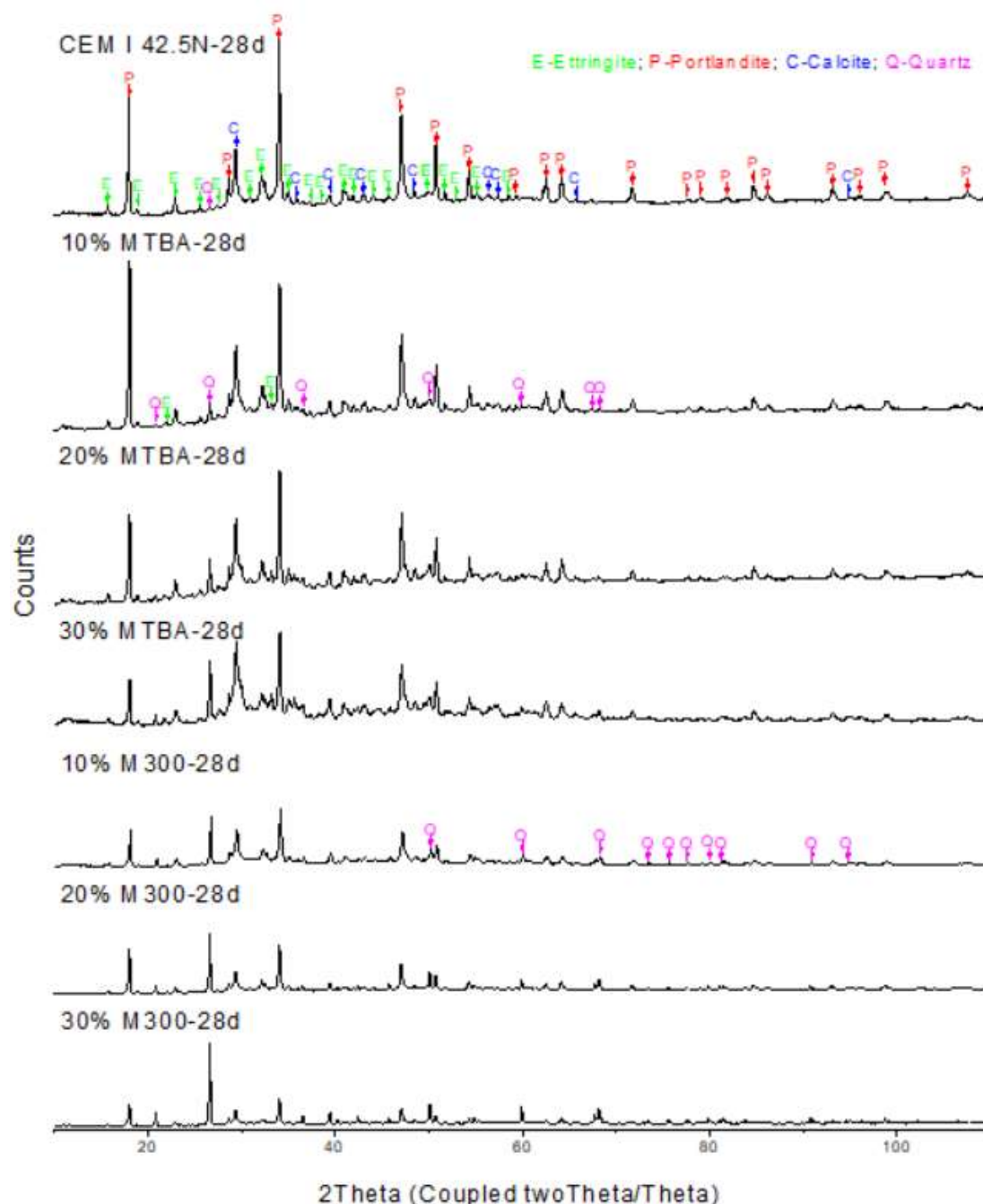


Fig. 7-16 XRD diffractograms of paste with different ratio of MTBA and M300

The effect of blending higher ratio MTBA into cement is quite obvious that a significant drop in intensity of main peaks was detected in both hydration products

(main peaks of portlandite at 18° , 34° and 47° , the main peak of ettringite at 32°). In addition, other subpeaks of portlandite and ettringite became weaker accompanied with the decrement of intensity, and some of them even vanished with the increase of MTBA replacement ratio in the paste. Meanwhile, higher intensity of quartz peaks was detected in 20% MTBA and 30% MTBA pastes, especially the main quartz peak at around 26.6° . Moreover, the same story holds for the peaks representing calcite (main peak at around 29.3°), which mainly comes from filler or clinker in cement paste.

By blending higher ratio M300 into the cement, even sharper peaks of quartz were detected (main peak at around 26.6°). While the peaks of portlandite and ettringite became even lower, and some of which even vanished. However, a decrement of intensity was observed in calcite peaks with the increment M300 replacement ratio, which is exactly opposite from the result in MTBA group. Accordingly, the growth of calcite peaks is proportional to the increment of MTBA substituting level, and the appearance of calcite in hardened cement paste could be partly attributed to the addition of MTBA.

7.1.2.3.2. TGA

MTBA and M300 were blended with pure cement with a replacement ratio from 10% to 30%, and TGA was conducted on 28-day pastes to investigate the effect of various replacement ratio. TG and DTG curves are summarized in Fig. 7-17 and Fig. 7-18. It is obvious that three peaks occurred on the DTG curves as well, which correspond to the dehydration of several kinds of hydration products, the dihydroxylation of CH and the decomposition of calcium carbonate with the increase of temperature separately. Characteristic values of TGA, DTG and DSC curves of the three phases are summarized in Table 7-7 (details of data are given in Appendix B, C, and D).

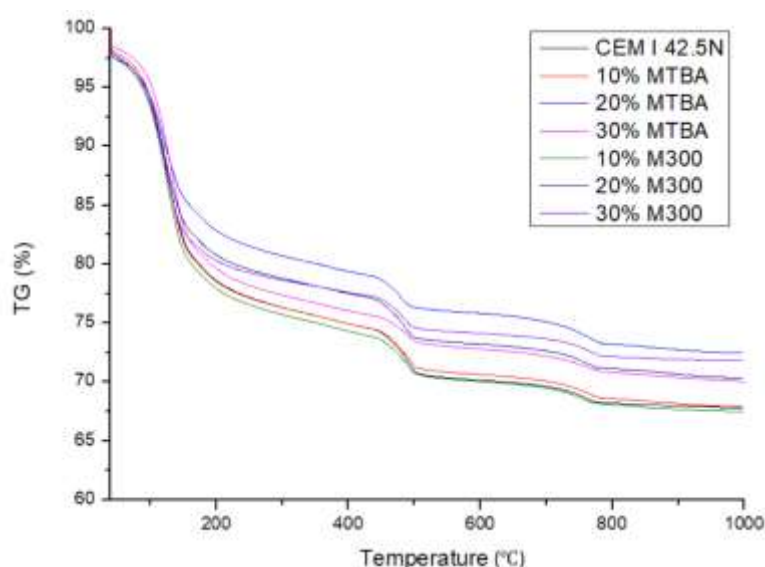


Fig. 7-17 TGA curves of cement paste with different replacement ratio of MTBA and M300

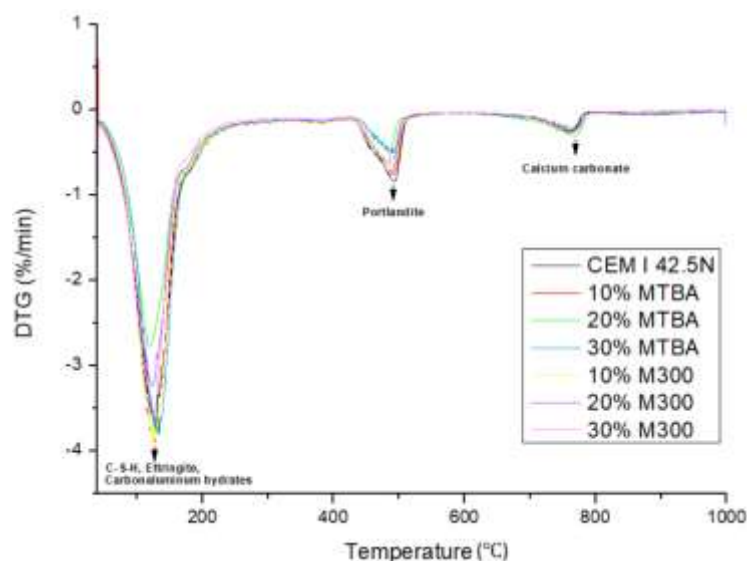


Fig. 7-18 DTG curves of cement paste with different replacement ratio of MTBA and M300

Table 7-7 Characteristic values of TGA, DTG and DSC curves of cement paste with different replacement ratio of MTBA and M300

		CEM I	10%	20%	30%	10%	20%	30%
		42.5N	M300	M300	M300	MTBA	MTBA	MTBA
105 – 300°C	Mass loss in TG (%)	8.53	8.07	7.02	7.07	8.90	7.55	7.12
	Peak in DTG (°C)	126.5	124.0	123.4	123.9	127.0	120.5	133.7
	Area in DSC (mW/mg)	488.6	518.6	397.9	408.6	466.6	374.1	482.2
400 – 550°C	Mass loss in TG (%)	2.69	2.30	2.44	1.86	2.39	1.81	1.38
	Peak in DTG (°C)	493.5	489.1	487.7	486.0	492.0	479.4	491.2
	Area in DSC (mW/mg)	117.01	93.65	103.5	81.71	101.33	77.89	59.91
700 – 900°C	Mass loss in TG (%)	0.43	0.02	0.53	0.41	0.31	0.47	0.01
	Peak in DTG (°C)	760.9	752.2	759.5	768.2	765.0	766.1	763.9
	Area in DSC (mW/mg)	11.96	7.81	16.08	13.78	7.60	14.01	7.60

The total amount of hydration product was estimated by the weight loss of CH and non-evaporable water content of TGA curve using the method mentioned in the previous chapter. Results are presented in Table 7-8 and Fig. 7-19. It is obvious that pure cement contains the highest content of both CH and non-evaporable water, while both MTBA and M300 showed a decrease amount of hydration products with an increasing amount of replacement ratio. However, it is weird that 20% M300 contains even higher content of CH than 10% M300, which might be attributed to experimental error, and the test should be repeated or modified in future investigations.

Table 7-8 CH and non-evaporable water content of cement paste with different replacement ratio of MTBA and M300

Content (%)	CEM I 42.5N	10% M300	20% M300	30% M300	10% MTBA	20% MTBA	30% MTBA
CH	2.69	2.30	2.44	1.86	2.39	1.81	1.38
Non-evaporable water	11.35	9.43	9.34	9.11	11.06	9.83	9.54

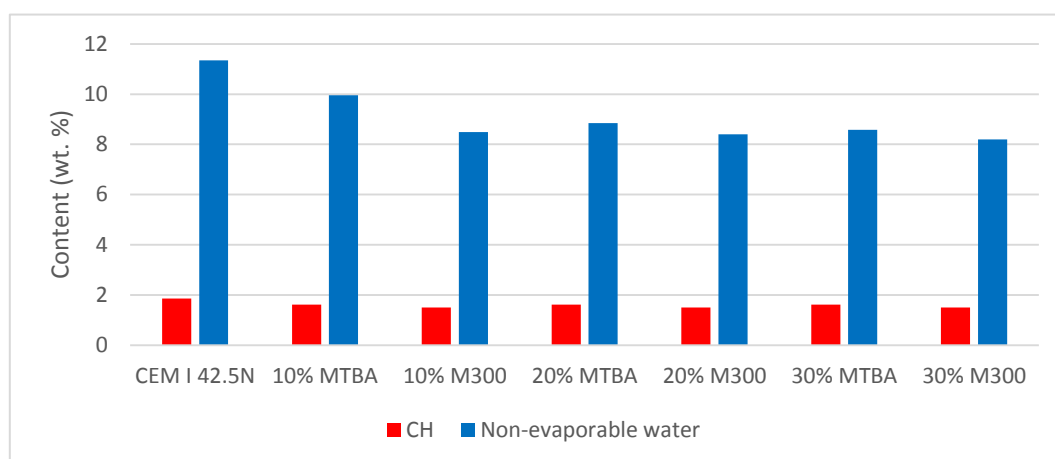


Fig. 7-19 Hydration product of cement paste with different replacement ratio of MTBA and M300 per weight of binder

In conclusion, MTBA exhibited a much better performance in compressive strength, heat development and amount of hydration products than M300, which proves again the contribution of MTBA to the hydration process. Accordingly, MTBA is regarded as a potential substitute material in cement.

7.2. Investigation on concrete level

In this chapter, the performance of MTBA in concrete was tested on the concrete level. B40 concrete was selected as a reference, and MTBA was blended with cement with 10% replacement ratio which works as binder in concrete with a w/c ratio of 0.5.

7.2.1. Workability

The workability of different concrete mixtures was determined according to the slump test. The height of slump was measured immediately after removal of the mold by determining the difference between the height of the mold and that of the highest point of the slumped test specimen (as shown in Fig. 7-20).



Fig. 7-20 Slump measurement

The slump height of B40 concrete and that with 10% MTBA were 5 mm and 10 mm separately, which indicates that the addition of MTBA would result in a negative impact on the consistency of the concrete mixture. This could be attributed to the existence of nonreactive phases in MTBA (quartz and organics), so that the adhesion of binder decreased with the addition of MTBA.

7.2.2. Compressive strength

The compressive strength of concrete cubes (100*100*100 mm in dimension) was tested on 1, 7, 14 and 28 days, and the results are illustrated in Fig. 7-21. A decrement of compressive was detected with the addition of MTBA, which is in parallel with the result of paste compressive strength test. The drop in compressive strength could be attributed to the nonreactive phases in MTBA. However, the compressive strength of concrete with 10% MTBA in cement is still considerable. This decrement could be compensated by denser mixture design (improve packing density) or lower water to cement ratio.

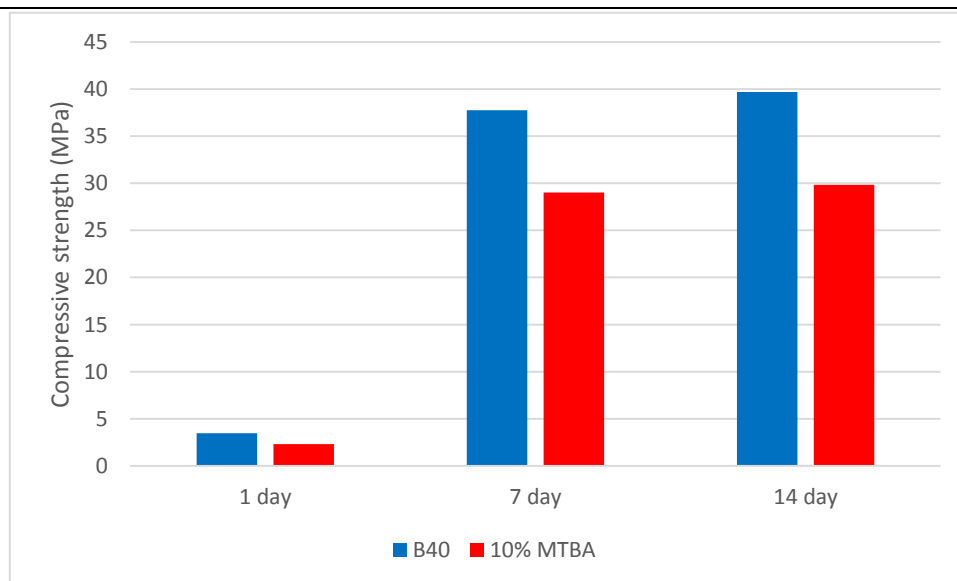


Fig. 7-21 Compressive strength of B40 concrete and 10% MTBA replacement in cement

However, only one cube was tested in each group since the massive production of MTBA is extremely difficult to be accomplished in the lab. The test should be repeated in future investigations if possible.

8. Results and discussion

In this chapter, the results of the experiments in previous chapters are summarized and discussed in perspective of the problem statement and the research goal.

8.1. Investigation on substitution materials

In this part, the characterization of raw BA was performed and the properties including crystalline phases and chemical compositions were compared with that of pure cement to find out the problems of as-received BA. Pretreatment was carried out to solve the problems so that the properties of BA could be improved as a substitute material in concrete. Finally, BA samples were characterized again to reveal the effects of different treatment methods.

8.1.1. Characterization of raw BA

At the beginning, as-received BA was characterized, including morphology, crystalline phases and chemical composition.

According to the result of the ESEM test, a high-porosity morphology of BA particles was observed, which would result in strength decrement when used as substitution material in cement with the following two mechanisms. Firstly, the strength of concrete with BA substitution would drop directly since pores and microcracks reduced the strength of BA particle itself and result in failure easily. Furthermore, the pores on BA particles work as water reservoirs affecting moisture transport in concrete [26, 55], extra water absorption may eventually reduce the amount of water available to react with cement and indirectly affect the strength development.

Crystalline phases of as-received BA were detected by XRD test. A large number of peaks representing quartz (SiO_2), calcite (CaCO_3), akermanite ($\text{Ca}_2\text{MgSi}_2\text{O}_7$) and magnetite ($\text{Fe} + 2\text{Fe}_2 + 3\text{O}_4$) have been observed in BA. Comparing with pure cement more nonreactive crystalline phases and less reactive amorphous phases were detected, which is consistent with the poor reactivity of BA reported in the literature review.

Elemental compositions of BA were determined by XRF. Results showed that BA samples contain more SiO_2 , Fe_2O_3 and Al_2O_3 , and less CaO than cement, which is in parallel with XRD result that a large number of quartz peaks were detected.

Unburned organic contents were checked by LOI test. Relatively high unburned organic contents were detected in BA samples which is nonreactive and inhibiting the hydration reaction when used as substitute materials in concrete and should be removed.

The metallic aluminum content was determined by dissolving test, and high content of that was detected which would generate a large amount of hydrogen bubbles in cement paste and result in a decrement in strength. The metallic aluminum should be removed as well before used as substitute in concrete.

8.1.2. Pretreatment

According to the result of raw BA characterization, the metallic aluminum content was the biggest issue to be solved in BA at the first place. Both chemical and physical treatment were performed on BA to get rid of the aluminum.

Additionally, a mortar strength test was performed after removing the metallic aluminum to reveal the effect of treatment by blending MBA into cement powder and comparing to that of the same amount of BFS and M300. No severe expansion or obvious air bubbles were detected in all samples which proved the remaining metallic aluminum content is already acceptable, and both physical and chemical treatment were effective enough to remove the aluminum (metallic aluminum content of CBA is even lower than that in MBA). Here samples with CBA were not casted since both the metallic aluminum content in MBA and CBA are acceptable and CBA contains less reactive phases according to XRD results so that a lower strength than MBA could be expected. The compressive strength of mortar with MBA is lower than that with pure cement and same ratio of BFS, which indicates that the reactivity of MBA is lower than that of cement and BFS. However, the compressive strength of mortar with MBA is still higher than that with the same amount of M300 with no reactivity. Therefore, MBA is already good enough to be used as filler in concrete.

Subsequently, it was decided to perform thermal treatment to get BA samples activated by generating reactive phases and investigate the feasibility of treated BA to be used as binder substitution materials in concrete. Furthermore, the unburned organic matters and remaining metallic aluminum in BA could be removed as well by thermal treatment.

8.1.3. Characterization of treated BA

The particle size distribution, morphology, crystalline phases and chemical composition of treated BA samples were checked again to reveal the effect of different treatment methods.

The particle size distribution of each type of treated BA sample was controlled at the same level, which is even finer than that of the reference cement powder and contribute to denser packing in cement paste.

The ESEM showed that the number and diameter of pores on BA particles became much smaller after thermal treatment, which would work much better in cement substitution.

Crystalline phases of treated BA samples were determined by XRD. Comparing with as-received BA, no significant difference was observed in MBA and CBA, which indicates that the grinding or chemical washing process didn't generate new phases. However, it is observed that both the intensity and width of peaks are decreased in CBA comparing that in BA and MBA, and those reactive amorphous crystalline phases were dissolved together with the metallic aluminum during the chemical treatment. As for QMBA and MTBA, thermal treatment mainly accelerates the decomposition of calcite as well as the oxidation of metallic iron and aluminum content, while some reactive phases such as wollastonite are generated at the same time. Comparing with QMBA, MTBA is more desirable since more peaks of reactive phases and oxidation phases were detected which would contribute more to strength development and mitigate the expansion and swelling due to metallic metals.

According to the result of XRF, a similar elemental composition has been observed among all kinds of treated BA. However, the silica oxide content became higher after

treatment while the calcium oxide content dropped. Meanwhile, the treatment also further removed the hazard contents such as heavy metals (Al, Mg, Cu and Zn) and salts (chloride and SO_3).

The metallic aluminum content of treated BA samples was determined again by dissolving tests. The result showed that both chemical treatment with sodium solution and physical treatment with grinding and sieving are effective enough to remove the metallic aluminum content in as-received BA. The aluminum content in MTBA is even lower than that in MBA, which proved that thermal treatment accelerated the oxidation of remaining metallic aluminum content in BA samples.

8.2. Investigation on cement paste level

In cement paste, the study was divided into two parts. In the first part, same amount of BA samples with different pretreatment methods were blended into the cement paste to show the effect of different treatment method, and the optimum pretreatment method was found out within this research. Furthermore, different ratio treated BA samples were blended into cement and investigate the effect of different replacement ratio so that maximum replacement ratio was derived.

The performances of different pastes were evaluated by compressive strength, hydration heat and hydration products (TGA and XRD), in which the compressive strength respond to the quality of BA substituted cement intuitively, and hydration heat and products could help explain how much BA contribute to the hydration process comparing to pure cement and the decrement in compressive strength

8.2.1. Effect of different treatment method

The compressive strength of different pastes follows the trend pure cement > MTBA > MBA > M300 > CBA. The result indicates that both MBA and MTBA would contribute more to the hydration process and strength development than pure sand, while the performance of CBA is even worse than pure sand.

The hydration heat development was measured for each paste from 0 to 120 hours, and heat flow and cumulative heat development were derived. There is no significant difference between the maximum heat flow of pure cement and 10% MTBA, however the maximum heat flow of MBA and M300 decreased 12.18% and 9.29% separately. Meanwhile, a remarkable delay of the peak value of heat flow is observed in 10% MBA group and the maximum heat release rate is even smaller than 10% M300. In the cumulative heat measurement, cement blended with 10% MB A exhibited even slower early-stage heat development than 10% M300. Eventually, at the end of 5 days, the cumulative heat of 10% MBA and 10% MTBA nearly reached the same level, which is 2.23% lower than that of pure cement. Meanwhile, the cumulative heat of 10% M300 is 15.47% lower than pure cement. Therefore, the addition of MBA retarded the hydration process and the early-stage performance is even worse than pure sand, which is in parallel with the result of mortar strength test that the 1-day strength of 10% and 30% MBA is lower than that with the same amount of M300. In addition, according to hydration heat development, thermal treatment mainly activated the BA and accelerate the early-stage heat development.

Crystalline phases of pastes were examined by XRD at the age of 28 days. It was

found that the XRD curve of 10% MTBA is almost identical to that of pure cement, which means the kind and amount of hydration products detected by XRD of two mixtures are at the same level. However, in pastes with 10% MBA, 10% CBA and 10% M300 that a dramatic drop was observed in the intensity of peaks corresponding to calcite, portlandite and ettringite, and some of the peaks even vanished. The results proved the poor hydration degree of those mixtures, which is also in agreement with the result of compressive strength tests. Meanwhile, peaks refer to nonreactive quartz were detected in all groups with BA substitution.

Amount of main hydration products (portlandite and non-evaporable water) were estimated by the mass loss during the TG analysis. The result is also in agreement with strength test that amount of hydration products of MTBA is the highest among all substitute materials

In conclusion, the ability of cement replacement of different substitute materials follows the trend that $MTBA > MBA > M300 > CBA$. Therefore, route of the best pretreatment method within this study is given in Fig. 8-1. The result also indicates MBA is already good enough to be used as filler substitute material in concrete which is much better than M300 with no reactivity. Moreover, proper thermal treatment could further get BA activated which could be potentially used as binder substitution materials. However, whether thermal treatment is suitable and applicable in the industry is still debatable since it could be highly energy consuming or highly polluting.



Fig. 8-1 Route of the best pretreatment method within this study

8.2.2. Effect of various replacement ratio

The compressive strength of paste with 10% MTBA was promising that the 7-day and 28-day results only dropped 4.3% and 28.5% compared with pure cement. However, a significant drop in compressive strength was observed with the increasing amount of blended MTBA. On the other hand, the performance of MTBA is still much better than that of M300, which proved that the thermal treatment provided certain amount of activity for BA and contributed to the hydration process. Moreover, it is also observed that there is almost no difference between 1-day and 7-day compressive strength of pure cement and 10% MTBA while the strength dropped a lot at the end of 28 days, which might be attributed to the finer particle size distribution of MTBA than cement that more reactive phases were consumed at the early-stage of reaction.

The hydration heat development was measured for each paste from 0 to 120 hours. The decrement of both peak heat flow and cumulative heat development were detected with the increasing of MTBA and M300 substitution rate. However, the performance of 30% MTBA is still better than 10% M300.

Crystalline phases of hydration products in different mixtures were checked by XRD.

The effect of blending higher ratio MTBA into cement is obvious that a significant drop in intensity of main peaks was detected in both hydration products (portlandite and ettringite) while the intensity of quartz peaks became higher, which is in agreement with the characterization of substitution materials that high content of quartz was detected in BA. By blending higher ratio M300 into the cement, even sharper peaks of quartz were detected while the peaks of portlandite and ettringite became even lower. However, a decrement of intensity was observed in calcite peaks with the increment M300 replacement ratio, which is exactly opposite from the result in MTBA group. The appearance of calcite in hardened cement paste could be partly attributed to the addition of MTBA.

The amount of main hydration products (portlandite and non-evaporable water) were estimated by the mass loss during TGA test. Both MTBA and M300 showed decrease amount of hydration products with an increase amount of replacement ratio.

In conclusion, a maximum replacement ratio of MTBA is derived as 10% that the compressive strength of cement paste at 28 days decreased by less than 30%. Moreover, the results of hydration heat and crystalline phases of paste with 10% MTBA substitution is still promising that is almost identical to pure cement. Furthermore, the strength development of paste with 10% MTBA is much worse than that of pure cement, which might be attributed to the finer particle size distribution that more reactive phases were consumed at the early-stage of reaction. Finally, the strength of paste with BA substitution could be further improved by optimizing the pretreatment method or adjusting mixture design.

8.3. Investigation on concrete level

MTBA with 10% replacement ratio was selected here as binder substitution in B40 concrete mix. Workability and compressive strength were tested.

A higher slump value was detected in the fresh concrete mixture with MTBA, which indicates that the addition of MTBA would result in a negative impact on the consistency of the concrete mixture. This could be attributed to the existence of nonreactive phases in MTBA.

A decrement of compressive was detected with the addition of MTBA, which is in parallel with the result of paste compressive strength test. The drop in compressive strength could be attributed to the nonreactive phases in MTBA. This decrement could be compensated by denser mixture design (improve packing density) or lower water to cement ratio.

9. Conclusions and recommendations

9.1. General conclusions

According to the experiments and results presented in previous chapters, the following conclusions are made with respect to the compositions, properties and different kinds of pretreatment methods for MSWI BA. The influence of BA addition as a binder and as a filler on chemical, physical and mechanical properties of cement paste and concrete were evaluated.

- Relatively identical chemical compositions were detected from as-received BA and Portland cement powder, which indicates that the potential application of BA to be used as cement substitute material in concrete. However, the content of each substance varies between BA and cement.
- The as-received BA contains high content of impurity substance, such as glass, bricks, metals, and unburned organics etc. Meanwhile, a high-porosity morphology was observed under ESEM detection. Moreover, high content of metallic aluminum was detected as well according to the dissolving test, which will result in a large amount of hydrogen bubbles in cement paste. Therefore, proper pretreatments are required to improve the properties of BA before they could be used in cement.
- Two methods were proposed to get rid of the metallic aluminum content in BA, including chemical (CBA: immersing in sodium hydroxide solution) and physical (MBA: a combination of grinding and sieving) treatments. Both methods were proved to be effective enough to remove the metallic aluminum, and the aluminum content after chemical treatment was even lower. However, chemical treatment is less desired since more crystalline phases were attacked by alkaline solution as well during the treatment, which is proved by the paste strength test that the compressive strength of paste with 10% CBA is lower than that with 10% MBA and 10% M300.
- Thermal treatments were performed as well on BA samples to get them activated by generating new reactive phases, which were detected by XRD. Two methods were proposed here either by quenching (QMBA) or heating up to 1000°C (MTBA) to generate reactive phases and remove the unburned organics, and the result of a preliminary compressive strength test showed that MTBA performed much better than QMBA, which was selected for further investigation.
- A denser matrix with few pores or microcracks of MTBA were observed under ESEM detection after thermal treatment. Meanwhile, XRD results showed that more reactive phases were generated in MTBA than that in QMBA, which is in parallel with the compressive strength test.
- The effect of different treatment methods was evaluated by blending them into cement pastes, and compressive strength of different ages, hydration heat development and amount of hydration products were checked separately. The results indicate that the ability of cement replacement of different substitute materials follows the trend that BFS > MTBA > MBA > M300 > CBA.
- The hydration heat development measurement revealed that the addition of MBA

in cement would result in the retardation in heat release that the hydration process could be weakened and extended. However, this effect was not detected in pastes with MTBA, and the result of cumulative heat measurement also showed that the thermal treatment mainly activated the BA and accelerate the early-stage heat development.

- Hydration products were checked by XRD and TGA tests. It was promising that the XRD result of 28-day pastes with 10% MTBA is almost identical to that of pure cement. The amount of main hydration products (CH and non-evaporable water) were estimated according to mass loss in TGA, and the content of those in MTBA is also the highest among all substitute materials.
- The performance of CBA is even worse than that of pure sand with no reactivity, which may be ascribed to the existence of unburned organics and that the reactive phases were dissolved by chemical treatment. On the other hand, MBA works better than M300 in cement paste, which proves the contribution of BA to hydration process since the grinding and sieving process does not generate new crystalline phases at all.
- According to the result of compressive strength, hydration heat development and hydration products, the performance of MTBA is much better than that of M300 at the same replacement ratio, which proves that MTBA is a potential substitute material in cement. However, the performance of pastes with MTBA substitution decreased with the increase replacement ratio.
- In general, MTBA could be a suitable substitute material in cement, and a reasonable replacement ratio is about 10% in cement that there is almost no difference in 1-day and 7-day compressive strength between pure cement paste and that with 10% MTBA. The drop in 14-day and 28-day compressive strength could be attributed to the finer particle size distribution of treated BA comparing to pure cement that more reactive phases were consumed at the early-stage of reaction.
- The result of this study also indicates MBA is already good enough to be used as filler substitute material in concrete since the 7-day and 28-day compressive strength of mortar strength with 10% MBA is higher than that with same amount of M300. Meanwhile, it is also observed that 1-day strength of mortar with 10% MBA is lower than that with 10% M300, which is in agreement with the hydration heat measurement in cement pastes, and the addition of MBA would result in retardation in early-stage of hydration reaction.
- Moreover, proper thermal treatment could further get BA activated which could be potentially used as binder substitution materials. However, whether thermal treatment is suitable and applicable in industry is still debatable since it could be highly energy consuming or highly polluting.

9.2. Recommendations

According to the results of this study, the following recommendations are given both in industry and future investigation fields:

- The decrement of strength while blending BA into cement is mainly due to the

appearance of unburned organic matters and metallic aluminum contents. However, this effect could be mitigated by modifying the incineration process within the plant. The properties of BA could be improved with a more adequate combustion process, e.g. municipal solid waste could be crushed in smaller particles before incineration so that the organics could be further removed or the temperature of combustion could be increased so that the oxidation of metallic aluminum could be accelerated.

- The MSW incineration could be combined with cement clinker production since high temperature occurred in both processes. Furthermore, a high calcium content waste material could be introduced together with the incineration of MSW since BA contains much lower of Ca than pure cement according to XRF results. Accordingly, a much better performance of BA in cement is expected.
- The BA treatment method proposed in this study is only a suggestion since the process of grinding and heating may vary in different labs and plants. Proper tests are required to achieve the same effect of treatment.
- The TG analysis should be repeated if possible in future studies so that the experimental error could be eliminated and the accuracy of hydration products content in hydration product could be guaranteed. Moreover, the method of hydration product estimation could be modified since a certain amount free water and physical bond water could contribute to the mass loss of non-evaporable water as well. The samples should be pre-dried by frozen vacuum so that the water resulting in mass loss in TG before 105°C could be completely removed and the effects are eliminated as well.

References

1. Hoornweg, D. and P. Bhada-Tata, *What a waste: a global review of solid waste management*. 2012.
2. Leckner, B., *Process aspects in combustion and gasification Waste-to-Energy (WtE) units*. Waste management, 2015. **37**: p. 13-25.
3. Wiles, C.C., *Municipal solid waste combustion ash: State-of-the-knowledge*. Journal of hazardous materials, 1996. **47**(1-3): p. 325-344.
4. Li, M., et al., *Characterization of solid residues from municipal solid waste incinerator*. Fuel, 2004. **83**(10): p. 1397-1405.
5. Sabbas, T., et al., *Management of municipal solid waste incineration residues*. Waste management, 2003. **23**(1): p. 61-88.
6. Bosmans, A., et al., *The crucial role of Waste-to-Energy technologies in enhanced landfill mining: a technology review*. Journal of Cleaner Production, 2013. **55**: p. 10-23.
7. Hjelm, O., *Disposal strategies for municipal solid waste incineration residues*. Journal of Hazardous Materials, 1996. **47**(1-3): p. 345-368.
8. Van der Sloot, H., D. Kosson, and O. Hjelm, *Characteristics, treatment and utilization of residues from municipal waste incineration*. Waste Management, 2001. **21**(8): p. 753-765.
9. Chimenos, J., et al., *Characterization of the bottom ash in municipal solid waste incinerator*. Journal of hazardous materials, 1999. **64**(3): p. 211-222.
10. Klein, R., et al., *Temperature development in a modern municipal solid waste incineration (MSWI) bottom ash landfill with regard to sustainable waste management*. Journal of Hazardous Materials, 2001. **83**(3): p. 265-280.
11. Saffarzadeh, A., et al., *Impacts of natural weathering on the transformation/neoformation processes in landfilled MSWI bottom ash: a geoenvironmental perspective*. Waste management, 2011. **31**(12): p. 2440-2454.
12. Kersten, M., et al., *Speciation of Cr in leachates of a MSWI bottom ash landfill*. Environmental science & technology, 1998. **32**(10): p. 1398-1403.
13. Lin, C.-F., C.-H. Wu, and H.-M. Ho, *Recovery of municipal waste incineration bottom ash and water treatment sludge to water permeable pavement materials*. Waste Management, 2006. **26**(9): p. 970-978.
14. Birgisdottir, H., et al., *Environmental assessment of roads constructed with and without bottom ash from municipal solid waste incineration*. Transportation Research Part D: Transport and Environment, 2006. **11**(5): p. 358-368.
15. Toraldo, E., et al., *Use of stabilized bottom ash for bound layers of road pavements*. Journal of environmental management, 2013. **121**: p. 117-123.
16. Siddique, R., *Use of municipal solid waste ash in concrete*. Resources, Conservation and Recycling, 2010. **55**(2): p. 83-91.
17. Pera, J., et al., *Use of incinerator bottom ash in concrete*. Cement and Concrete Research, 1997. **27**(1): p. 1-5.
18. Ginés, O., et al., *Combined use of MSWI bottom ash and fly ash as aggregate in concrete formulation: environmental and mechanical considerations*. Journal of Hazardous Materials, 2009. **169**(1-3): p. 643-650.
19. del Valle-Zermeño, R., et al., *Aggregate material formulated with MSWI bottom ash and APC fly ash for use as secondary building material*. Waste management, 2013. **33**(3): p. 621-627.

20. Forteza, R., et al., *Characterization of bottom ash in municipal solid waste incinerators for its use in road base*. Waste management, 2004. **24**(9): p. 899-909.
21. Song, G.-J., et al., *Characteristics of ashes from different locations at the MSW incinerator equipped with various air pollution control devices*. Waste Management, 2004. **24**(1): p. 99-106.
22. Meima, J.A. and R.N. Comans, *Geochemical modeling of weathering reactions in municipal solid waste incinerator bottom ash*. Environmental Science & Technology, 1997. **31**(5): p. 1269-1276.
23. Meima, J.A. and R.N. Comans, *The leaching of trace elements from municipal solid waste incinerator bottom ash at different stages of weathering*. Applied Geochemistry, 1999. **14**(2): p. 159-171.
24. Arickx, S., T. Van Gerven, and C. Vandecasteele, *Accelerated carbonation for treatment of MSWI bottom ash*. Journal of hazardous materials, 2006. **137**(1): p. 235-243.
25. Bethanis, S., C. Cheeseman, and C. Sollars, *Properties and microstructure of sintered incinerator bottom ash*. Ceramics International, 2002. **28**(8): p. 881-886.
26. Tang, P., et al., *Characteristics and application potential of municipal solid waste incineration (MSWI) bottom ashes from two waste-to-energy plants*. Construction and Building Materials, 2015. **83**: p. 77-94.
27. Verbinnen, B., et al., *Recycling of MSWI bottom ash: a review of chemical barriers, engineering applications and treatment technologies*. Waste and Biomass Valorization, 2017. **8**(5): p. 1453-1466.
28. Wiles, C.C. and P.B. Shepherd, *Beneficial use and recycling of municipal waste combustion residues: a comprehensive resource document*. 1999: National Renewable Energy Laboratory Golden, USA.
29. Eymael, M.T., W. De Wijs, and D. Mahadew, *The use of MSWI bottom ash in asphalt concrete, in Studies in Environmental Science*. 1994, Elsevier. p. 851-862.
30. Li, X.-G., et al., *Utilization of municipal solid waste incineration bottom ash in blended cement*. Journal of Cleaner Production, 2012. **32**: p. 96-100.
31. Tang, P., et al., *Application of thermally activated municipal solid waste incineration (MSWI) bottom ash fines as binder substitute*. Cement and Concrete Composites, 2016. **70**: p. 194-205.
32. Pal, S., A. Mukherjee, and S. Pathak, *Investigation of hydraulic activity of ground granulated blast furnace slag in concrete*. Cement and Concrete Research, 2003. **33**(9): p. 1481-1486.
33. Proctor, D., et al., *Physical and chemical characteristics of blast furnace, basic oxygen furnace, and electric arc furnace steel industry slags*. Environmental science & technology, 2000. **34**(8): p. 1576-1582.
34. Ramsden, A. and M. Shibaoka, *Characterization and analysis of individual fly-ash particles from coal-fired power stations by a combination of optical microscopy, electron microscopy and quantitative electron microprobe analysis*. Atmospheric Environment (1967), 1982. **16**(9): p. 2191-2206.
35. Müller, U. and K. Rübner, *The microstructure of concrete made with municipal waste incinerator bottom ash as an aggregate component*. Cement and Concrete Research, 2006. **36**(8): p. 1434-1443.
36. Pecqueur, G., C. Crignon, and B. Quénée, *Behaviour of cement-treated MSWI bottom ash*.

- Waste management, 2001. **21**(3): p. 229-233.
37. Pan, J.R., et al., *Recycling MSWI bottom and fly ash as raw materials for Portland cement*. Waste Management, 2008. **28**(7): p. 1113-1118.
38. Lam, C.H.K., J.P. Barford, and G. McKay, *Utilization of municipal solid waste incineration ash in Portland cement clinker*. Clean technologies and environmental policy, 2011. **13**(4): p. 607-615.
39. Bertolini, L., et al., *MSWI ashes as mineral additions in concrete*. Cement and Concrete Research, 2004. **34**(10): p. 1899-1906.
40. Gupta, V., et al., *Removal of dyes from wastewater using bottom ash*. Industrial & engineering chemistry research, 2005. **44**(10): p. 3655-3664.
41. Wei, Y., et al., *Mineralogical characterization of municipal solid waste incineration bottom ash with an emphasis on heavy metal-bearing phases*. Journal of Hazardous Materials, 2011. **187**(1-3): p. 534-543.
42. Andreola, F., et al., *Reuse of incinerator bottom and fly ashes to obtain glassy materials*. Journal of hazardous materials, 2008. **153**(3): p. 1270-1274.
43. Rendek, E., G. Ducom, and P. Germain, *Carbon dioxide sequestration in municipal solid waste incinerator (MSWI) bottom ash*. Journal of hazardous materials, 2006. **128**(1): p. 73-79.
44. Qiao, X., et al., *Characterization of alkali-activated thermally treated incinerator bottom ash*. Waste management, 2008. **28**(10): p. 1955-1962.
45. Aubert, J., B. Husson, and A. Vaquier, *Metallic aluminum in MSWI fly ash: quantification and influence on the properties of cement-based products*. Waste Management, 2004. **24**(6): p. 589-596.
46. Wan, X., et al., *A study on the chemical and mineralogical characterization of MSWI fly ash using a sequential extraction procedure*. Journal of Hazardous Materials, 2006. **134**(1-3): p. 197-201.
47. Kim, B. and M. Prezzi, *Evaluation of the mechanical properties of class-F fly ash*. Waste management, 2008. **28**(3): p. 649-659.
48. Nathan, Y., et al., *Characterization of coal fly ash from Israel*. Fuel, 1999. **78**(2): p. 205-213.
49. Zhang, S., et al., *Waste glass as partial mineral precursor in alkali-activated slag/fly ash system*. Cement and Concrete Research, 2017. **102**: p. 29-40.
50. Richardson, I., et al., *The characterization of hardened alkali-activated blast-furnace slag pastes and the nature of the calcium silicate hydrate (CSH) phase*. Cement and Concrete Research, 1994. **24**(5): p. 813-829.
51. Jaturapitakkul, C. and R. Cheerarot, *Development of bottom ash as pozzolanic material*. Journal of materials in civil engineering, 2003. **15**(1): p. 48-53.
52. Kim, B., M. Prezzi, and R. Salgado, *Geotechnical properties of fly and bottom ash mixtures for use in highway embankments*. Journal of Geotechnical and Geoenvironmental Engineering, 2005. **131**(7): p. 914-924.
53. Bayuseno, A. and W.W. Schmahl, *Understanding the chemical and mineralogical properties of the inorganic portion of MSWI bottom ash*. Waste Management, 2010. **30**(8-9): p. 1509-1520.
54. Brami, Y., et al., *Surface chemical characteristics of coal fly ash particles after interaction with seawater under natural deep sea conditions*. Environmental science & technology, 1999. **33**(2): p. 276-281.
55. Andrade, L.B., J. Rocha, and M. Cheriaf, *Evaluation of concrete incorporating bottom ash as a*

- natural aggregates replacement*. Waste Management, 2007. **27**(9): p. 1190-1199.
56. Vegas, I., et al., *Construction demolition wastes, Waelz slag and MSWI bottom ash: A comparative technical analysis as material for road construction*. Waste management, 2008. **28**(3): p. 565-574.
57. Zevenbergen, C., et al., *Weathering of MSWI bottom ash with emphasis on the glassy constituents*. Journal of geochemical exploration, 1998. **62**(1-3): p. 293-298.
58. Izquierdo, M., et al. *Use of bottom ash from municipal solid waste incineration as a road material*. in *International ash utilization symposium, 4th, Lexington, KY, United States*. 2001.
59. Gunning, P.J., C.D. Hills, and P.J. Carey, *Production of lightweight aggregate from industrial waste and carbon dioxide*. Waste management, 2009. **29**(10): p. 2722-2728.
60. Filipponi, P., et al., *Physical and mechanical properties of cement-based products containing incineration bottom ash*. Waste Management, 2003. **23**(2): p. 145-156.
61. Pera, J., A. Wolde, and M. Chabannet, *Hydraulic activity of slags obtained by vitrification of wastes*. Materials Journal, 1996. **93**(6): p. 613-618.
62. Jurič, B., et al., *Utilization of municipal solid waste bottom ash and recycled aggregate in concrete*. Waste Management, 2006. **26**(12): p. 1436-1442.
63. Hjelm, O., J. Holm, and K. Crillesen, *Utilisation of MSWI bottom ash as sub-base in road construction: first results from a large-scale test site*. Journal of hazardous materials, 2007. **139**(3): p. 471-480.
64. Olsson, S., E. Kärrman, and J.P. Gustafsson, *Environmental systems analysis of the use of bottom ash from incineration of municipal waste for road construction*. Resources, conservation and recycling, 2006. **48**(1): p. 26-40.
65. Su, L., et al., *Copper leaching of MSWI bottom ash co-disposed with refuse: effect of short-term accelerated weathering*. Waste management, 2013. **33**(6): p. 1411-1417.
66. Heasman, L., H. van der Sloot, and P. Quevauviller, *Harmonization of leaching/extraction tests*. Vol. 70. 1997: Elsevier.
67. Van der Sloot, H., R. Comans, and O. Hjelm, *Similarities in the leaching behaviour of trace contaminants from waste, stabilized waste, construction materials and soils*. Science of the Total Environment, 1996. **178**(1-3): p. 111-126.
68. Chandler, A.J., et al., *Municipal solid waste incinerator residues*. Vol. 67. 1997: Elsevier.
69. Arickx, S., et al., *Effect of carbonation on the leaching of organic carbon and of copper from MSWI bottom ash*. Waste Management, 2010. **30**(7): p. 1296-1302.
70. Dijkstra, J.J., H.A. Van Der Sloot, and R.N. Comans, *The leaching of major and trace elements from MSWI bottom ash as a function of pH and time*. Applied Geochemistry, 2006. **21**(2): p. 335-351.
71. Dugenez, S., et al., *Municipal solid waste incineration bottom ash: characterization and kinetic studies of organic matter*. Environmental science & technology, 1999. **33**(7): p. 1110-1115.
72. Saikia, N., et al., *Assessment of Pb-slag, MSWI bottom ash and boiler and fly ash for using as a fine aggregate in cement mortar*. Journal of Hazardous materials, 2008. **154**(1-3): p. 766-777.
73. Meima, J.A., A. van Zomeren, and R.N. Comans, *Complexation of Cu with dissolved organic carbon in municipal solid waste incinerator bottom ash leachates*. Environmental Science & Technology, 1999. **33**(9): p. 1424-1429.

74. Rendek, E., G. Ducom, and P. Germain, *Influence of organic matter on municipal solid waste incinerator bottom ash carbonation*. Chemosphere, 2006. **64**(7): p. 1212-1218.
75. Ito, R., et al., *Removal of insoluble chloride from bottom ash for recycling*. Waste Management, 2008. **28**(8): p. 1317-1323.
76. Meima, J.A., et al., *Carbonation processes in municipal solid waste incinerator bottom ash and their effect on the leaching of copper and molybdenum*. Applied Geochemistry, 2002. **17**(12): p. 1503-1513.
77. Chimenos, J., et al., *Short-term natural weathering of MSWI bottom ash as a function of particle size*. Waste Management, 2003. **23**(10): p. 887-895.
78. Van Gerven, T., et al., *Carbonation of MSWI-bottom ash to decrease heavy metal leaching, in view of recycling*. Waste Management, 2005. **25**(3): p. 291-300.
79. Chen, C.-G., et al., *The effects of the mechanical–chemical stabilization process for municipal solid waste incinerator fly ash on the chemical reactions in cement paste*. Waste Management, 2013. **33**(4): p. 858-865.
80. Shi, C. and J. Qian, *High performance cementing materials from industrial slags—a review*. Resources, Conservation and Recycling, 2000. **29**(3): p. 195-207.
81. Chou, J.-D., M.-Y. Wey, and S.-H. Chang, *Evaluation of the distribution patterns of Pb, Cu and Cd from MSWI fly ash during thermal treatment by sequential extraction procedure*. Journal of hazardous materials, 2009. **162**(2-3): p. 1000-1006.
82. Hyks, J., et al., *Leaching from waste incineration bottom ashes treated in a rotary kiln*. Waste Management & Research, 2011. **29**(10): p. 995-1007.
83. Arickx, S., et al., *Influence of treatment techniques on Cu leaching and different organic fractions in MSWI bottom ash leachate*. Waste management, 2007. **27**(10): p. 1422-1427.
84. Qiao, X., et al., *Novel cementitious materials produced from incinerator bottom ash*. Resources, Conservation and Recycling, 2008. **52**(3): p. 496-510.
85. Yang, S., et al., *Existence of Cl in municipal solid waste incineration bottom ash and dechlorination effect of thermal treatment*. Journal of hazardous materials, 2014. **267**: p. 214-220.
86. Hu, Y., M. Bakker, and P. De Heij, *Recovery and distribution of incinerated aluminum packaging waste*. Waste management, 2011. **31**(12): p. 2422-2430.
87. Song, Y., et al., *Feasibility study on utilization of municipal solid waste incineration bottom ash as aerating agent for the production of autoclaved aerated concrete*. Cement and Concrete Composites, 2015. **56**: p. 51-58.
88. Penilla, R.P., A.G. Bustos, and S.G. Elizalde, *Zeolite synthesized by alkaline hydrothermal treatment of bottom ash from combustion of municipal solid wastes*. Journal of the American Ceramic Society, 2003. **86**(9): p. 1527-1533.
89. Aubert, J., B. Husson, and N. Sarramone, *Utilization of municipal solid waste incineration (MSWI) fly ash in blended cement: Part 1: Processing and characterization of MSWI fly ash*. Journal of hazardous materials, 2006. **136**(3): p. 624-631.
90. Lumley, J., et al., *Degrees of reaction of the slag in some blends with Portland cements*. Cement and Concrete Research, 1996. **26**(1): p. 139-151.
91. Wang, Y., *Performance assessment of cement-based materials blended with micronized sand: microstructure, durability and sustainability*. 2013.
92. Sha, W., E. O'Neill, and Z. Guo, *Differential scanning calorimetry study of ordinary Portland*

- cement*. Cement and Concrete Research, 1999. **29**(9): p. 1487-1489.
93. Noumowe, A., *Effet de hautes températures (20-600° C) sur le béton: cas particulier du béton a hautes performances*. 1995, Lyon, INSA.
94. Zhou, Q. and F.P. Glasser, *Thermal stability and decomposition mechanisms of ettringite at< 120 C*. Cement and Concrete Research, 2001. **31**(9): p. 1333-1339.
95. Nonnet, E., N. Lequeux, and P. Boch, *Elastic properties of high alumina cement castables from room temperature to 1600 C*. Journal of the European Ceramic Society, 1999. **19**(8): p. 1575-1583.
96. Khoury, G., *Compressive strength of concrete at high temperatures: a reassessment*. Magazine of concrete Research, 1992. **44**(161): p. 291-309.
97. Alarcon-Ruiz, L., et al., *The use of thermal analysis in assessing the effect of temperature on a cement paste*. Cement and Concrete research, 2005. **35**(3): p. 609-613.
98. Nguyen, V., *Rice husk ash as a mineral admixture for ultra high performance concrete*. 2011.
99. Ye, G., *Experimental study and numerical simulation of the development of the microstructure and permeability of cementitious materials*. 2003.
100. Shi, C. and R.L. Day, *Comparison of different methods for enhancing reactivity of pozzolans*. Cement and Concrete Research, 2001. **31**(5): p. 813-818.
101. Ferrari, S., H. Belevi, and P. Baccini, *Chemical speciation of carbon in municipal solid waste incinerator residues*. Waste Management, 2002. **22**(3): p. 303-314.
102. Van Zomeren, A. and R.N. Comans, *Contribution of natural organic matter to copper leaching from municipal solid waste incinerator bottom ash*. Environmental science & technology, 2004. **38**(14): p. 3927-3932.
103. Low, N.M. and J.J. Beaudoin, *Flexural strength and microstructure of cement binders reinforced with wollastonite micro-fibres*. Cement and concrete research, 1993. **23**(4): p. 905-916.
104. Callebaut, K., et al., *Nineteenth century hydraulic restoration mortars in the Saint Michael's Church (Leuven, Belgium): Natural hydraulic lime or cement?* Cement and Concrete Research, 2001. **31**(3): p. 397-403.
105. Gartner, E., et al., *Hydration of Portland cement*. Structure and performance of cements, 2002. **2**: p. 57-108.
106. Bullard, J.W., et al., *Mechanisms of cement hydration*. Cement and Concrete Research, 2011. **41**(12): p. 1208-1223.
107. Shi, C. and R.L. Day, *A calorimetric study of early hydration of alkali-slag cements*. Cement and Concrete Research, 1995. **25**(6): p. 1333-1346.
108. Weeks, C., R.J. Hand, and J.H. Sharp, *Retardation of cement hydration caused by heavy metals present in ISF slag used as aggregate*. Cement and concrete composites, 2008. **30**(10): p. 970-978.
109. Zhang, Y.M., W. Sun, and H.D. Yan, *Hydration of high-volume fly ash cement pastes*. Cement and Concrete Composites, 2000. **22**(6): p. 445-452.
110. Berry, E.E., et al., *Hydration in high-volume fly ash concrete binders*. Materials Journal, 1994. **91**(4): p. 382-389.
111. Lerch, W., *The influence of gypsum on the hydration and properties of Portland cement pastes*. 2008.
112. Gallucci, E., P. Mathur, and K. Scrivener, *Microstructural development of early age hydration*

shells around cement grains. Cement and Concrete Research, 2010. **40**(1): p. 4-13.

Appendix A Results of compressive strength tests

A1 Compressive strength of mortar

Table A-1 Compressive strength of mortar with pure cement, 10% MBA, 30% MBA, 10% BFS, 30% BFS, 10% M300 and 30% M300

Strength (MPa)	CEM I 42.5 N	10% MBA	30% MBA	10% BFS	30% BFS	10% M300	30% M300
1 day	5.717	3.853	1.737	5.566	4.795	3.849	3.911
	5.078	2.768	1.426	6.574	3.815	5.717	3.752
	5.535	3.996	1.430	5.698	3.927	4.791	3.946
	Average	5.443	3.539	1.531	5.946	4.179	4.786
7 day	30.171	20.317	18.472	19.704	15.028	18.419	16.324
	27.160	21.275	15.879	22.761	12.989	18.966	15.292
	32.078	21.455	14.164	26.139	13.210	20.936	12.207
	Average	29.803	21.016	16.172	22.868	13.742	19.440
28 day	34.656	27.052	19.158	31.761	24.430	25.219	17.067
	37.771	26.298	18.970	40.052	27.806	25.516	19.169
	46.397	25.002	17.793	26.380	23.355	22.987	18.583
	Average	39.608	26.117	18.640	32.731	25.197	24.574

A2 Compressive strength for paste

Table A-2 Compressive strength of pastes with pure cement, 10% M300, 10% CBA, 10% MBA and 10% MTBA

Strength (MPa)	CEM I 42.5N	10% M300	10% CBA	10% MBA	10% MTBA
7 day	18.400	13.300	9.998	15.113	12.060
	15.703	14.431	19.578	12.307	23.019
	22.104	9.750	7.285	16.586	18.709
	Average	18.736	12.494	12.287	14.669
31.90328 day	41.834	19.392	17.191	27.995	33.036
	39.516	16.493	22.569	27.390	24.693
	44.152	24.864	8.076	20.556	31.903
	Average	41.834	20.250	15.945	25.314

Table A-3 Compressive strength of pastes with pure cement, 10% M300, 10% MTBA, 20% M300, 20% MTBA, 30% M300 and 30% MTBA

Strength (MPa)	CEM I 42.5N	10% M300	10% MTBA	20% M300	20% MTBA	30% M300	30% MTBA
1 day	2.310	2.604	2.604	1.395	1.953	0.961	1.395
	3.581	2.001	3.565	1.287	1.829	0.884	1.240
	-	1.907	2.542	1.054	1.783	1.149	1.194
	Average	2.946	2.217	2.904	1.245	1.855	0.998
7 day	18.400	13.300	12.060	8.076	10.308	4.077	13.858
	15.703	14.431	23.019	14.400	10.804	7.022	6.526
	22.104	9.750	18.709	9.282	11.331	7.502	5.309
	Average	18.736	12.494	17.929	10.586	10.814	6.200
14 day	35.422	18.121	22.616	21.624	18.152	9.487	21.469
	33.916	17.764	27.514	14.958	23.686	13.937	15.345
	34.708	18.003	24.013	13.377	19.485	8.936	13.108
	34.682	17.963	24.714	16.653	20.441	10.787	16.641
28 day	41.834	19.392	33.036	19.051	16.912	14.354	14.400
	39.516	16.493	24.693	18.043	24.693	11.223	25.282
	44.152	24.864	31.903	20.306	20.275	10.494	14.635
	Average	41.834	20.250	29.877	19.133	20.627	12.024

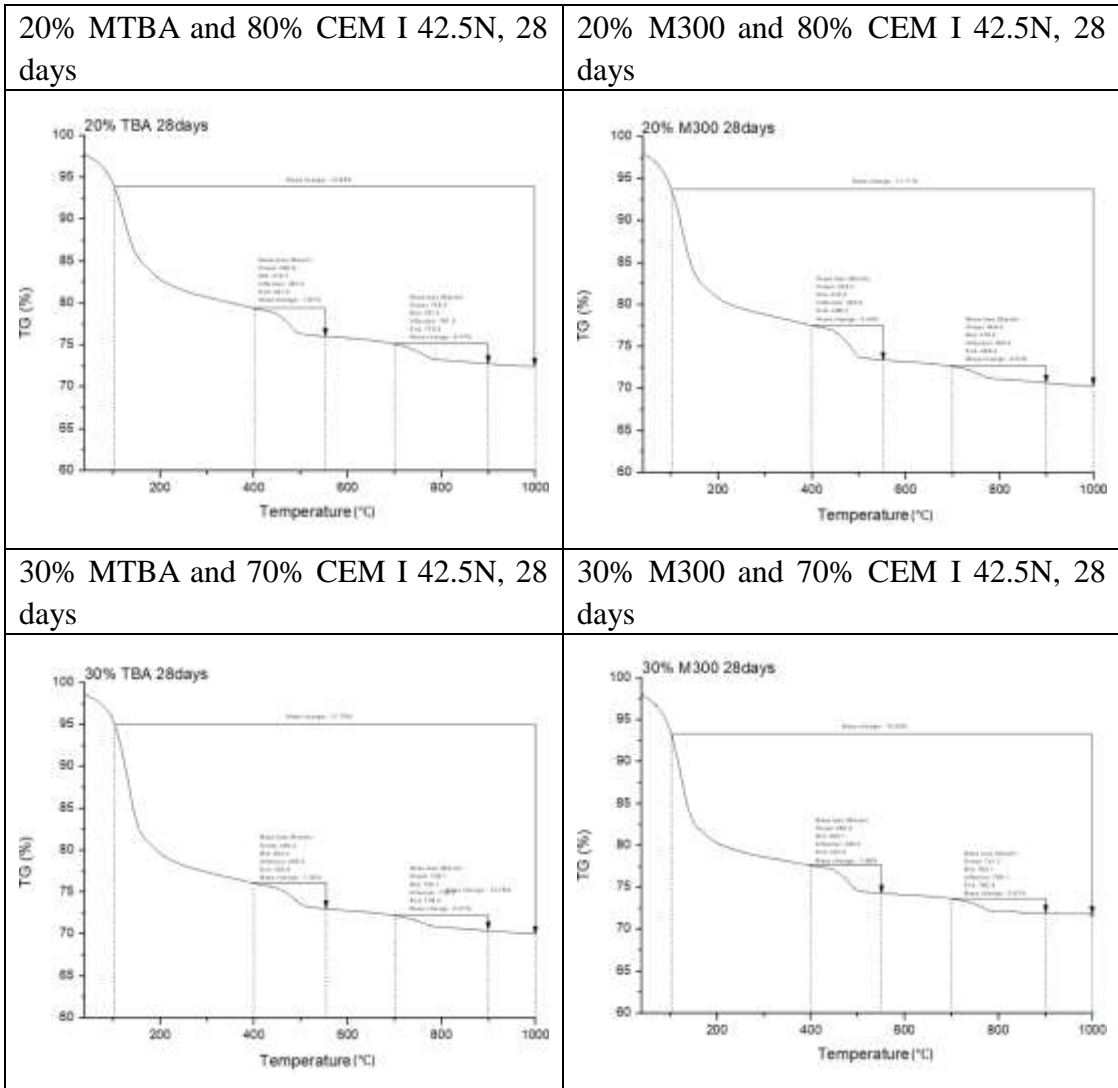
A3 Compressive strength of concrete

Table A-0-4 Compressive strength of B40 concrete and substituted with 10% MTBA

Strength (MPa)	CEM I 42.5N	10% MTBA
1 day	3.47	2.30
7 day	37.76	29.03
14 day	-	-
28 day	-	-

Appendix B Results of TGA tests

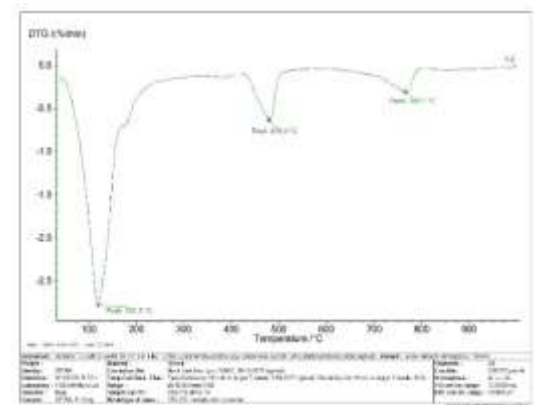
CEM I 42.5N, 28 days	10% M300 and 90% CEM I 42.5N, 28 days
10% CBA and 90% CEM I 42.5N, 28 days	10% MBA and 90% CEM I 42.5N, 28 days
10% MTBA and 90% CEM I 42.5N, 28 days	



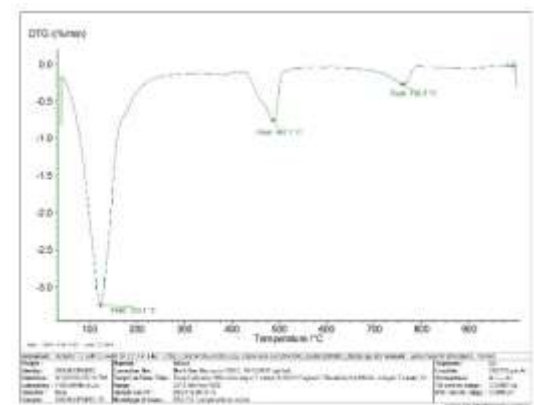
Appendix C Results of DTG tests

CEM I 42.5N, 28 days	10% M300 and 90% CEM I 42.5N, 28 days
10% and 90% CEM I 42.5N, 28 days	10% MBA and 90% CEM I 42.5N, 28 days
10% MTBA and 90% CEM I 42.5N, 28 days	

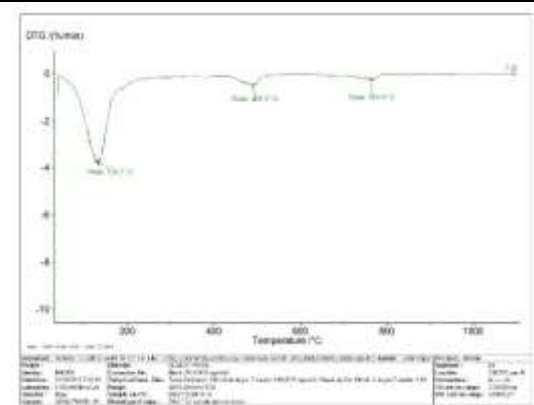
20% MTBA and 80% CEM I 42.5N, 28 days



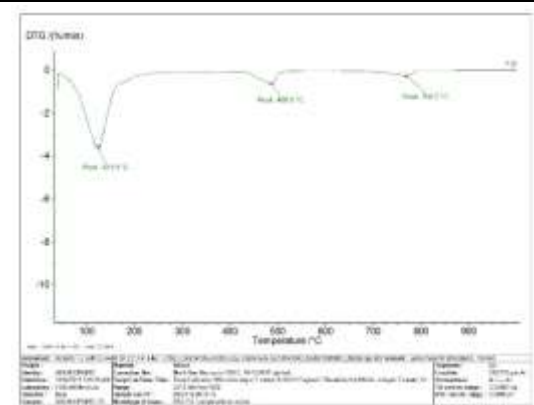
20% M300 and 80% CEM I 42.5N, 28 days



30% MTBA and 70% CEM I 42.5N, 28 days



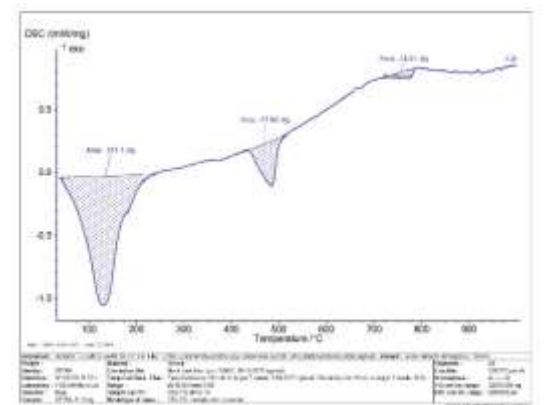
30% M300 and 70% CEM I 42.5N, 28 days



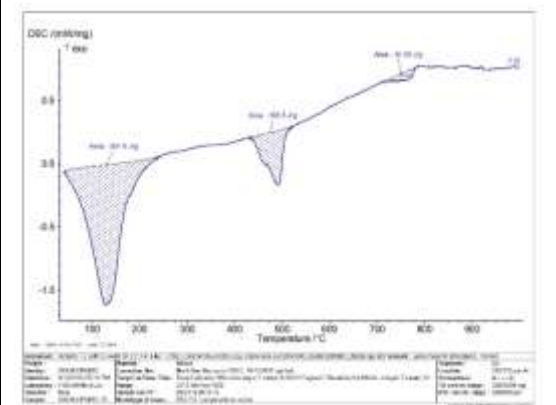
Appendix D Results of DSC tests

CEM I 42.5N, 28 days	10% M300 and 90% CEM I 42.5N, 28 days
10% CBA and 90% CEM I 42.5N, 28 days	10% MBA and 90% CEM I 42.5N, 28 days
10% MTBA and 90% CEM I 42.5N, 28 days	

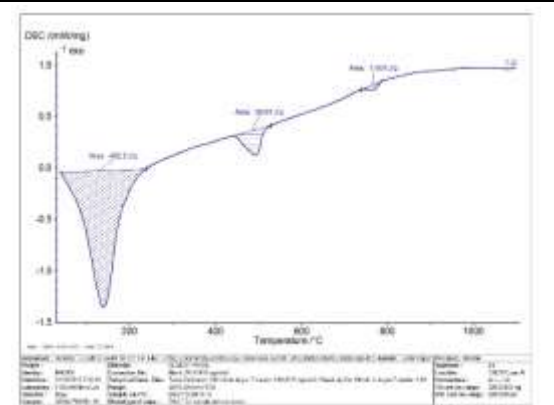
20% MTBA and 80% CEM I 42.5N, 28 days



20% M300 and 80% CEM I 42.5N, 28 days



30% MTBA and 70% CEM I 42.5N, 28 days



30% M300 and 70% CEM I 42.5N, 28 days

